3D Analysis of CT Images for Fenestrated Endovascular Aneurysm Repair

Thesis submitted in accordance with the requirements of

Faculty of Medicine at the University of Liverpool

For the degree of

Doctor of Medicine

By

Olufemi Ayoadeleke Oshin

BEng(Hons), MBChB, MRCS (Ed)

Regional Vascular Unit

Royal Liverpool University Hospital

Liverpool, L7 8XP, UK.

&

Department of Clinical Engineering

University Of Liverpool, L69 3GA, UK

May 2012

Dedicated to

My wife Emma and my parents:

Ayo Oshin and Abosede Ogunbanke

ABSTRACT

Successful endovascular aneurysm repair (EVAR) relies upon seal and fixation of the endograft in order to exclude the aneurysm from systemic circulation. In the absence of an adequate infra-renal aortic neck, endovascular aneurysm repair of abdominal aortic aneurysms is only possible using a fenestrated stent-graft. These devices extend the proximal sealing zone of the stent-graft into the visceral aorta and maintain perfusion to the gut and other end organs through specially created fenestrations in the stent-graft fabric. As such target vessel patency is an important marker of success. The aim of this study is to evaluate the relationship between the design/ planning of fenestrated stent-grafts and target vessel patency by; 1) exploring the modes and mechanisms of threat to target vessel patency 2) quantifying observer variability during assessment of aorto-iliac anatomy 3) investigating the potential consequences of planning errors.

A synthesis of published fenestrated EVAR (FEVAR) case series showed that after median follow up of 20 months, approximately 4% of target vessels are lost. The modes and mechanisms of these events was subsequently investigated by analysing the Royal Liverpool University hospital's case series in detail using a core laboratory for image analysis and a panel of experienced endovascular specialists. The most common mode of target vessel loss was shuttering either as a consequence of a planning issue or intra-operative difficulty, thereby supporting an association between assessment of aorto-iliac anatomy and early threat to target vessel patency.

Since target vessel separation in the longitudinal and circumferential direction cannot be measured directly, the reproducibility of these measurements may be used as a proxy for accuracy. Inter and intra-observer variability of target vessel measurements for FEVAR was quantified by analysing the vessel separation measurements of two blinded observers. Intra-observer variability was limited to 4.9mm between repeat measurements but increased to 7.4mm between different observers. This was predominantly a consequence of the subjective nature of image interpretation since neither measurement technique or image work station had a significant influence on variability. Further studies also appear to support this finding by demonstrating a potential relationship between specific morphological features of the aorta and the variability of observer measurements.

However quantification of inter intra-observer variability of target vessel measurements does not provide additional information about the potential effects of measurement error (mismatch between stent-graft design and the native aorta occurs) upon target vessel patency. Inter and intra-observer variability was contextualised by investigating the material properties of a Cook™ fenestrated stent-graft and subsequently the forces acting upon target stents when mismatch occurs. These studies show that fenestrated stent-grafts display a remarkable degree of tolerance and the forces are unlikely to result in significant distortion of target vessel stents.

It may not be possible to eliminate measurement error during the design stage of fenestrated endovascular aneurysm repair. Successful fenestrated endovascular

aneurysm repair is possible within the limits of intra and inter-observer variability identified in this study. This has implications for broadening the application of fenestrated EVAR from the elective setting to emergent intervention. However, such use must be tempered with caution since the long-term consequences of fenestrated stent-graft/ aorta mismatch are as yet unknown and the deliberate use of mismatched devices may introduce intra-operative difficulty that hampers successful endovascular repair.

Acknowledgements

Mr SR Vallabhaneni; Consultant Vascular Surgeon, the Royal Liverpool University Hospital

Dr T.V How; Senior Lecturer, Institute of Ageing and Chronic Disease, University of Liverpool

Mr J.A. Brennan; Consultant Vascular Surgeon, the Royal Liverpool University Hospital

Mr R.K. Fisher; Consultant Vascular Surgeon, the Royal Liverpool University Hospital

Dr R.G. McWilliams; Consultant Interventional Radiologist, the Royal Liverpool University Hospital

The late **Mr G.L. Gilling-Smith**; Consultant Vascular Surgeon, the Royal Liverpool University Hospital

Mr J. Blackhurst; Technician, Institute of Ageing and Chronic Disease, University of Liverpool

Ms J. Houghton; CT Clinical Lead Radiographer, the Royal Liverpool University Hospital

Mr A. Topping; Laboratory Technician, Faculty of Engineering, University of Liverpool

Mr A. England; Lecturer in Medical Imaging, University of Liverpool

Contents

Chapter 2 Endovascular Aneurysm Repair (EVAR)

Abbreviations and Acronyms

CTA	Computed Tomography Angiography
EVAR	Endovascular aneurysm repair
FEVAR	Fenestrated Endovascular Aneurysm repair
MMP	Matrix Metalloproteinase
OSR	Open Surgical Repair
SMA	Superior Mesenteric Artery

Chapter 1

Abdominal Aortic Aneurysms

1.1 Aneurysm

The word aneurysm originates from the Greek word aneurysma (ανεύρυσμα) denoting swelling. The most widely used definition of aneurysm is an abnormal focal dilation of an artery which exceeds 1.5 times the artery's nominal diameter. Aneurysms may be classified according to aetiology or morphology. True aneurysms comprise all the normal layers of the arterial wall; tunica intima, tunica media and tunica adventitia. The most frequently occurring true aneurysms are those affecting the infrarenal aorta, usually referred to as abdominal aortic aneurysms (AAA). Pseudoaneurysms form as a consequence of a defect in the arterial wall (usually trauma) resulting in the accumulation of blood in tissues adjacent to the artery. This collection of blood may progressively enlarge and eventually rupture.

From a large autopsy series, Brunkwall et al reported the relative frequencies of aneurysm location in patients with aortoiliac aneurysms as follows: abdominal aorta only 65%; thoracic aorta only 19%; aorto-iliac segment 13%, thoracoabdominal aorta 2% and isolated iliac 1% (Brunkwall et al., 1989). Abdominal aortic aneurysms are also associated with aneurysms of peripheral arteries and up to 10% of patients with AAA also have a concomitant popliteal artery aneurysm. Conversely a popliteal artery aneurysm is associated with an AAA in 35%.

1.2 Epidemiology

The prevalence of asymptomatic abdominal aortic aneurysms ranges between 0.5 and 3.2 % in the USA and in Europe varies from 8.2% in the UK to 4.2% in Denmark (Pearce, 2009) and initially appeared to be on an increasing trend. This was thought to be due to an increase in detection and a true rise in incidence (Fowkes et al., 1989). However more recent evidence has suggested that changes in risk factor management (smoking and hypertension) has in fact lead to a reduction in the prevalence of clinically relevant AAA (Anjum and Powell, 2012, Von Allmen and Powell, 2012). In men, its prevalence ranges from 1.3 to 8.9% and 1 to 2% in women (Sakalihasan et al., 2005). Aortic aneurysms are therefore five times (Hannawa et al., 2009, Katz et al., 1997, Lederle et al., 2001) as common in men compared with women. Aneurysm incidence rises rapidly in the male population above the age of 50 with a peak incidence in the eighth decade of life. In women, this rise is delayed but also peaks at age 80. Abdominal aortic aneurysms are much less common in men of African, Asian and Hispanic heritage and are thus primarily a disease of elderly Caucasian men. Indeed aortic aneurysms are 3.5 times more common in Caucasian elderly males than their African-American counterparts (Katz et al 1978; LaMorte 1995).

1.3 Aetiology

There are specific connective tissue disorders such as Ehlers-Danlos and Marfan's syndrome which are responsible for the formation of a proportion of aneurysms. In addition, aneurysms may also be formed due to infective pathogens, most notably *Salmonella enterica*. The vast majority of abdominal aortic aneurysms however, are referred to as 'atherosclerotic aneurysms' despite

the fact that both the formation and evolution of these aneurysms represent a unique pathological process, distinct from occlusive arterial disease. As such these aneurysms are better described as degenerative aneurysms. Age, male gender, racial origin, smoking history, occlusive arterial disease, hypertension and hypercholesterolemia are all independent risk factors (Table1). Of these, smoking appears to be the strongest risk factor with an almost six-fold increase in the relative risk of AAA formation.

Familial clustering of aortic aneurysms has also been reported (Johansen and Koepsell, 1986, Verloes et al., 1995) suggesting a genetic component in the aetiology of aneurysms. Fifteen to twenty-five per cent of first-degree relatives are noted to have abdominal aortic aneurysms compared with age-matched controls. The aneurysms tend to occur 5 to 7 years earlier than the general population and occur with greater frequency in women. Furthermore brothers of a patient with an aortic aneurysm have an 18-fold increase in the relative risk of AAA development in their lifetime (Verloes et al., 1995). Although this increase in prevalence may be explained by the presence of a common environmental agent to which these families are exposed (such as cigarette smoke), the influence of the proband's gender on AAA formation supports a strong genetic component. Furthermore if the proband is male, the risk of AAA development in a first degree relative is 7%, rising to 12% in females (Rutherford, 2000).

Risk Factor	Odds Ratio	95% Confidence
Smoking History	5.6	4.2-7.3
Family history of AAA	2.0	1.6-2.4
Old age (7-year interval)	1.7	1.5-1.8
Coronary artery Disease	1.6	1.4-1.8
Hypercholesterolaemia	1.5	1.3-1.8
COPD	1.3	1.1-1.5
Height (7 cm interval)	1.2	1.1-1.3
Deep vein thrombosis	0.7	0.5-0.9
Diabetes Mellitus	0.5	0.4-0.7
Black race	0.5	0.4-0.7
Female gender	0.2	0.1-0.7

Table 1. Independent risk factors for abdominal aortic aneurysms. *From Lederle FA, Johnson GR et al: Prevalence and associations of abdominal aortic aneurysms detected through screening: Aneurysm Detection and Management (ADAM) Veterans Affairs Cooperative Study Group, Ann Intern Med 126(6): 441, 1997*

1.4 Pathogenesis

Aneurysm formation is associated with significant and well documented changes in the structural elements of the aortic wall. The mechanical properties of a healthy human aorta are mainly dependent upon two major structural proteins; collagen and elastin. Elastin is predominantly found in the media and is arranged in a lamellar fashion with alternating layers of concentrically oriented vascular smooth muscle cells which impart active properties to the aortic wall. Elastin and the smooth muscle cells together maintain a uniform distribution of tensile forces

throughout the arterial wall and a physiological viscoelastic response to the oscillatory stress generated by the cardiac cycle. Collagen on the other hand is a load bearing protein primarily found in the adventitia. In contrast to elastin, collagen's main function is to limit the distension of the artery by providing stiffness and tensile strength as it can be stretched to 2-4% of its original length only.

Since aneurysm formation is associated with risk factors such as smoking, male gender and coronary artery disease, it is understandable that a causal link was drawn between atherosclerosis and aneurysm formation. The proposed mechanism was degenerative changes in the arterial wall and ischaemia of the vasa vasorum as a result of atherosclerosis leading to aneurysm formation. This proposed pathological process appears to be supported by the findings of Zarins et al who were able to initiate aneurysm formation in monkeys fed a high cholesterol diet (Zarins et al., 1992). However atherosclerosis as a causative mechanism fails to explain why dilation occurs in the abdominal aorta instead of the pattern of occlusive disease observed in the peripheral and coronary arteries. Furthermore studies have shown that arterial occlusive disease primarily affects the intima whereas aneurysms result from a degenerative process of the media (Xu et al., 2001).

Histologically the wall of an aneurismal artery is characterised by medial thinning and loss of elastin. Such changes in the architectural characteristics have been described by Zarins et al after crush injuries to the arterial wall (Xu et al., 2001), with consequent aneurismal change afterwards. In addition normal ageing,

arterial trauma and inflammation may induce degradation of elastin in the media through elastolyis. Therefore the pathogenesis of the abdominal aortic aneurysm appears to be a complex process in which proteolysis, inflammation and hemodynamic forces play a role in the degeneration and remodelling of the arterial wall.

1.4.1 *Haemodynamic forces*

The structure and composition of the media varies throughout the aorta with a tendency towards a lower elastin/collagen ratio at in the infra-renal portion of the abdominal aorta (Reed et al., 1992) therefore the most distal portion of the aorta is less compliant than more proximal sections. In addition the aorta tapers as it approaches its bifurcation resulting in an increased pulse pressure which is accentuated by the peripheral vascular resistance of the lower limbs. Indeed it has been shown in some studies that lower limb amputees appear to have at an increased risk of developing aortic aneurysm (Vollmar et al., 1989, Wills et al., 1996).

This variation in elastin concentration may explain the predilection of aneurysms for the infra-renal aorta. Furthermore the half-life of elastin (40-70 years) is a potential reason why aortic aneurysms are a disease of the elderly. However the absence of elastin does not necessarily lead to aneurysm formation. Indeed aneurysm formation after endarterectomy of either the carotid or femoral arteries has not been reported and would therefore suggest that the mechanical forces acting upon the aorta do not fully explain this pathological process.

1.4.2 *Proteolysis*

Expansion of aortic aneurysms is associated with an increase in total protein, collagen content and a reduction in elastin concentration and suggests that the extracellular matrix of the media is a metabolically active region of the aortic wall. Indeed both elastase and collagenase activity have been demonstrated providing direct evidence of proteolytic activity. Furthermore, normal homeostatic mechanisms appear to be inhibited as evidenced by the reduced capacity of aortic tissue to inhibit elastastolytic enzymes.

A family of zinc-dependent enzymes have been discovered with specific proteolytic action on the extracellular matrix. These enzymes, known as the matrix metalloproteinases (MMP) can be subdivided into three main groups depending on their particular affinity for a substrate. MMPs are produced by inflammatory cells such as neutrophils and macrophages as well as mesenchymal cells e.g. fibroblasts. Although they are involved in normal physiological processes such as wound healing and the remodelling of structural proteins, MMPs can influence the activity of membrane receptors, disrupt cell-cell interaction and induce apoptosis. Therefore the activity of MMPs is tightly regulated and controlled. This is achieved through the regulation of growth factors, and a family of tissue inhibitors of metalloproteinases (TIMP- 1, 2 and 3).

The increased enzymatic activity within aneurismal tissue highlights the central role that proteolytic degradation plays in aneurysm pathogenesis. Direct evidence of the role of MMPs in AAA formation has been difficult to obtain due to the

technical aspects of measuring their activity. It is believed that this is because of the binding properties of their inhibitor TIMP-1; therefore indirect evidence has been gathered by measuring MMP/TIMP-1 ratios.

Although several MMPs have been directly implicated in aneurysm formation-nominally MMP-2, MMP-3, MMP-9, and MMP-12, MMP-9 appears to be an important factor in the pathogenesis of abdominal aortic aneurysms. In 1991 Vine and Powell found increased elastolytic activity in AAA tissue compared with normal aorta and were able to show that the principal enzyme involved was MMP-9 (Vine and Powell, 1991). In the same year, Senior et al also demonstrated the ability of MMP-3 and MMP-9 to cleave elastin (Senior et al., 1991). Indeed the significance of MMP-9 with regards to AAA pathogenesis is clearly demonstrated in a study by Pyo et al where MMP-9 null mice failed to develop aneurysms despite elastase infusion (Pyo et al., 2000).

MMP-9 levels within the wall of aortic aneurysms have also been shown to correlate closely with aneurysm diameter (Petersen et al., 2002). At smaller diameters MMP-2 levels predominate whereas at larger diameters the ratio of MMP-2/MMP-9 shifts in favour of MMP-9. Whilst continued aneurysm expansion may be mediated by MMP-9, mechanical failure of the aneurysm wall occurs when aortic wall stress exceeds the tensile strength of the aneurysm wall. In this respect, MMP-9 appears to play a pivotal and synergistic role since the degradation products of the extra cellular matrix are capable of activating MMP-1, an enzyme elevated in ruptured abdominal aortic aneurysms (Wilson et al., 2008). However these degradation products are not inhibited by the presence of

TIMP, thus proteolysis of the extra cellular matrix may result in an unregulated positive feed-back loop of continued collagen destruction that ultimately results in aneurysm rupture.

1.4.3 *Inflammation*

Histological examination of abdominal aortic aneurysm specimens has shown infiltration by inflammatory cells. In a study by Koch et al, frank evidence of inflammation was demonstrated in the majority of explanted abdominal aortic aneurysm tissue (Koch et al., 1990) and has been reproduced in other studies since. In addition further evidence for the role of inflammation in aortic aneurysm pathogenesis is derived from the fact that inflammatory cells are capable of both secreting and activating the matrix metalloproteinases involved in the destruction of the extracellular matrix. Indeed a positive correlation between elastolytic activity and inflammation has been demonstrated as well as a proportional relationship between aortic aneurysm diameter and inflammatory markers (Vine and Powell, 1991).

Increased cytokine activity has also been implicated in AAA formation, particularly IL-6, IL-10, TNF-α, and interferon-γ. Elevated levels of TNF-α have been demonstrated in explanted aneurismal tissue (Newman et al., 1994). The association between abdominal aortic aneurysms and TNF-α has elucidated the understanding of aortic aneurysm pathogenesis in two ways. First TNF-α is a cytokine secreted by macrophages and secondly it is known to have angiogenic properties (associated with elevated MMP production) thereby strengthening the association between inflammation, matrix metalloproteinases and the pathogenesis of aortic aneurysm formation (Wills et al., 1996).

Further support for the role of inflammation in AAA pathogenesis was provided in a study by Dawson et al in 2006 which showed a significant reduction in IL-10 levels when comparing 99 patients awaiting abdominal aortic aneurysm repair and 100 post-operative patients (Dawson et al., 2006). Although there was no significant difference in IL-6 and CRP between the two groups, sub-group analysis showed that in patients where the aneurysm wall remained intact (endovascular aneurysm repair) there was a significant reduction in the level of inflammatory markers compared with those patients in whom the aneurysm wall excised (open surgical repair). Thus the aneurysm wall itself appears to be a site of inflammation.

The clear evidence of an inflammatory process occurring within the abdominal aortic aneurysms implies that at some point, the abdominal aorta sustained some form of injury thereby stimulating an inflammatory response. Indeed several pathogens have been associated with aneurysm formation, most notably infectious agents such as *Chlamydia pneumoniae*, *cytomegalovirus*, *Herpes simplex* and *Treponema pallidum* (syphilis). Furthermore treatment with doxycycline has been shown to reduce expansion rate in aneurysms in both the rodent model (Petrinec et al., 1996, Curci et al., 1998) and humans (Mosorin et al., 2001). However whilst the rodent model appears promising, the applicability of these findings to the human model is limited by the small sample size and follow up periods of study conducted using human subjects.

One other proposed mechanism of the initial injury sustained by the aorta in order to trigger an inflammatory response is oxidative stress. Oxidative stress may lead to cell damage at the genetic level and one of the most prevalent causes of this mode of injury to the cardiovascular system is smoking. Furthermore considering the fact that smoking is strongly associated with an increased propensity for both the formation and rapid expansion of abdominal aortic aneurysms, it is highly likely that it is an aetiological factor triggering the inflammatory response associated with the formation of abdominal aortic aneurysms.

Aortic aneurysm formation therefore represents a complex interaction between inflammatory, immune and proteolytic mediators that result in a dynamic process of tissue destruction and remodelling. This is a process influenced by hemodynamic forces, ageing and specific mechanisms of arterial injury such as oxidative stress and pathogens. Although pathogens are specific causes of aneurismal disease, the vast majority of aneurysms are non-specific in origin and emphasizes the important but as yet unclear role of genes in the cellular response to stimuli associated with aneurismal disease.

1.5 Natural history of abdominal aortic aneurysms

Abdominal aortic aneurysms are usually incidental discoveries following investigation for an unrelated ailment or clinical examination by a medical professional. The vast majority remain asymptomatic until the aneurysm ruptures. In some patients the mass effect of aneurysm may result in back pain, whilst others may present with acute limb ischaemia as a result dislodgement of thrombus from the aneurysm into the peripheral circulation. Left untreated, aneurysms will continue to expand until they rupture.

1.5.1 *Expansion of abdominal aortic aneurysms*

The expansion of abdominal aortic aneurysms is neither steady nor predictable. Enormous variation has been observed between patients however it is recognised that a loose relationship exists between maximal aneurysm diameter and expansion rate. Even when using aneurysm diameter to categorise growth rate,

considerable variation is reported in published literature and may be a reflection of the techniques used to calculate expansion rate.

The most common method used is linear expansion rate which calculates expansion rate by dividing the difference between maximum aneurysm diameter at the start and end of follow up by the length of follow up. However since the growth pattern of can vary both between individuals and in the same person, estimating the linear expansion rate of an aneurysm can be unreliable. Indeed both quiescent periods and growth spurts have been demonstrated when analysing individual patients' growth patterns.

In the longest study of aortic aneurysm expansion rate published, Brady et al showed that a quadratic model of expansion rate was a better fit for the variations in aneurysm growth compared with linear expansion (Brady et al., 2004). In addition, they also confirmed the previously reported association between smoking and increased expansion rate. Current smokers in this study had a significantly faster expansion rate (0.4 mm per annum) compared with non-smokers. However this effect did not appear to be dose dependent nor was it associated with a life-time exposure to nicotine in terms of pack years and therefore suggests a more complicated relationship between smoking and the metabolic process of aneurysm formation than first thought.

1.5.2 *Aneurysm rupture risk*

Aneurysm rupture risk is usually determined from studies of patients unfit for intervention, necropsy studies or trials for small aneurysm surveillance. Although

more sophisticated prediction models and systems have been pioneered, these actually involve invasive methods or expensive equipment and thus far have not been sufficiently validated to be of clinical benefit.

However even accepted systems of assessing aneurysm rupture risk have the potential for inaccuracy. Observational studies of patients with known abdominal aortic aneurysms tend to overestimate rupture risk since it is assumed that most sudden deaths are the result of ruptured aneurysms, but since there is a significant correlation between ischemic heart disease and abdominal aortic aneurysm, death as a result of a myocardial infarction equally as likely without the benefit of a post-mortem examination. Necropsy studies on the other hand are prone to overestimating rupture risk since autopsies only take place in a small sample of the population and are unable to include patients who survive with large aneurysms.

1.6 Population screening of abdominal aortic aneurysms

A ruptured aortic aneurysm results in a catastrophic bleed into the abdominal cavity mandating emergent surgical attention. It is estimated that the acute nature of AAA rupture results in pre-hospital mortality in the order of 50%. Of the patients who reach hospital, mortality rates of 30 to 65% have been reported (Spronk et al., 2011). As such a ruptured abdominal aortic aneurysm has an overall mortality of 80% (Lee et al., 2004). Furthermore the estimated cost of emergency surgery for ruptured AAA is £11,176 (CI £9,636 - £13,358) as

opposed to the cost of elective repair, £6,909 (CI £6,458 -£7,531) and represents significant resource utility (Multicenter aneurysm screening study group, 2002). It therefore follows that early identification of people with AAA will improve mortality from ruptures in the community.

Two UK based randomised control trials Multi-centre Aneurysm Screening Study (MASS) and Chichester reported a reduction in the risk of aneurysm related death with acceptance rates of 80.2% and 80.5% respectively for men aged 65 (Ashton et al., 2002, Scott et al., 2001). Whilst screening has a survival benefit in men, screening in women does not reduce mortality as a result of the low prevalence of aortic aneurysms in women (Scott et al., 2002).

Although screening will inevitably increase the requirement for elective surgery, it is expected that the increased workload will be equivalent to approximately one extra AAA repair per month for a District General Hospital serving 400,000 people (Young et al., 2007). The Multi-centre Aneurysm Screening Study (MASS) estimates the initial cost of starting an aneurysm screening program to be the region of £ 2.2 million. In addition the current screening program in Gloucestershire has reported running costs of £43,000 per annum. However compared with other successful screening programs; the cost of AAA screening is encouraging- £23.40 per patient compared with £40 in breast screening.

1.7 Surveillance

The timing of intervention for aortic aneurysms is largely determined by considering the risk of surveillance and the perceived of intervention. The risk of rupture is strongly associated with maximal aortic aneurysm diameter whilst surgery associated with a defined mortality risk, particularly when one considers the fact that the majority of patients with aortic aneurysms have co-morbidities that affect both the respiratory and cardiovascular system. It therefore follows that for the same individual, intervention after the aneurysm reaches a certain diameter is likely to be beneficial whereas below this size, treatment is likely to result in net harm.

With the exception of patients with significant co-morbidities, there is a clear distinction between net harm and benefit when the aneurysm is either very small (< 4cm) or large (> 6cm). However it was unclear whether prophylactic surgery for small aneurysms conferred a survival advantage over prophylactic surgery. As a result two trials were designed to answer this question.

The UK Small Aneurysm Trial (UKSAT) and the US ADAM study reported in 1998 and 2002 respectively (The UK Small Aneurysm Trial Participants, 1998, Lederle et al., 2002). These studies compared surveillance of small (4 -5.5 cm) abdominal aortic aneurysms with the outcomes of surgical intervention. Both studies concluded that there was no survival difference between the two options; therefore surveillance of small aortic aneurysms was safe.

From the results of the UKSAT and ADAM studies, one may infer that in the majority of individuals, 5 to 5.5cm represents a threshold for intervention

however the value of this diameter is dependent upon the perceived risk of intervention. Reported mortality rates between 1 to 10% for open surgery range have been published. This wide variation is thought to be the product of both patient selection and reporting bias. Randomised controlled trials often involve specifically chosen institutions and are therefore unlikely to represent "real-world" practice. As such published mortality rates are usually a reflection of practice in specialist and high volume centres. Indeed there is compelling evidence to suggest that high volume centres are associated with better patient outcome (Young et al., 2007).

Patient selection is also clearly important since patient fitness governs both post-operative mortality and morbidity. There is clear evidence that a correlation exists between both morbidity and mortality and American Society of Anaesthesiology (ASA) grade (Prause et al., 1997). Given that factors associated abdominal aortic aneurysm formation are also the co-morbidities associated with poor outcome (COPD, hypercholesterolaemia, coronary heart disease and age) it is not surprising that many patients fall into higher ASA groups. Several risk prediction models such as Glasgow Aneurysm Score (GAS), VBHOM (Vascular Biochemistry, Haematology Outcome Models) and Estimation of Physiologic Ability and Surgical Stress (E-PASS) and V-POSSUM (Vascular Physiological and Operative Severity Score for the enUmeration of Mortality and Morbidity) have been developed to aid the decision making process. Although these models can accurately predict mortality and morbidity rates within a given population (Tang et al., 2007), it is currently not possible to determine with absolute certainty whether a given individual will survive repair of their aneurysm.

Therefore the decision to intervene in patients with abdominal aortic aneurysms remains a clinical judgement made by vascular surgeons informed by the individualities of each patient presenting with an aortic aneurysm.

1.8 Surgical Intervention

1.8.1 *History*

Although many credit John Hunter, the British surgeon with the technique of aneurismal ligation, this technique was probably first recorded by the Greek surgeon Antyllus in 2 AD (Friedman and Friedman, 1989). In his writings he advised ligation of aneurysm but warned against resection of the aneurysm itself in case the ligatures slipped and resulted in haemorrhage. Hunter reported success with this technique when dealing with popliteal aneurysms but a significant proportion of his patients suffered limb loss or death as a result of gangrene if insufficient collateral circulation did not develop following this procedure (Galland, 2007). Following this, most "therapeutic management" for aneurismal disease was based on the prevention of rupture by inducing fibrosis of the aneurysm wall or thrombosis of the sac.

The first glimpse of modern aortic aneurysm surgery did not emerge until the first reported resection of a coarcted aorta (Crafoord, 1947) and in the 1950's reports began to emerge of aortic resection and replacement with human homografts (Creech et al., 1956). However these homografts were prone to failure and limited the applicability of this technique due in part to problems with availability and was only resolved through the efforts of vascular surgeon ME

DeBakey (1908-2008). In 1955 he performed the first successful resection of a thoracoabdominal aortic aneurysm using the DeBakey Dacron graft- the first artificial arterial graft of its kind.

1.8.2 *Technique for Open abdominal aortic aneurysm repair*

Although refinements have been made in the technique of open aneurysm surgery, it has remained relatively unchanged since its inception almost 60 years ago. Initially both the thoracic and abdominal cavities were opened to access the aorta with resection of the aneurysm and an end-to-end anastomosis for the Dacron conduit. Modern open abdominal aortic aneurysm surgery consists of a midline laparotomy which provides sufficient access to the aneurysm. Complete excision of the aneurysm sac is no longer practiced as this is unnecessary, technically demanding and ultimately dangerous.

Instead the graft material is now sutured using an inlay technique whereby the aneurysm is exposed and the diseased aorta replaced (Orr and Davies, 1974). The graft itself is then protected by covering it with the redundant tissue of the aneurysm sac- a technique known as aneurysmorraphy first described by Rudolph Matas (1860-1957), but later adopted and popularised by Oscar Creech in 1966 (Creech, 1966).

1.8.3 *Complications of Open abdominal aortic aneurysm repair*

Despite that fact that the technique for modern open aneurysm repair is approximately 60 years old, the morbidity and mortality from open aneurysm

repair has not improved significantly. A major factor in this is the fact that blood flow through the aorta has to be temporarily arrested by cross-clamping the aorta in order to effect aneurysm repair. This has the effect of significantly increasing the peripheral vascular resistance and thus the workload of the heart in particular the left ventricle. In addition, prolonged ischaemia results in the formation of metabolites that are both cardio and nephrotoxic. In conjunction with the severe fluid shifts and blood loss associated with open abdominal aortic aneurysm repair, it is not uncommon for patients to succumb to cardiovascular complications such as myocardial infarction or cardiac dysrhythmias following surgery. Furthermore, renal dysfunction as a result of fluid balance changes and ischaemia from cross-clamping the aorta above the renal arteries and respiratory complications as a result of poor respiratory effort as a result of significant abdominal pain after surgery are also common.

Although complications such as the erosion of graft material into the bowel (aorto-enteric fistulae) and pseudoaneurysms at the anastomosis between the graft and native aortic tissue have been reported at medium and long-term follow up, these are relatively rare and infrequent occurrences underpinning the durability of open surgical repair in patients who survive the initial procedure.

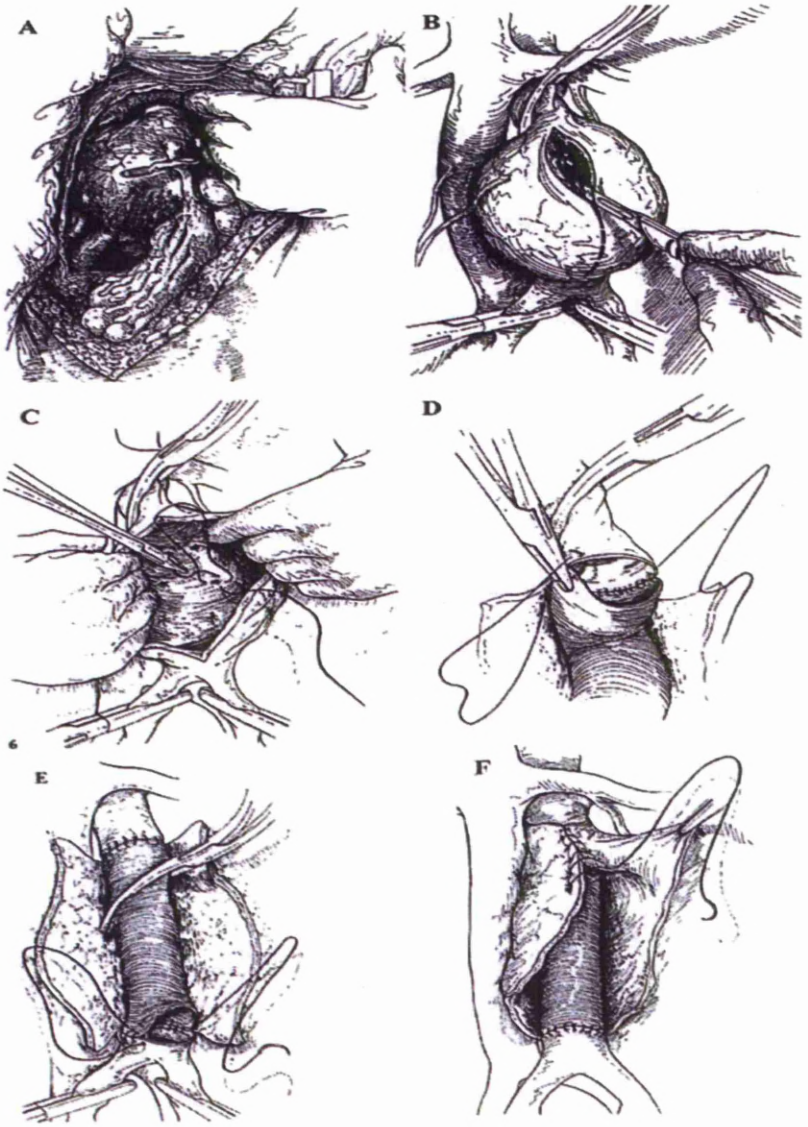

Figure 1.2 Endoaneurysmorhaphy A: Exposure of the aneurysm sac. B: Once the aneurysm has been controlled with clamps it is opened. C: Control of back bleeding lumbar arteries by oversewing. D: Proximal anastomosis of the synthetic graft. E: Distal anastomosis of synthetic graft. F: Redundant aneurysm sac is used as a protective barrier between the synthetic graft and bowel. *(From "Vascular and Endovascular Surgical Techniques" Third Edition. Ed: RM Greenhalgh, WB Saunders.)*

1.9 *Summary*

Aneurismal degeneration of the abdominal aorta is a common condition affecting men over the age of 65. Since it is an asymptomatic condition, it often presents as an incidental finding or acute circulatory collapse in the event of a rupture. Whilst surgery has provided effective treatment for this condition over the last 60 years, open aneurysm repair nonetheless represents a significant physiological insult in a cohort of patients already compromised by their co morbidities.

Chapter 2

Endovascular Aneurysm Repair (EVAR)

2.1 Introduction

Open abdominal aortic aneurysm surgery has remained the gold standard for abdominal aortic aneurysm repair since its description by Dubost in the 1950's (Dubost et al., 1952). However open surgery is associated with considerable morbidity and mortality since it relies on opening the abdominal compartment (laparotomy). Furthermore it prolongs hospital length of stay, utilisation of intensive care facilities and in some cases, convalescence. As such both Parodi and Volodos to developed and reported the first endovascular devices independently of each other (Volodos et al., 1991, Parodi et al., 1991). This new technique combined the principles of endoluminal and minimally invasive surgery with a resultant paradigm shift in the management of abdominal aortic aneurysms.

Parodi reported five successful cases of patients in whom an endovascular device had been deployed. The aim of this new technology was to exclude the aneurysm sac by ensuring continuity of blood flow using minimally invasive techniques. It was expected that this technique would minimise post-operative morbidity and mortality and thus allow aneurysm treatment to be offered to high risk patients.

Indeed Parodi theorised that the mortality benefit of EVAR would be such that small aneurysms could be treated since the threshold for intervention was reliant on the observed mortality of open surgery (Parodi et al., 1991).

2.2 Principles of endovascular aneurysm repair

Two important concepts underpin endovascular aneurysm repair; seal and fixation. Seal refers to the isolation of the aneurysm sac from systemic circulation by channelling blood through the stent-graft or conduit. Seal may be compromised by both minor and major displacement of the stent-graft, therefore a durable repair relies on the ability of the stent-graft to maintain its position through fixation to the native aorta. These factors are very closely related to the morphology of the aneurysm. As such clinical success and outcome is mainly dependent on the patient anatomy unlike open aortic surgery where patient fitness governs outcome.

2.3 Anatomical considerations

The application of EVAR is limited by certain anatomical criteria, principally the "neck" of the aneurysm and access to the aneurysm itself. The aneurysm's neck refers to the distance between the lowermost renal vessel and the beginning of the aneurysm sac. It is now widely accepted that a neck length of 10-15mm or more is required for successful standard EVAR. Since the neck of the aneurysm plays a crucial role in the durability of EVAR, neck quality is also important.

Whilst excessive calcification and thrombus are relative contra indications to EVAR, the morphology also has an important role since seal and fixation are often both reliant to a large degree on friction generated by the stent-graft/ aortic interface. Ideally the infra-renal segment of the aorta should be circular and straight with no angulation- in effect a cylinder. However it is unusual to encounter such necks in clinical practice since aneurismal degeneration often leads to elongation and subsequent angulation of the aorta.

The minimally invasive nature of EVAR means that access to the aneurysm itself is important and is in itself another limiting factor in applicability. Usually access to the aneurysm is obtained via the common femoral artery which has a nominal diameter of 6-8 mm dependent on gender. Introduction of the stent-graft relies upon compaction of the stent graft into a sheath that is then manoeuvred into position under fluoroscopic (x-ray) guidance. However the degree of compression is limited by the bulk of the stent-graft fabric and metal which make up the stents. Therefore access to the aneurysm sac is limited by the relative calibre of the delivery system and the diameter of the artery used to gain access to the aneurysm. Whilst this varies with stent design and manufacturer, stenosis, tortuousity and calcification (which limits compliance) of the external iliac artery are additional factors that may also hinder device introduction.

Collectively these anatomical features can limit the applicability of EVAR and early experience suggested that up to 55 per cent of patients would be

anatomically suitable for EVAR (Armon et al., 1997, Treiman et al., 1999). However in modern times poor access is no longer a major barrier to EVAR and may be improved using a variety of techniques. Open surgical options include sewing a synthetic tube onto the larger common iliac artery in order to avoid excessive tortuosity or calcification of external iliac artery or endarterectomy prior to device introduction.

Innovative endovascular techniques have also been reported. An example is the process known as "paving and cracking". Here the diseased segment of artery is first "paved" using a covered stent and then dilated or "cracked" by angioplasty thus relining the damage to the arterial wall that inevitably ensues from this technique. Furthermore improvements in stent design (notably the use of suprarenal fixation with hooks or barbs) now mean that in experienced hands, aneurysms with neck lengths approaching 10mm may be offered treatment. As a consequence of the combined improvements in stent-graft technology, clinical experience and the use of adjunctive manoeuvres, the applicability of EVAR has increased (Carpenter et al., 2001) leading some to state that the use of EVAR is limited only by the imagination and the ingenuity of individual clinicians.

2.4 Outcomes of EVAR

Following its introduction in 1991, evidence for the clinical efficacy of EVAR was derived from case reports, observational studies from single institutions and multicentre registries, most notably the EUROSTAR registry. Data from these sources suggest that EVAR had better clinical outcomes compared with open surgical repair; however like all data from these sources the objectivity of the conclusions drawn were hampered by problems such as patient heterogeneity, publication bias and the absence of a true control group. Robust evidence for the efficacy of EVAR was not available till the advent of three major randomised controlled trials- UK EVAR 1 (UK EVAR trial 1 participants, 2005), UK EVAR 2 (UK EVAR 2 trial participants, 2005) and the Dutch DREAM trial (Prinssen et al., 2004a). The UK EVAR 1 study randomised 1082 patients from 41 UK centres fit for open surgical repair to either open surgical repair (OSR) or EVAR. This was a similar model to the DREAM trial where 345 patients were randomised. The UK EVAR 2 addressed the question of patient fitness as a determinant of outcome and randomised 338 patients to either EVAR or conservative management. More recently two other trials; the outcomes following endovascular vs open repair for abdominal aortic aneurysm (OVER) trial from the USA (Lederle et al., 2009) and the ACE trial from France (Becquemin, 2009) have also reported.

2.4.1 *30-day survival*

All four trials demonstrated a lower 30-day mortality in the EVAR group compared with the open surgical repair (OSR) group. The UK EVAR trial 1

reported mortality of 1.7% vs 4.7% for EVAR and OSR respectively. This difference was highly significant (p= 0.009) and was equivalent to a crude odds ratio of 0.35 in favour of endovascular aneurysm repair. This early survival advantage was also persistent when in-hospital mortality was taken into consideration (EVAR 2.1% vs. OSR 6.2%, p = 0.001). The DREAM trial also produced similar results (EVAR 1.2% vs. OSR 4.6%) and had a better odds ratio in favour of EVAR (0.25), however these figures did not reach statistical significance (p = 0.1). The OVER trial reported mortality in the EVAR group as 0.5% vs 3% in the OSR group; p = 0.04 however the ACE trial showed no significant difference in 30-day mortality between EVAR and OSR 0.6% vs 1.3%; p = 1.0.

The difference between the trials is probably explained by the fact that both the DREAM and ACE trials were underpowered. In the DREAM trial in order to demonstrate a difference between the two treatment arms with 80% power, 450 patients were required but as a result of time constraints imposed by the funding body for the DREAM trial, the investigators were only able to recruit 351 patients. Similarly the ACE trial struggled with recruitment, primarily as a consequence of difficulties encountered with funding for endovascular stent-grafts. Three hundred and six patients were recruited into this trial and by the time the trial was published, only 299 patients of the original target of 600 participants were available for analysis. As such both the DREAM and ACE trials probably reported on an insufficient number of patients to demonstrate a significant difference in survival between the EVAR and OSR groups. Therefore

the most robust evidence for the efficacy of EVAR can only be derived from analysis of the UK EVAR 1 and OVER trials. Both trials also show significant advantages with EVAR in terms of morbidity and health resource utility. In addition the DREAM trial in particular was also able to show significant improvements in early complication rates with regards to specific body systems and blood loss. It would therefore appear that EVAR confers a significant survival advantage over the OSR group that is probably a consequence of eliminating the physiological burden of aortic cross-clamping and laparotomy.

2.4.2 *Mid-term and late survival*

The mid-term results of UK EVAR trial 1 showed that at 4 years follow up, although all-cause mortality was similar in the two groups, aneurysm related morality was still lower in the EVAR group (4% vs 7%; $p = 0.04$) by virtue of the sustained benefit of its lower 30-day mortality compared with OSR. This finding was also reproduced in the DREAM trial at two years, but all-cause mortality was unaffected by the type of repair. Furthermore in the ACE trial, all-cause mortality was not improved by EVAR, thus one might conclude that in patients at low risk from OSR, EVAR provides no survival advantage but is associated with additional resource utility as a result of surveillance.

The late results of EVAR from the UK EVAR trial showed that the initial advantage of EVAR was subsequently negated by a late surge in aneurysm related mortality. This has important ramifications since the aim of intervention in patients with aneurysms is the prevention of death as a result of rupture as

opposed to prolonging life expectancy. As such aneurysm related mortality (defined as death from rupture, stent-graft related events and peri-operative death) is a more reliable indicator of the efficacy of EVAR. The convergence of the survival curves between the two groups (EVARE and OSR) is not necessarily an indictment of EVAR. Indeed one might argue that the EVAR trials are largely historic and much more is known in the present day about mitigating the potential complications of EVAR and patient selection. It is anticipated that the long-term results of the OVER trail will answer this question since this will reflect contemporaneous practice.

The fact that mid-term survival is unaffected by the treatment modality suggests that the underlying pathology (i.e. the aneurysm) and patient co-morbidity may be more significant determinants of survival than treatment modality. This is demonstrated in the UK EVAR 2 trial where patients deemed unfit for open repair were randomised to either EVAR or conservative management. Overall mortality at 4 years was 64% with no difference in either all cause or aneurysm related mortality between the two groups. However in a post hoc analysis, follow up was divided into the first 6 months after randomisation and the period after 6 months. The hazard ratios for aneurysm related mortality comparing the EVAR and no intervention groups were 1.67 (95% CI 0.72 to 3.86) and 0.53 (95% CI 0.20 to 1.39) in the two time periods respectively and suggests that the initial disadvantage of EVAR may be followed by longer term benefit.

It would therefore appear that there is a subset of patients who will derive no benefit from EVAR. It should be noted however that there were no objective criteria used to define patients unfit for open surgical repair in the UK EVAR Trial 2 study. Indeed this decision was left to the discretion of the trial participants. Whilst this may reflect "real world practice", the patients in this trial were probably a broad spectrum of individuals of which a proportion may have been considered for inclusion into UK EVAR trial 1, thereby highlighting the subjective nature of patient assessment for aneurysm surgery.

2.4.3 *Complications*

Whilst there is little doubt that EVAR has reduced both peri-operative mortality and aneurysm related death, secondary intervention has been reported in 10-34% of cases (Verhoeven et al., 2004) and may be performed either as an elective or acute/unplanned basis. They range from interventions performed for incidental discoveries during surveillance such as embolectomy following endograft limb occlusion to conversion to open repair in order to prevent late rupture of the aneurysm.

2.4.3.1 *Endoleak*

Endoleak is defined as a condition associated endoluminal vascular grafts, defined by the persistence of blood flow outside the lumen of the endoluminal graft but within the aneurysm sac or adjacent vascular segment being treated by the graft (White et al., 1997). They may be categorised according to the timing of

their onset- early (within the first 30 days) or late, however the most useful and widely accepted classification system relates the endoleak to its origin. The overall prevalence of endoleaks ranges from 10 to 45% (Carrafiello et al., 2008) and may represent impending or actual failure of endovascular repair and usually correlates with the type of endoleak in question.

2.4.4.1 *Type 1 Endoleak*

These result from inadequate seal (apposition between the stent-graft and native aorta) at either the proximal or distal fixation point of the endograft (landing zones); thus the aneurysm sac remains perfused at systemic pressures. As such this type of endoleak is associated with a high risk of secondary rupture after endovascular repair, mandating early intervention. Predisposing factors to the formation of a type 1 endoleak are usually anatomical in origin and include a short sealing zone and extensive neck calcification or angulation.

2.4.4.2 *Type 2 Endoleak*

These endoleaks arise from retrograde perfusion of the aneurysm sac such as the lumbar or inferior mesenteric arteries. Unlike type 1 endoleaks, their significance remains controversial although there is increasing evidence supporting the hypothesis that these endoleaks are benign. In the early days of EVAR, these endoleaks were viewed as a procedural failure and were the basis for a significant number of secondary interventions. It is now recognised that up to 40% will seal spontaneously. Although some have been associated with sac expansion, these endoleaks are low pressure endoleaks and as such the risk of sac

rupture is much lower than that associated with type 1 endoleaks. Indeed only 4 secondary ruptures after EVAR attributable to a type 2 endoleak have been reported in the world literature (Jones et al., 2007). On this basis, most clinicians now adopt a conservative approach to type 2 endoleaks since intervention may result in considerable morbidity.

2.4.4.3 *Type 3 Endoleak*

These are endoleaks resulting from a problem with the stent-graft itself and encompass separation of the endograft components (main body and stent-graft limbs) and fabric tears or holes due to erosion or fracture of the metallic component of the stent-graft. Similar to type 1 endoleaks, these endoleaks expose the aneurysm sac to systemic pressure and as such secondary intervention is recommended.

2.4.4.4 *Type 4 Endoleaks*

Type 4 endoleaks were seen with early stent-grafts when completion angiograms demonstrated a faint "blush" of contrast. This was due to extravasation of contrast through the stent graft fabric exacerbated by anticoagulation of patients during the procedure. These sealed spontaneously and are rarely seen with modern devices.

2.4.4.5 *Type 5 Endoleaks*

A type 5 endoleak is by definition sac expansion without an identified endoleak and is thought to be a result of ultra-filtration through the stent-graft material (commonly those made from PTFE).

2.4.5 *Migration*

Migration has been defined as the longitudinal movement of all or part of a stent-graft or attachment system for a distance of 5 mm or more relative to anatomic landmarks determined before discharge (Lifeline Registry of Endovascular Aneurysm Repair Steering Committee, 2001). Since isolation of the aneurysm sac from systemic circulation depends on apposition of the stent-graft to the native aorta, migration may potentially result in the formation of a type 1 endoleak with the attendant risk of secondary rupture. However the point at which stent-graft migration becomes a significant problem remains controversial. As such Greenberg and co-workers have more recently proposed redefining migration as twice the resolution of imaging study (Greenberg et al., 2004). Although these definitions provide robust and reproducible mechanisms for defining migration *radiologically*, migration in itself does not necessarily represent failure of endovascular repair. Loss of device fixation raises doubts about durability however the length of aortic neck that remains in contact with the stent-graft is arguably of more significance since this distance better reflects the risk developing a type 1 endoleak as a result of device migration.

Stent-graft design has a significant influence on the propensity for migration. Early designs relied on the radial force exerted by the metallic component of the stent-graft on the aortic wall. By selecting a stent-graft with a larger nominal diameter than the aortic neck (oversizing), the radial force exerted on the aorta is increased leading to improved seal and fixation; as such most device companies recommend oversizing stent-grafts by 10 to 20%. Whilst an undersized endograft may compromise seal, excessive stent-graft oversizing may result in endoleak as a result of stent-graft infolding or progressive dilation of the proximal aortic neck leading to subsequent migration. Although this has been demonstrated *in vitro* (Schurink et al., 1999), these fears have not been corroborated by clinical studies (Petrik and Moore, 2001, Dias et al., 2001, Sampaio et al., 2004). Although the radial force exerted by oversized stent-grafts on the aorta is related to the displacement force and therefore migration resistance, this effect is marginal when compared to the displacement force needed to extract stent-grafts anchored by hooks and barbs. Indeed utilising hooks and barbs has been shown to add anchoring strength and increase fixation 10-fold (Malina et al., 1998, Resch et al., 2000).

More recently the role of the iliac system and distal fixation has also emerged as a contributing factor to migration. In animal experiments, Akro et al showed that complete utilisation of the iliac system significantly increased the fixation strength of commercial stent-grafts (Murphy et al., 2007). Later in retrospective analysis, Zarins et al confirmed these findings by showing that iliac limbs with

closer proximity to the iliac bifurcation resulted in greater stability even in the presence of sub-optimal proximal device fixation (Heikkinen et al., 2006).

2.4.6 *Iliac Limb Occlusion*

Limb occlusion is an important complication after EVAR with an incidence approaching 15% (Conner et al., 2002, Krajcer et al., 2002). The majority occlude with the first three months of surveillance; however limb occlusion has been reported as late as three years following the index procedure (Cochennec et al., 2007). The aetiology of limb occlusion may be categorised according to anatomical factors or graft-related problems. Device-related problems include dissection during introduction and a tendency for devices with unsupported limbs to kink within the iliac arteries. Indeed during short term follow up, unsupported limbs appear to be 15 times more likely to require secondary intervention to maintain patency than supported limbs (Fairman et al., 2002).

Specific anatomical features predisposing to limb occlusion include iliac artery angulation, kinking of the iliac limbs following primary deployment and stenosis due to pre-existing vessel disease or calcification. Gender has also been reported as a factor associated with limb occlusion and is thought to occur because of the propensity for smaller vessels in women. The association between the size of the iliac artery and the risk of limb occlusion also appears to be important. In one study, Carroccio et al found that iliac limbs of 14mm or less were twice as likely

to occlude as those greater than 14mm (Carroccio et al., 2002). This observation is also supported by other studies which show that extension of the endograft limb into the external iliac artery was also associated with an increased risk of limb occlusion; probably related to a combination of reduced luminal diameter and increased tortuosity of the external iliac artery (Sivamurthy et al., 2006, Oshin et al., 2010b).

2.5 Surveillance

Although the benefits of EVAR compared with open surgical repair have been demonstrated conclusively in several studies, the potential risk of complications following this procedure mandates lifelong surveillance. Ideally surveillance after EVAR should have a high degree of specificity and sensitivity in order to detect endograft related adverse events. In centres offering endovascular aneurysm repair, this has historically been based on contrast enhanced computed tomographic angiography (CTA) performed at regular intervals following the index procedure. One such protocol is the EUROSTAR protocol which recommends surveillance images at 1, 3, 6, 12, 18 and 24 months followed by annual imaging thereafter.

CTA has remained the gold standard for surveillance imaging after EVAR because the high specificity and sensitivity it offers for the major complications following EVAR. However in addition to the high addition cost to EVAR as a whole (Prinssen et al., 2004b), concern has been raised regarding the cumulative

exposure of patients to ionising radiation (Brenner and Hall, 2007) and the potential for renal dysfunction as a result of contrast induced nephropathy (Walsh et al., 2008). Although frequent CTA after EVAR provides a wealth of information about aneurysm diameter, freedom from endoleak and stent-graft integrity, in the context of improved clinical outcome with successive generations of stent-grafts (May et al., 2000, Resch et al., 2001) both the intensity and utility of routine CTA after EVAR has been questioned.

Several authors now advocate the use of duplex ultrasound scanning (DUS) as the imaging modality of choice since recent studies have shown that it is at least as efficacious as CTA in determining clinically significant endoleaks (Chaer et al., 2009, Beeman et al., 2009, Schmieder et al., 2009a). Indeed there is growing evidence that the requirement for secondary intervention after EVAR can be based on aneurysm sac expansion in the majority of cases and as such is an event that may be monitored regularly using DUS alone. Indeed in one study, periodic CT scans were shown to be of benefit to less than 10% of patients after EVAR (Dias et al., 2009a).

2.6 Secondary intervention after EVAR

Historically, surveillance frequently resulted in secondary intervention after EVAR since the significance of certain complications was poorly understood. Early studies reported secondary intervention rates of 2.1% per annum (Hinchliffe et al., 2003, Conner et al., 2002) and in a study by Laheij et al based on the EUROSTAR registry, secondary intervention of one form or another had

been performed in 38% of patients at 4 years follow up (Laheij et al., 2000). However the significant intervention rates reported in this study is largely a reflection of the use of first generation stent-grafts. In this study 26% of the devices were still in use by the time the study was repeated again in a study by Hobo and Buth which showed freedom from secondary intervention had improved to 86% at 4 years (Hobo and Buth, 2006).

The relatively high frequency of secondary intervention compared with open surgical repair is frequently cited as a potential disadvantage of EVAR and evidence of poor long-term durability. However secondary intervention may be categorised by the invasiveness of the procedure namely: (a) trans-abdominal procedures (usually conversion to open repair), (b) extra-anatomic (bypass) procedures and (c) trans-femoral interventions.

The minimally invasive nature of a trans-femoral procedure is an important consideration when comparing secondary intervention after EVAR and open repair. In the UK EVAR 1 trial, 20% patients in the EVAR group required secondary intervention after 4 years follow up compared 5% in the open surgery cohort. Even taking into account secondary interventions performed for type II endoleaks (now recognised as largely benign) there was still a significant trend towards a higher rate of secondary intervention in the EVAR group. However the majority of secondary interventions in the open group were trans-abdominal in nature, whilst trans-femoral procedures formed the bulk of secondary intervention sin the EVAR group; a finding replicated by other authors (Hobo and Buth, 2006, Lalka et al., 2005, Conrad et al., 2009, Becquemin et al., 2004).

Indeed Hobo et al found that of 2846 patients, of undergoing secondary interventions, 23% were trans-abdominal as opposed to trans-femoral interventions which accounted for 60% all secondary interventions.

Therefore although EVAR is associated with a frequent requirement for secondary procedures, these are often minor in nature. Furthermore potentially life-threatening problems such as type endoleaks and stent-graft migration may be remedied without the need for graft explantation using endovascular techniques. This lends weight to the assertion by some that since EVAR is an evolving technique, these results reflect early experience with EVAR and are not representative of modern day practice.

Late rupture (confirmed or imminent) is the usual indication for trans-abdominal procedures after EVAR and represents ultimate failure of the stent-graft. Rupture after EVAR is relatively infrequent with rates 0 to 1% per annum at late follow up (Fransen et al., 2003, Pitton et al., 2009), however these procedures are associated with significant mortality that exceed that of open repair even in the elective setting. The main risk factors for secondary rupture are endoleak (type 1 and 3), migration and maximal aneurysm diameter; however the influence of experience must also be taken into account. In a review of aneurysm rupture after EVAR, Schlosser and co-workers showed a dramatic rise in the reported cases of aneurysm rupture between the year 2000 and 2004; a time period correlating with increased uptake of EVAR world-wide. In recent years the incidence of secondary rupture has decreased and may be driven largely by a combination of

improved stent-graft technology and experience, though reporting bias cannot be excluded.

The decision to perform a secondary intervention is based on a balance between the perceived risk to individual patients as a result of problems discovered during surveillance and the intervention being proposed and is largely informed by the experience of individual clinicians. Over the years there has been a tendency to perform fewer secondary interventions as knowledge of the behaviour of stent-grafts and the natural history of issues brought to the fore by surveillance has increased. In 2003 studies reported a median secondary intervention rate of 6.6% per year compared with 4.5% in 2009 case series (Nordon et al., 2009b). Such a reduction reflects both improving technology and a greater willingness of clinicians to some complications conservatively. Indeed some authors are now beginning to advocate secondary intervention directed by patient symptoms (Black et al., 2009).

2.7 Summary

Endovascular aneurysm repair represents a paradigm shift in the management of abdominal aortic aneurysms. Two major large randomised control trials have demonstrated beyond doubt the feasibility and early benefits of EVAR compared with open surgical repair especially in patients perceived to be at high risk from laparotomy. However EVAR has unique complications and whilst it is now clear that some of these complications do not adversely affect the long-term durability of this technique, the fact that the aneurysm sac remains intact poses a continued

and tangible risk of late rupture throughout the patient's lifetime. As such continued surveillance is mandatory in order to identify and correct late failure of endovascular stent-grafts.

Chapter 3

Fenestrated EVAR (FEVAR): A Review

3.1 Introduction

Aortic aneurysm formation primarily results in an increase in the nominal diameter of the aorta. However expansion also occurs in the longitudinal direction and given the confined space within the abdominal cavity, considerable distortion of the abdominal aorta can occur. In concert with short aortic necks and aneurysmal disease affecting both the visceral aorta and iliac arteries, it is not surprising that standard EVAR has been limited to 60% of patients with aneurysms (Wolf et al., 2000). Open repair may be an option in patients unsuitable for standard EVAR; however those that require supra-renal or supra-celiac cross clamping of the aorta in particular are inevitably faced with the prospect of enduring considerable physiological insult. As a result, mortality rates of up to 15.3% (Green et al., 1989) have been reported.

The problems relating to a sub-optimal distal sealing zone have largely been addressed by a combination of experience, improved technique (Oshin et al., 2010b) and advances in stent-graft design (Donas et al., 2011, Torsello et al., 2011). However ensuring adequate seal and fixation in patients with aneurysms in close proximity to or involving the visceral segment of the aorta continued to

be a contraindication to wholly endovascular aneurysm repair until the advent of fenestrated stent-grafts.

These custom-made stent-grafts are manufactured with holes (fenestrations) in the stent-graft fabric designed to align perfectly with the branch vessels of the visceral aorta. This innovation permits the utilisation of the visceral aorta as a proximal sealing zone thereby expanding the application of EVAR to include aneurysms in which the proximal neck is of inadequate length. There are currently several commercially available variations in the design of fenestrated stent-grafts however at the time the studies in this thesis were undertaken, only one manufacturer (Cook Medical) created fenestrated stent-grafts.

3.2 Planning a fenestrated stent-graft

Precise planning is a prerequisite for fenestrated endovascular aneurysm repair (FEVAR). The customised nature of these stent-grafts inevitably results in significant additional expense (typically a fenestrated device costs £25-30,000 compared with circa £6,000 for standard endovascular stent-grafts). Furthermore inaccurate planning may introduce additional complexity to primary deployment. This may ultimately result in failure to correctly align the target vessel ostium and the fenestration with subsequent target vessel loss.

3.2.1 *Image acquisition*

Planning begins with a dataset of images of the aortoiliac anatomy. For the purposes of fenestrated and standard EVAR planning, this consists of high quality computerised tomography (CT) images. First introduced 1960s by the physicist Sir Godferey Hounsfield, computed tomography is an imaging modality that relies on the detection of x-rays that pass through the body. As the x-ray beam penetrates the body, its energy is absorbed or attenuated to varying degrees in a manner proportional to tissue density. Images are therefore created based on the intensity of the x-ray beam that is detected.

Unlike plain x-ray films, the images generated are perpendicular to the long axis of the subject (z axis), achieved by rotating the x-ray tube and detector (gantry) around the patient. Each revolution thus produced an image of a thickness determined by the width of the x-ray beam. Historically CT scanners required each clockwise revolution to be followed by an anti-clockwise revolution in order to avoid entanglement of the power cables. Therefore to scan a region of interest e.g. the abdomen, the patient would be advanced after each revolution by a distance equal to the slice thickness of the scanner resulting in a time consuming process that limited the application of CT.

The introduction of power slip rings eliminated the requirement for alternating clockwise and anti-clockwise rotation resulting in continuous rotation of the gantry whilst the patient is advanced through the scanner. With these modern

scanners, the gantry effectively moves in a helical trajectory around the patient with the advantage of shorter scan times. The scanning speed that may be achieved with helical scanner may also be increased by altering the relationship between table feed, gantry rotation and the width of the x-ray beam (collimation); otherwise known as pitch.

Pitch is given by the equation:

$$\frac{Table\ movement/rotation}{Collimation\ (slice\ thickness)}$$

The gantry rotation and table speed is usually constant therefore pitch is mainly determined altering collimation. Whilst increasing pitch allows quicker scanning of regions of interest, there is a corresponding reduction in image quality since the scanner software interpolates the gaps in the raw helical data acquired to create an image.

3.2.2 *Post-acquisition image processing*

Complex vascular anatomy invariably associated with aneurismal degeneration precludes the measurements of the abdominal aorta using axial CTA images only. One of the advantages of helical CT angiography is the ability to create a volumetric representation of the human body. Each helical CT dataset may be sub-divided in two smaller fragments called voxels. Using mathematical

algorithms these voxels may be reconstructed in order to provide a more accurate representation of the anatomy in question. At present there are two methods for image reconstruction; these are multi planar reconstruction (MPR) semi-automated centre reconstruction.

MPR utilises manual manipulation of the coronal, sagittal and transverse planes to create a composite image in an arbitrary plane defined by the operator. The parameters of the reconstructed images may be set by the operator however the accuracy of the reconstructions is dependent on the voxels themselves. Voxels that are equal in all directions are said to be isotropic and produce the best reconstructions compared with anisotropic voxels which tend to produce distorted images. However the latter is dependent on both the resolution and slice thickness of the scanner. On occasion the course of the abdominal aorta is such that an accurate representation of the anatomy cannot be achieved in a single plane. Under these circumstances the most accurate way to measure vessel separation is the utilisation of semi-automated centre line reconstruction.

Semi-automated centre line reconstruction begins with the selection of start and end points within the region of interest by the operator. Using the start point as an origin (O), the algorithm traverses a small step to point (A) in the direction of the destination point (D). The magnitude of the step is variable depending on the parameters chosen by the operator or the software itself. At point A, a new plane is created perpendicular to the vector OA. The boundary of the aorta is determined within tissue plane by utilising the difference in enhancement in caused by the intravascular contrast. The cross sectional area of the aorta in this

image is assumed to be a polygon and as such its centre may be determined using the technique described by Bashien et al (Bashein G, 1994, Isokangas et al., 2003). Once the centre (C) has been determined, the vector OA is altered to a new vector OC. The process is repeated again this time using point C as the origin. The accumulation of each successive vector thus forms the centre line of flow.

Where vessel separation is important such as fenestrated endovascular aortic aneurysm repair, some commercially available software allows the centre line to be stretched to generate an image in a single plane. This stretch view of the aorta allows visualisation of these side branches of the aorta thereby permitting the measurement of vessel separation.

3.2.3 *Target vessel measurement*

Target vessel measurement begins following the acquisition of adequate images. Since fenestrations are created in the fabric of the stent-graft, knowledge of the circumferential and longitudinal separation of the target vessels is essential. Longitudinal target vessel separation is usually measured first using either cut plane maximum intensity projections (MIP) or semi-automated central line reconstructions. The distance from a fixed point (usually the bottom of the coeliac axis) to the centre of each target vessel is measured and recorded on a planning sheet. Alternatively some individuals prefer to use a schematic diagram to demonstrate the relative positions of the target vessels (Fig 3.1).

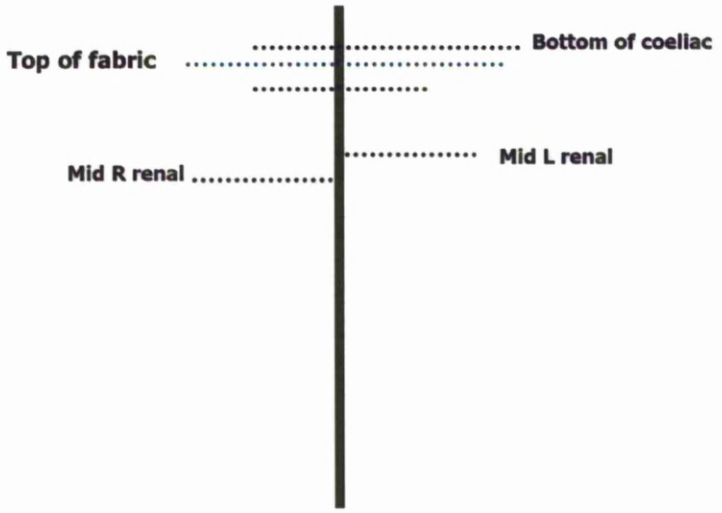

Figure 3.1 Schematic drawing on longitudinal target vessel positions.

Although knowledge of the longitudinal target vessel separation is important, planning the positions of the fenestrations on the stent graft is complicated technical limitations introduced during the fabrication process. The Cook fenestrated stent-graft consists of a series of individual "Z shaped" stents stitched to a Dacron fabric tube. The fenestrations used to maintain visceral artery perfusion are strategically placed into the fabric tube and may be sub-divided into three groups: scallops, small and large fenestrations.

A scallop may be formed to allow the incorporation of one or more vessels at the proximal part of the stent-graft. These fenestrations have a nominal width of 10 mm in order that they can be placed between points of a Gianturco Z-stent and height (length from fabric edge to bottom of scallop) that ranges from 6 to12 mm. Small fenestrations are usually 6 or 8mm in diameter and are frequently reinforced with a nitinol ring. In order to maintain alignment with the intended target vessel, the position of these fenestrations is normally maintained with a

balloon expandable stent. Small fenestrations must be created at least 15 mm inferior to the proximal aspect of the graft, so as to remain free from any crossing struts. Large fenestrations are normally located at least 10 mm below the top of the fabric with a nominal diameter between 8 and 12 mm. They may be traversed by one of the struts of the proximal Gianturco Z-stents of the graft therefore balloon expandable stents are not usually used with these fenestrations. By using a combination of fenestrations and scallops (usually two fenestrations for the renal arteries and a scallop for the superior mesenteric artery) endovascular stent-grafts may be customized to suit individual patient anatomy.

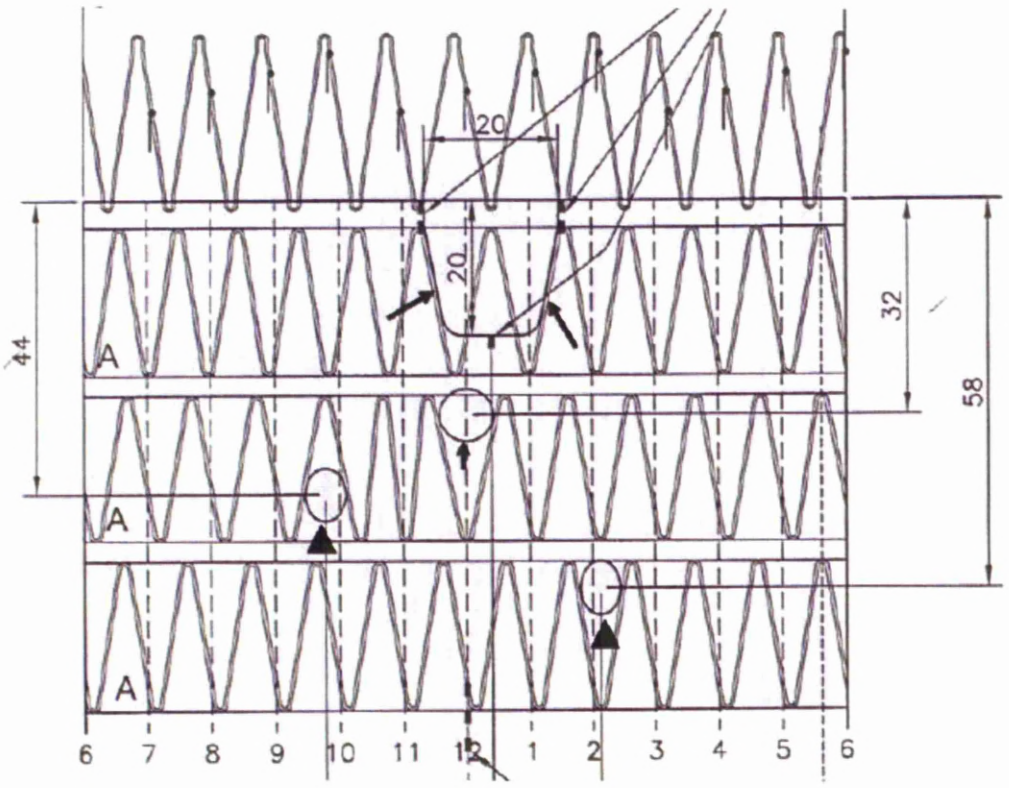

Figure 3.2 Technical limitations of fenestration positioning. Small fenstrations have to be palced in positions whre they will not be traversed by the Gianturco Z-stents and scallops are placed so that their edges may be stitched directly to the struts of the Gianturco Z-stents.

Finally the CTA images are examined in the axial plane. A protractor is used to determine the "clock-face" position of the target vessels (Figure 3.3). The inner aortic diameter is also measured at the level of the fenestration in order to aid correct positioning of the fenestration during fabrication.

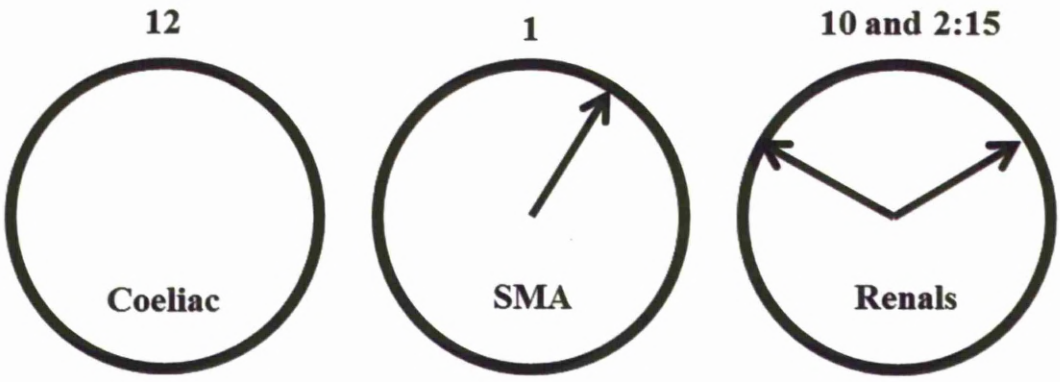

Figure 3.3. Target vessel "clock-face" positioning.

3.3 Deployment of fenestrated stent-grafts: Technique

Advanced endovascular procedures such as the repair of aneurysms using complex or standard stent grafts are ideally performed in operating theatres with fixed fluoroscopy facilities. However such facilities are usually expensive and require considerable changes to the theatre environment. Thus, in practice endovascular procedures often take place in an operating theatre with a mobile image intensifier and "floating" operating table. This allows optimal image generation by manipulating the position of both the patient and the image intensifier.

Fenestrated endovascular aneurysm repair may be performed utilising either general or regional anaesthesia, however the former is preferred by most clinicians since these procedures are usually lengthy. The patient is placed in a supine position and access to the aorta obtained via both femoral arteries either percutaneously or through open dissection through a transverse or oblique groin incision. Prophylactic antibiotics and 5000 international units (IU) unfractionated heparin are then administered intravenously. Further doses of heparin may be given according to the patient's body weight to maintain adequate anticoagulation.

Following this, a stiff guidewire is inserted through one of the femoral vessels (usually the right) into the arch of the aorta under fluoroscopic guidance. In the contralateral femoral vessel, a catheter with multiple side-holes is manoeuvred into the aneurysm. A separate puncture is also made in this vessel through which a large sheath is inserted. This sheath permits the introduction of the target vessel stents and so obviates the need for multiple separate punctures in the contra lateral vessel.

The delivery system is then introduced in to the ipsilateral access artery over the stiff guide wire using the bones of the vertebral column as a guide to the approximate position of the renal vessels. This has the advantage of minimising the volume of contrast medium administered to the patient. The stent-graft is then orientated such that the anterior and posterior stent-graft markers form a cross. Subsequently, the delivery sheath is partially withdrawn to release the stents incorporating the fenestrations whilst a "top cap" continues to constrain

the proximal bare metal sealing stent of the fenestrated stent-graft. At this stage, further corrections to the orientation of the fenestrated stent-graft may be made in order to align the target vessels with the gold markers of their individual fenestrations. The position of the C-arm of the image intensifier is therefore crucial at this point since image foreshortening due to lateral or posterior angulation of the aorta along its course creates a potential risk of error in stent-graft orientation. After achieving a satisfactory position, the delivery sheath is partially withdrawn and the stent-graft cannulated with a multi-purpose angulated catheter inserted in the large access sheath in the contralateral femoral artery. At this stage, a small degree of rotational freedom is still possible because the stent-graft may be partially constrained by "diameter reducing ties". These are essentially loops of prolene suture that are held together by a steel rod at the posterior of the graft that prevent complete expansion of the Gianturco Z-stent so that some rotational freedom is possible to aid cannulation.

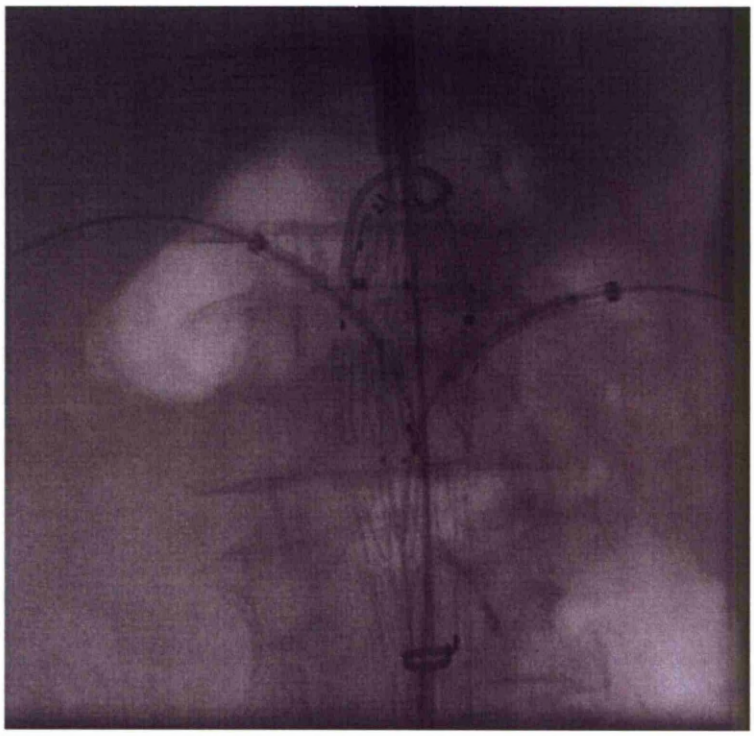

Figure 3.4 Partial deployment of fenestrated stent-graft.

Access to each target vessel is achieved by selective catheterisation of each fenestration and infusing short bursts of radio-opaque contrast to delineate the path of the intended target vessel. In addition, the C-arm is repositioned in order to optimise the images showing the relationship between the ostium of the target vessel and the gold markers of the fenestration. A soft guidewire is manoeuvred into the vessel, over which the catheter is advanced. The soft guidewire is exchanged for a slightly stiffer guide wire and the catheter replaced with a sheath containing the stent that will be used to maintain the fenestration's position relative to the target vessel. Once all target vessels have been cannulated, the diameter reducing ties and device top cap are released to complete the deployment of the proximal section of the fenestrated stent-graft. After deployment of the main body of the stent-graft, the stents in the visceral vessels

are deployed such that approximately a third of the stent protrudes into the lumen of the main body to allow flaring of this portion of the stent. A variety of renal stents may be used to secure the fenestrations. Historically covered stents were reserved for use in only in situations where apposition between the stent graft fabric and native aorta was expected to be poor and bare stents selected when satisfactory seal was expected. However there is now emerging evidence that covered stents may protect against neointimal hyperplasia seen in bare metal stents thereby improving long-term target vessel patency (Mohabbat et al., 2009).

The bifurcated distal component of the fenestrated stent graft is then deployed using the stiff wire initially placed in the arch of the aorta (now in the lumen of the fenestrated proximal body) as a guide. After deployment of the iliac limbs, all stiff wires are removed and a final completion angiogram is performed to identify any endoleaks and ensure adequate placement of the stent-graft and perfusion of target vessels.

3.4 Outcomes of Fenestrated EVAR

Endovascular aneurysm repair is an accepted alternative to open surgical repair, however the role of fenestrated EVAR has yet to be defined. As in standard EVAR, there is a potential risk of complications such as migration, endoleak and stent-graft thrombosis. Furthermore the incorporation of fenestrations in the stent-graft fabric provides a focus for potential problems relating to target vessel patency. In order to be a viable alternative to juxta renal aneurysm repair, FEVAR must demonstrate safety, efficacy and long-term durability however to date there is no randomised controlled trial examining the efficacy of FEVAR. Therefore the best evidence available is via pooled results from the individual cohort series.

3.4.1 *Methods*

A literature search for related articles was performed of the MEDLINE and Embase medical databases for articles published between 1999 and 2009. Keywords such as "fenestrated endovascular aneurysm repair", "fenestrated stent-graft", "para-renal aortic aneurysm" and "juxta-renal aneurysm" were used to identify potentially relevant articles. In addition a further search was conducted using a combination of the following Medical Subject Headings (MeSH) terms: Zenith; juxta-renal AAA; para-renal AAA; Fenestrated stent-graft. Eligible articles were English language peer reviewed studies describing the use and clinical outcomes of FEVAR. Exclusion criteria were systematic reviews, case reports, articles pertaining to or describing the technique of

FEVAR and studies consisting of fewer than 10 subjects were excluded from analysis. A flow diagram of the literature search is given in Figure 3.5 and a summary of the articles used in this review is given in Table 3.5. The following data was extracted from each study; author, year of study, primary technical success, configuration of target vessels, 30 day and later mortality, target vessel loss, median follow up and secondary intervention or complications. Aneurysm related mortality was defined as 1) a death occurring within 30-days of the procedure, 2) death within 30 days of any intervention intended to maintain exclusion of the aneurysm or 3) death due to aneurysm rupture (UK EVAR trial 1 participants, 2005) and renal impairment was defined as a rise in serum creatinine to 2 mg/dl or a 30% or a rise in creatinine following FEVAR. The outcome data for each study was pooled and the weighted mean value with confidence intervals derived.

3.4.2 *Results*

3.4.2.1 *Early and late mortality*

All studies reported both perioperative (30-day) and late mortality. Overall peri-operative mortality after fenestrated EVAR was 10/509 (weighted proportion 1.3%, 95% CI 0.6 to 2.8%). Causes of mortality in the early post-operative period are given in Table 3.6. Sixty-nine patients (weighted proportion 8.4%, 95% CI 6 to 11.2%) died in early follow up (median 20 months). Of these nine deaths (14%, 95% CI 6.7 to 23.9%) were aneurysm related.

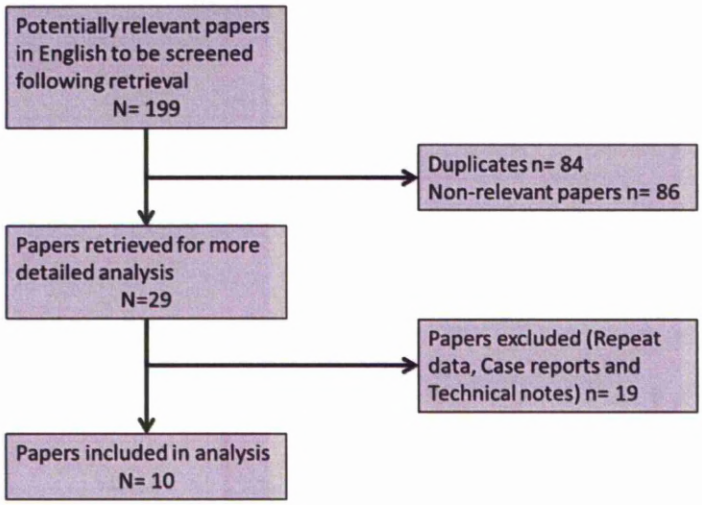

Figure 3.5 Chart of literature search for FEVAR papers

Cause of Death	Number
Bowel infarction	**3**
SMA loss (n = 2)	
IMA loss (n = 1)	
Myocardial Infarction	**3**
Aspiration Pneumonia	**1**
Multi-organ Failure	**3**
Significant bleeding (n = 2)	
Conversion to open surgery (n = 1)	

Table 3.6 Published 30-day mortality following fenestrated endovascular aneurysm repair

3.4.2.2 *Primary technical success and target vessel patency*

All publications reported primary technical success which ranged from 91 to 100%. In total 1189/1223 target vessels were preserved after the initial procedure, equivalent to an average technical success rate of 97% (95% CI 96 to 98%). There was a weak but positive correlation between technical success and mid-point of the published study however this was not statistically significant (r 0.28, p = 0.21), Figure 3.7. After median follow up of 20 months, 51 (4%, 95% CI 3 to 5%) target vessels had been lost. The majority of these target vessels (n = 40, 78%) were renal arteries. Of the remainder, 6 (11%) were SMAs, 1 (2%) a celiac artery and in 4 cases (8%) the target vessels was unspecified. Most occlusions occurred within the first year of follow up.

Author	Year	Country	Patients (n)	Target Vessels (n)	Weight
Anderson	2001	Australia	13	33	0.03
Halak	2006	Australia	17	35	0.03
Muhs	2006	Netherlands	38	87	0.07
O'Neill	2006	USA	119	302	0.25
Semmens	2006	Australia	58	116	0.09
Zeigler	2007	Germany	63	122	0.1
Scurr	2008	UK	45	117	0.1
Bicknell	2009	UK	15	40	0.03
Kirtsmondsun	2009	Sweden	54	134	0.11
Haulon	2009	France	87	237	0.19
			509	**1223**	

Table 3.6 Summary of published literature

As a function of time (figure 3.8), there was no significant correlation between the proportion of target vessels lost and mid-point of the publication (r, -0.17, p = 0.31) however there was a significant correlation between the number of target vessels in each individual study and proportion of target vessels lost; r, 0.58 and p = 0.03 (figure 3.9).

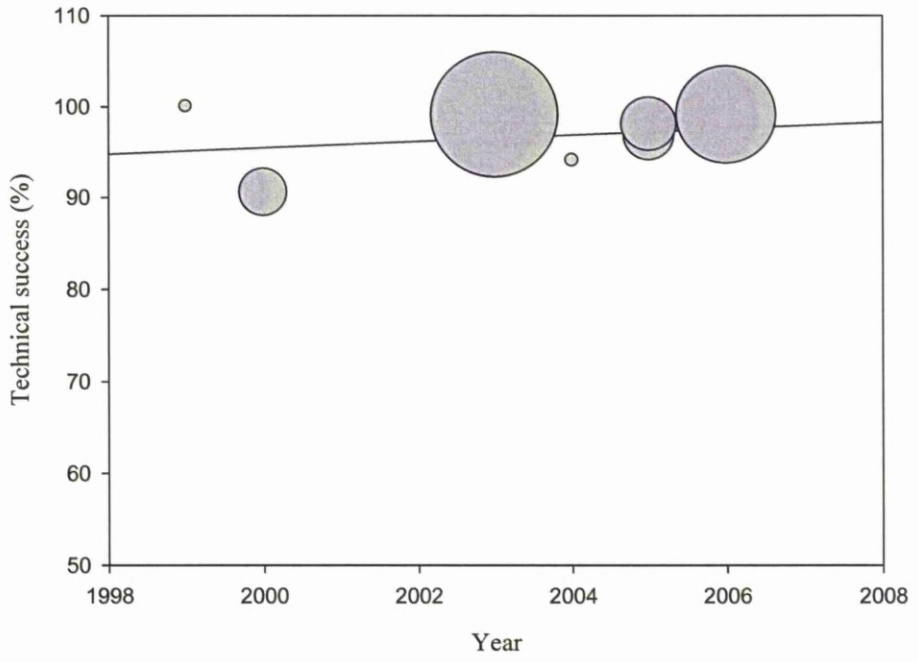

Figure 3.8 Trend of technical success of FEVAR as a function if time. The size of each circle is proportional to the size of each study on the analysis.

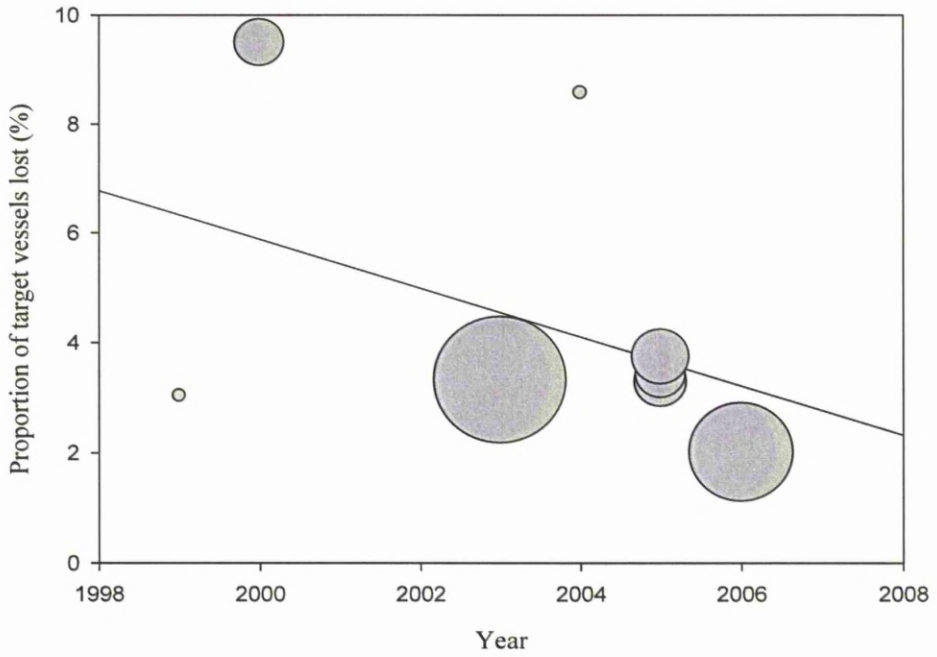

Figure 3.9 Target vessel loss from published literature as a function of time

3.4.2.3 *Renal dysfunction after FEVAR*

Nine studies reported early transient renal dysfunction following FEVAR. This was defined as an increase in serum creatinine by >2 mg/dl or a deterioration of pre-operative baseline renal function by >30%. Of these, 80/492 patients (16.22%, CI 13.2 to 19.7%) developed renal dysfunction. Nine studies reported the incidence of permanent dialysis dependence as a direct result of FEVAR. Permanent dialysis occurred in 6/451 patients (1.55 %, CI 0.5 to 2.9%).

3.4.2.4 *Endoleak*

All case series reported the number of type I endoleaks observed after the index procedure. Twenty-four type I endoleaks were observed in 509 patients (4.8%,

95% CI 3.1 to 6.9%). The most common management strategy for these endoleaks was the use of additional balloon expandable (Palmaz) stents. The modular design of the fenestrated stent-graft was a predisposing factor for the development of type III endoleaks. These occurred between the proximal and distal sections of the main body of the stent-graft or between the target vessel stent and the proximal main body as a result of dislocation. Overall, 12 type III endoleaks were reported (2.5% CI, 1.3 to 4.1%). These were managed successfully using additional balloon expandable stents.

3.4.2.5 *Secondary intervention*

All studies reported secondary intervention following FEVAR. This is summarised in Table 3.10. The cumulative secondary intervention rate at 20 months is 14.8% (95% CI 11.9 to 18%); the majority of which were performed using endoluminal techniques.

Reason for secondary intervention	**n**
Target vessel related	**14**
Type III endoleak (5)	
Stenosis (7)	
Stent fracture (2)	
Modular distraction	**10**
Type III endoleak (7)	
Impending type III endoleak (3)	
Sealing zone	**24**
Proximal type 1 endoleak (21)	
Distal type 1 endoleak (3)	
Access site	**7**
Groin (4)	
Brachial artery (3)	
Limb occlusion	**2**
Type II endoleak	**11**
Retroperitoneal haematoma	**2**
Limb extension	**2**
Limb stenosis	**1**
Conversion	**2**
Rupture (1)	
Aortic Occlusion (1)	
	75

Table 3.10 Secondary intervention after fenestrated endovascular aneurysm repair

Outcomes	Pooled results (%)	95% CI
Peri-operative mortality	1.3	0.6 to 2.8
Overall mortality	8.4	6 to 11.2
Technical success	97	96 to 98
Type 1 endoleak	1.8	0 to 3.3
Permanent dialysis	1.5	0.5 to 2.9
Target vessel loss	4.2	3.1 to 5.4
Secondary intervention	14.8	11.9 to 18

Table 3.5- Summary of outcomes for FEVAR

3.5 Discussion

The decision to offer EVAR as a therapeutic option is a careful balance between the perceived risk of aneurysm rupture, life expectancy of the patient and the estimated risk of complications and death from intervention. Furthermore consideration for endovascular repair must also involve a detailed appraisal of aneurysm morphology. Ideally a neck length of at least 10 to 15mm that is relatively straight and free from thrombus forms the optimal conditions for treatment with a standard endograft. However a significant proportion of patients do not fulfil these criteria and as a result the most frequent anatomical restriction

to the use of EVAR is an inadequate infra-renal aortic neck. For this reason, open repair of juxtarenal and para-renal aneurysms is the current gold standard for intervention whilst the efficacy of FEVAR is evaluated.

The short-term outcomes of FEVAR clearly demonstrate the technical feasibility of this technique. Perioperative mortality and technical success are comparable with the results of both institutional case series and the major EVAR trials. However when attempting to compare the results of FEVAR with open surgical repair for juxtarenal and para-renal aneurysms, bias as a result patient selection is an important consideration.

The combination of extensive visceral mobilisation to provide adequate exposure of the abdominal aorta and either supra-renal or supra-visceral aortic cross-clamping places the patient at increased risk of cardiopulmonary and renal complications (Sarac et al., 2002b). As such, open repair of these aneurysms is associated with a higher mortality risk than that of open infra-renal aneurysm repair (7% vs. 3% respectively) (Knott et al., 2008, Costin et al., 2006, Ockert et al., 2007). Therefore the cohort of patients undergoing open repair is likely to be composed of patients best able to tolerate the physiological insult associated with such major surgery.

The pooled perioperative mortality for open surgical repair ranges between 2.9% and 3.6% (Jongkind et al., 2010, Nordon et al., 2009a) and at first glance appears higher than the pooled perioperative mortality (1.4%) of FEVAR calculated in this study. Furthermore at a median follow up of 20 months, the crude all-cause mortality rate of 8.4 % (CI 6 to 11.2%) is superior to mid-term results of the UK EVAR trial 1 study and the results of open juxtarenal aneurysm repair (Faggioli et al., 1998b). Indeed in their systematic review, Nordon et al have also demonstrated a significant but marginal reduction in mortality in favour of FEVAR. However these findings must be interpreted with caution due to the lack of standardisation amongst the selected studies. The case series from which these data were extracted frequently report that the patients selected for FEVAR are those with a higher than average risk of mortality. The morphological and physiological basis for these assertions is unclear and as such the evidence supporting the superiority of FEVAR over open repair is controversial. Indeed the mid-term results of FEVAR potentially reflects outcomes in patients that are excellent surgical candidates in which case the perceived benefit of FEVAR over open surgery may be exaggerated. Therefore direct comparison between the clinical outcomes of endovascular repair and open surgery out with the conditions of a clinical trial is difficult and potentially misleading.

Overall, the rate of secondary intervention following successful deployment of a fenestrated stent-graft is comparable to the reported secondary intervention rate after standard EVAR. The presence of a type 1 endoleak was the most common reason for secondary interventions after FEVAR and is often associated with angulated aortic necks. The presence of an endoleak represents a failure to

completely exclude the aneurysm from systemic circulation with a potential risk of subsequent rupture. Indeed one case of rupture after FEVAR has been reported (Ziegler et al., 2007) as a result of a type 1 endoleak. Such endoleaks potentially present a challenging post-operative complication as attempts to correct them could compromise target vessel patency, however in practice the majority of these endoleaks were rectified using giant Palmaz stents without sequelae to the target vessels stents.

In addition, to type 1 endoleaks, the discovery of type 3 endoleaks are also a significant cause for concern during follow up. Modular stent-grafts (proximal main body containing fenestrations, distal main body incorporating stent-graft bifurcation and two iliac limbs) are now used instead of the standard three-piece system (single main body and two iliac limbs) initially pioneered by Anderson and co-workers (Anderson et al., 2001). A significant component of the caudal migratory force is generated when pulsatile blood flow in the aorta encounters the flow divider of an endovascular stent-graft (Mohan et al., 2002). With modular stent-grafts, this force acts at the interface between the two main body grafts resulting in component separation whereas in a three-piece system, the target vessel stents may be crushed since they are in effect resisting the migratory force generated at the flow divider. Component separation in this fashion accounts for the majority of type 3 endoleaks after FEVAR although some are also the result of target vessel stent separation from the proximal main body. As with type 1 endoleaks, this complication may be managed successfully with the use of ancillary stents.

Although the majority of complications arising as a consequence of FEVAR have potential to be technically demanding, secondary intervention is often a trans-femoral procedure thereby obviating the requirement for general anaesthesia. Given the complex nature of these stent-grafts and the potential consequences of target vessel loss, early recognition of these complications is reliant upon a robust surveillance protocol. Currently there is a trend towards reducing the burden of ionising radiation after EVAR by utilising alternative imaging modalities surveillance (Harrison et al., 2011, Schmieder et al., 2009b, Dias et al., 2009b). However FEVAR requires more frequent surveillance intervals than EVAR and the use of multiple imaging modalities in order to adequately identify impending threats to target vessel patency. This has implications for both the cost effectiveness of FEVAR and the risk of developing malignancies as a consequence of surveillance, however without medium and long-term outcome data, this situation is unlikely to change.

If initial technical success (cannulation of all intended target vessels) determines the feasibility of fenestrated EVAR, subsequent target vessel patency is a surrogate measure of durability. The majority of fenestrations are incorporated into the fabric of the stent-graft to maintain renal perfusion. Since dependence upon renal dialysis significantly reduces life expectancy, maintenance of renal artery patency is an important clinical end-point. During open repair, prolonged ischaemia during cross-clamping may result in irreversible ischaemia and subsequent dialysis. However the risk of such an event is largely limited to intra-operative period whereas following FEVAR, threat to target vessel patency appears to be a life-long risk.

Target vessels loss appears to be most prevalent in the first post-operative year and occur for a variety of reasons. Indeed in a study by Greenberg et al, (Mohabbat et al., 2009), no further target vessel loss was observed between the first year and a maximum follow up period of 48 months. Over time data has emerged supporting the use of ancillary stents to maintain alignment between the target vessel ostia and fenestration thereby reducing the risk of shuttering and subsequent occlusion. In addition, the type of ancillary stent used also appears to be important. It has been shown that the use of covered stents may improve target vessel patency by reducing the risk of in-stent stenosis as a result of intimal hyperplasia (Mohabbat et al., 2009), whilst a "closed cell" stent design may prevent fabric encroachment between interstices (Scurr et al., 2008a). The rate of target vessel loss reported in consecutive case series has not improved significantly over time despite high technical success rate. This may represent an inevitable post-operative complication of FEVAR however, clinically significant sequelae following target vessel loss appears to be a relatively infrequent occurrence.

Approximately 1.5% of patients undergoing FEVAR require permanent dialysis as a direct consequence of this procedure compared with 3.3% after open juxtarenal aneurysm repair however this difference may not be statistically significant (Nordon et al., 2009a). A possible explanation for this difference may be the potential mechanism of renal dysfunction. During open repair, ischaemia or embolization as a result of cross-clamping could potentially affect both kidneys whereas in FEVAR intraoperative problems arising from catheter manipulation or fenestration misalignment would likely affect one and not both

target vessels. In such situations, there may be deterioration in renal function without the development of new onset dialysis.

Potentially fenestrated endovascular aneurysm repair may offer superior outcomes compared with open surgery but this technique is hampered by several limitations. First the delivery system for these stent-grafts is large. As such small access vessels may limit its use in certain patients. Furthermore rotational freedom is essential for intra-operative alignment between the fenestrations and target vessel ostia. Indeed failure to correctly align the fenestrations as a result of iliac calcification, tortuosity and the presence of an infra-renal surgical graft have all been directly responsible for acute target vessel loss. Finally, the highly customised nature of these stent-grafts introduces a delay of at least 6 weeks. As such in contrast to standard infra-renal stent-grafts, there appears to be no role at present for FEVAR in emergent cases.

3.6 Summary

In the short to medium-term, the results of fenestrated endovascular aneurysm repair are encouraging and this technique may yet prove to be a good alternative to open juxtarenal aneurysm repair. As with standard EVAR, questions still remain unanswered regarding the durability of FEVAR, in particular the fate of target vessels. Ideally, a randomised trial comparing clinical outcomes between open surgery FEVAR is desirable however this does not appear forthcoming. Evaluation of the efficacy and durability of FEVAR will thus be reliant upon registry data or pooled analysis of case series reports. However if meaningful comparisons are to be drawn between these treatment options, it is essential that specific reporting standards (Boyle et al 2011) are met.

Chapter 4

Rationale for subsequent studies

The main objective of fenestrated endovascular aneurysm repair is the isolation of juxta-renal abdominal aortic aneurysms from systemic circulation whilst maintaining perfusion to the gut and kidneys. Although technically feasible, FEVAR is associated with a small but appreciable risk of target vessel occlusion. However despite the fact that fenestrated stent-grafts are customized for individual patients, the extent to which planning errors contribute to these serious and potentially catastrophic adverse events remains poorly understood.

The observation in almost all FEVAR series published to date that the majority of target vessel occlusions occur within the first year of follow up lead to a core laboratory analysis of the modes and mechanisms of target vessel loss. This was based on a standardized assessment protocol of threatened or confirmed target vessel loss using follow up data from the Liverpool Regional Vascular Unit EVAR database (Chapter 5).

Confirmation that both potential planning errors and unforeseen interaction between the stent-graft and native anatomy stent graft and native anatomy were a frequent cause of target vessel loss prompted further investigation into the anatomical assessment of aneurysms being considered for repair with fenestrated

stent-grafts. Particular attention was paid to the different planning strategies and image manipulation software utilized in the planning stage of FEVAR. In addition a qualitative and quantitative assessment of intra and inter-observer variability of target vessel measurement was performed (Chapter 6).

The finding that a certain degree of intra-observer variability in target vessel measurement exists was not surprising; however this variability was compounded by frequent and often significant inter-observer disagreement in the position of target vessels. Neither the image processing software nor measurement technique significantly contributed to this technique leading to the hypothesis that the perception of anatomical landmarks varies between individuals resulting in a degree of subjectivity in image assessment. Since individual patient anatomy could not be measured directly to determine which anatomical features resulted in increased variability between observers, phantoms depicting human aortas were created (Chapter 7).

For practical reasons an exhaustive investigation of all the possible variants of human aortic anatomy was not possible. The investigation so far had suggested a potential relationship between specific anatomical characteristics and the intra and inter-observer variability of target vessel measurements for fenestrated stent-graft design. However the clinical significance of this finding was unclear since statistically significant results may be of little clinical importance. The physical properties and tolerance of fenestrated stent-grafts was therefore studied to contextualize the subjectivity of the target vessel measurement (Chapter 8).

Currently fenestrated stent-grafts are designed as far as possible to exactly fit individual patient anatomy. However the observation that fenestrated stent-grafts possess a surprising degree of flexibility coupled with the potential for inter-observer variability when measuring target vessel separation appears to challenge this principle. This lead to the hypothesis that the integrity of the target vessel stents is not necessarily challenged by when there is discrepancy between native anatomy and fenestrated stent-grafts. A study was thus designed to elucidate the magnitude of the forces acting upon target vessel stents when mismatch occurs (Chapter 9).

Chapter 5

Target vessel loss after FEVAR

5.1 Introduction

It is estimated that approximately 60% of patients are suitable for endovascular aneurysm repair using a standard device. The utility of standard devices however is predominantly limited by aortic morphology and other anatomical features of patients considered for repair. Durable endovascular repair is reliant on seal and fixation of the device, however in the case of juxta and para-renal aneurysms the infra renal neck is of insufficient length to act as a sealing zone precluding standard endovascular aneurysm repair.

Endovascular repair of juxta-renal aneurysms therefore require devices with fabric extending above the renal artery origins and consisting strategically placed windows to target renal and visceral arteries. As such in addition to survival, target vessel patency is an important marker of outcome. In the mid-term, pooled results from published series report 423/460 target vessels remain patent (92%, CI 90.3-94.8). Although this represents a small proportion of target vessels, the potential consequence of target vessel loss is significant. Although some authors have commented on the potential reasons for target vessel loss little is known about the aetiology of target vessel loss after FEVAR.

The aim of this study therefore was to elucidate modes and possible mechanisms of actual or threatened loss of target vessel patency.

5.2 Material and Methods

5.2.1 *Patients*

The records of 65 consecutive patients in whom a fenestrated endovascular aneurysm repair was performed between 2004 and 2009 were reviewed. All patients were considered high risk for open surgery because of their co-morbidities or a hostile abdomen as a result of previous abdominal surgery. Each fenestrated stent-graft was deployed according to a standard method which has been previously described (Chapter 3).

A target vessel was defined as one in which a scallop or fenestration had been incorporated into the stent-graft design in order to maintain perfusion. Target vessels were confirmed as lost in cases where occlusion occurred either intra-operatively or during subsequent follow up. Threat to target vessel patency was defined in two ways; cases in which sub-optimal alignment of the stent-graft resulted in encroachment of the stent-graft fabric on the ostia of target vessels with or without clinical sequelae or patients in whom secondary intervention was required in order to maintain end organ perfusion.

5.2.2 *Follow-up protocol*

Follow-up imaging consisted of 3 imaging modalities; computed tomography angiogram (CTA), renal and mesenteric duplex scans (DUS) and plain abdominal radiographs (AXR). Surveillance imaging was conducted at discharge, 1 month, 6 months, 12 months and annually thereafter. In addition at each surveillance visit, routine laboratory studies were performed to monitor renal function by calculating the estimated glomerular filtration rate (eGFR) using the Modification of Diet in Renal Disease (MDRD) formula.

5.2.3 *Analysis*

A core-lab was created for analysis of the pre and post-operative images of patients in whom confirmed or threatened target vessel loss had occurred and conducted by an investigative panel (*Olufemi A Oshin*- Research fellow; *John A Brennan*- Consultant Vascular Surgeon; *Richard G McWilliams*- Consultant Interventional Radiologists and *Srinivasa R Vallabhaneni*- Consultant Vascular Surgeon). In order to obtain optimum visualization of each target vessel and identify the mode of target vessel threat, follow up CTA images were reconstructed and assessed by multi-planar reconstruction (MPR), three-dimensional (3D), and centreline of flow (CLF) techniques using 3D workstations Leonardo (Siemens Healthcare, Erlagen, Germany) and Aquarius (Terarecon, San Mateo, California, USA).

The operation notes were consulted in order to determine the potential mechanism of target vessel threat/loss. In cases where the mechanism of target

vessel loss was not obvious or where no intra-operative difficulty was reported, the spatial relationship between target vessels was measured in order to create a new stent-graft plan. This was compared to the initial stent-graft design in order to determine if a planning error was responsible for target vessel loss/threat.

5.3 Results

Fenestrations were created for a total of 179 target vessels in 65 patients treated with the Zenith (Cook Inc, Bloomington, IN, USA) abdominal aortic aneurysm (AAA) fenestrated endograft. The median follow-up was 39 months (range 0 to 86). Primary technical success was achieved in 97% (63/65) of patients and 30-day mortality was 1.5% (1/65).). Demographic data for the patient cohort is given in Table 5.1 and stent-graft configuration is summarized in Table 5.2.

Target vessel threat/ loss was identified in 15% of patients (n= 10). All problems relating to target vessel patency were identified within the first year of follow-up. Four target vessel occlusions occurred in 3 patients and in the remaining patients, target vessel patency was threatened in a total of 10 vessels. Freedom from occlusion was 95.5% at 83 months follow up. Secondary interventions were undertaken in three patients in order to maintain patency or revascularise threatened target vessels. Freedom from target vessel threat was 84.2% at 86 months follow up (Figure 5.3) and all target vessel problems were identified within the first 12 months of follow up.

Co-morbidities	
Gender M:F	58:7
Median age (range)	74 (54 – 87)
Median AAA diameter mm (range)	64 (55 – 92)
Ischaemic Heart Disease	38
Chronic Renal Failure	10
Diabetes mellitus	6
Congestive Cardiac Failure	4
Hypertension	32
Smoker	
Ex	40
Current	11
Never	14
ASA	
1	2
2	12
3	47
4	4
Previous aortic surgery	4
Median operation time (range)	

Table 5.1 Cohort demographic data

Mesenteric fenestrations	**Renal fenestrations**			
	0	1	2	3
None	0	4	3	0
SMA	0	2	45	1
SMA + Coeliac	0	0	10	0

Table 5.2 Distribution of vessels incorporated in fenestrated stent-grafts

Identified modes include distortion of the target vessel stent, partial shuttering of target vessel ostia and inadequate expansion of scallop fenestration. The possible mechanisms relate to stent-graft planning (n=3), primary deployment (n=5), unforeseen interaction between stent-graft and native aorta (n=2) and postoperative changes (n=4), with more than one mechanism at work in some.

A detailed analysis of the modes and mechanisms of target vessel threat/loss for each patient follows and is summarized in Table 5.14.

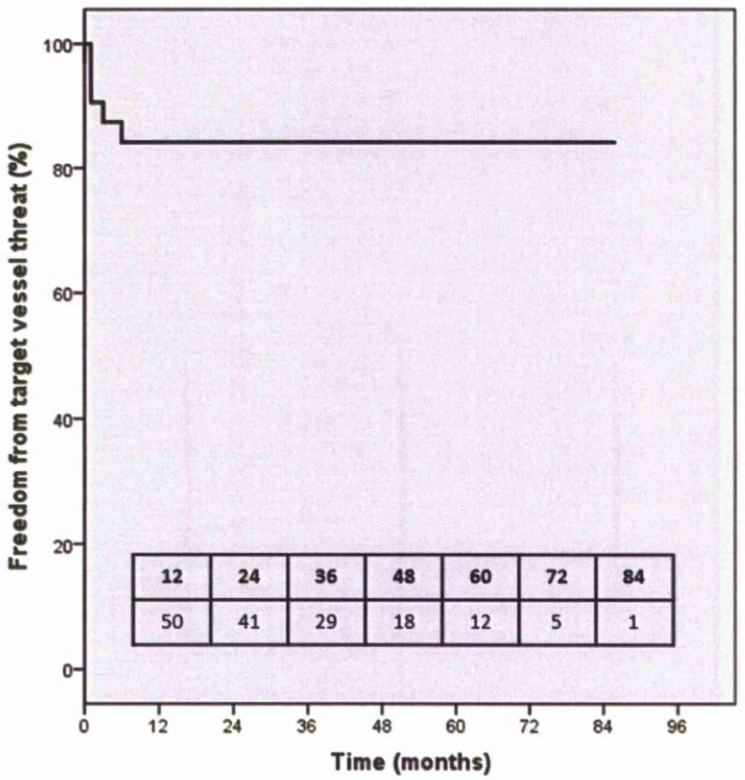

Figure 5.3 Freedom from target vessel threat

Patient 1 - Target vessel threat

This 84 year-old patient presented with a 6.4 cm juxtarenal aneurysm. A conical infra-renal neck and angulation of 80 degrees precluded endovascular repair with a conventional stent-graft. In February 2006, he underwent FEVAR with a stent-graft incorporating 8mm fenestrations for both the right renal artery and the SMA. The coeliac axis was occluded as was the left renal artery. Both fenestrations were successfully cannulated. The right renal was treated with an 8mm x 38mm Atrium stent (Atrium Medical, Rendementsweg, Netherlands) and the SMA with a 9mm x 27mm AVE stent (Medtronic, Minneapolis, USA). Completion angiography showed filling of all target vessels and no endoleak.

Post-operative abdominal pain prompted a mesenteric angiogram 15 days after the initial procedure. This revealed an SMA stenosis with a significant gradient as a result of indentation of the SMA stent from the nitinol ring of the fenestration (Figure 5.4). Angioplasty of the stenosis was attempted to correct this problem, but this was unsuccessful as 6 months later, the patient underwent iliac artery to SMA bypass to preserve flow to the SMA.

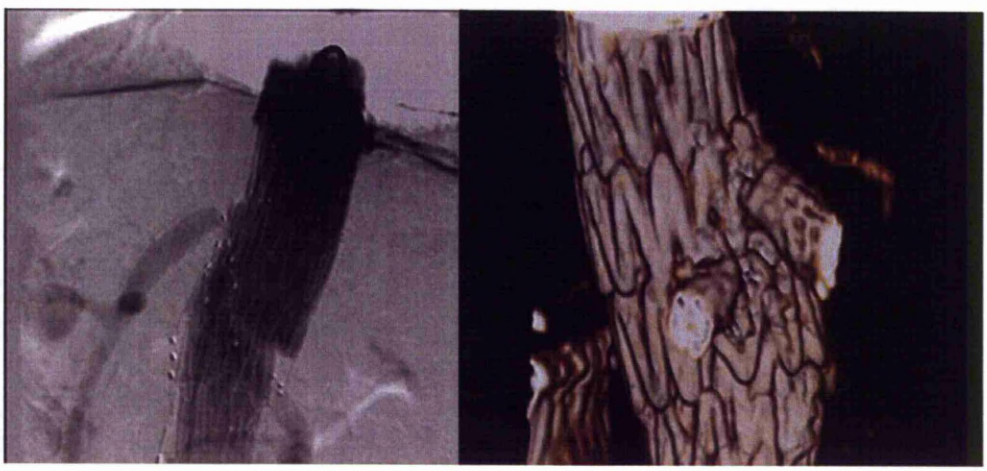

Figure 5.4 SMA stenosis as a result of caudal migration

Core-Lab analysis confirmed SMA stenosis as a result of proximal migration of the graft fabric between the interstices of the SMA stent. Analysis of the fenestrated stent-graft design revealed that the way in which the stent-graft would conform to the native aorta graft was considered in the planning process. However this was a subjective interpretation and it potentially lead to underestimation of inter-vessel separation. This is in combination with cephalad migration between the open cells of the SMA stent lead to target vessel threat in

the form of partial shuttering and stenosis. In this situation target vessel threat was the result of a possible planning error and unforeseen stent-graft/ aorta interaction.

Patient 2 - Target vessel threatened

This 66 year old patient with a 68 mm juxta renal aneurysm was treated with a fenestrated stent-graft incorporating 2 fenestrations for the renal arteries and a scallop for the SMA. Both renal fenestrations were stented with 7 x 22 mm Atrium stents (Atrium Medical, Rendementsweg, Netherlands). Completion angiography showed good filling of the renal arteries, however when the position of the SMA was checked with a lateral view, the scallop was mainly below the SMA. On subsequent surveillance imaging at one month, the SMA scallop was malpositioned to the left by 15^0 (equivalent to 30 minutes by clock-face position) (Figure 5.5). Since the scallop was deployed below the level of the target vessel, there was no compromise of gut perfusion.

As part of the core-lab analysis, the fenestrated stent-graft was re-planned using the patient's original CTA data-set. The new plan was identical to the original design and as such, planning error was unlikely to be responsible for target vessel threat in this patient.

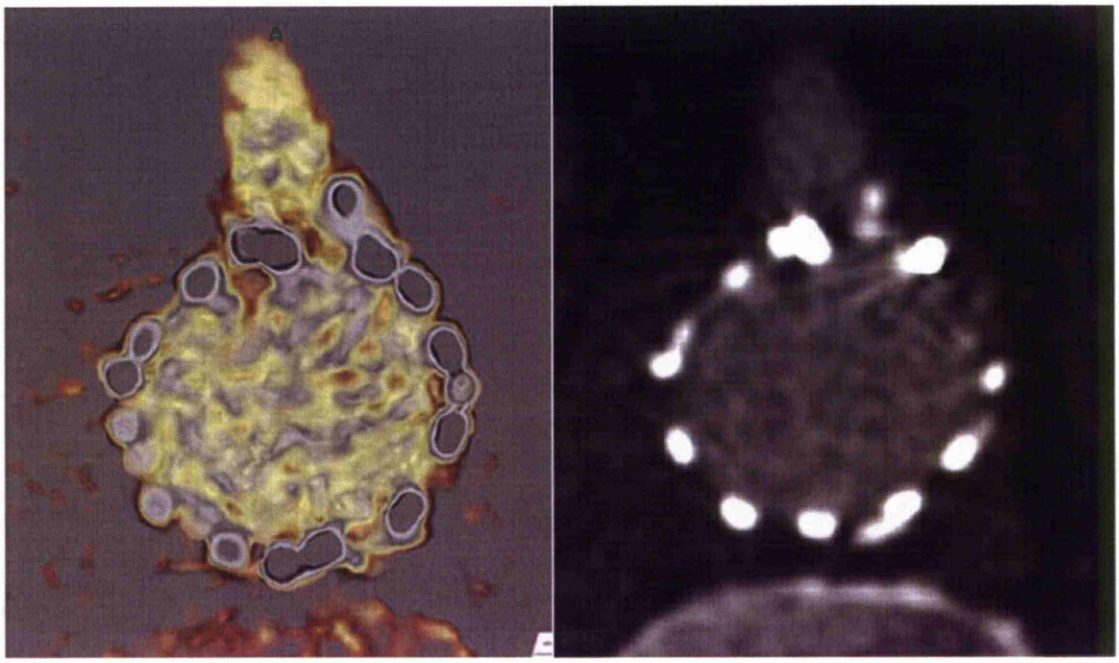

Figure 5.5 Malpositioning of SMA scallop by 30 minutes. Fortunately, the scallop was located below the target vessel and there was no clinical significant complication.

Angulation at the neck of the aneurysm and significant variation in the diameter of the proximal sealing zone that would have resulted in variation in oversize throughout the fenestrated segment of the stent-graft was noted upon analysis of neck morphology. In this patient, the aorta varied from 24 mm at the level of the renal artery to 30 mm at the level of the SMA. These anatomical features in combination could potentially hinder deployment of the stent-graft however no rotational difficulty was reported in the operation notes. The core-lab panel therefore concluded that target vessel threat was a result of unforeseen stent-graft/native aorta interaction caused by the introduction of the stent-graft.

Patient 3 - Target vessel threatened

This 64 year old patient with a 60 mm aortic aneurysm unsuitable for standard EVAR was repaired with a fenestrated stent-graft incorporating two renal fenestrations and a scallop for the SMA. Two Palmaz Genesis stents (Cordis, Waterloo, Belgium) were deployed in to both renal arteries. No intraoperative problems were reported but at 3 months, kinking of the right renal artery stent was noted. There was no compromise of renal function.

Core-lab analysis of this patient's records revealed no obvious planning issues and since no intra-operative difficulties were recorded, the panel concluded that target vessel threat was most likely due to unforeseen stent-graft aorta interaction leading to distortion of the right renal stent.

Patient 4 - Target vessel lost

This 65 year-old patient presented with an aneurysm measuring 55 mm in diameter and an infra-renal neck length of 10 mm. A fenestrated stent-graft was utilised in order to extend the proximal sealing zone. The left renal arterial anatomy was complex with 3 renal arterial branches, therefore the lowermost renal artery was sacrificed and a single scallop created for the main left renal artery.

Following alignment of the scallop, a wire was placed in the main left renal artery prior to stenting. Unfortunately this wire was lost and after it was reintroduced, it became apparent that the stent would not fully expand. Check angiography revealed that the wire had entered the smaller of the two remaining

renal vessels. Thus a 5 mm stent was inflated in an artery with approximate diameter of 3 mm. This resulted in occlusion of the accessory renal artery at 1 month however the intended target vessel remains patent.

The pre-operative images showed that the left main and accessory renal arteries originated from the aorta in the same axial plane. Core-lab analysis of this case therefore concluded that when the guide wire was being re-introduced, a superimposed image of the two left renal arteries (Figure 5.6) resulted in placement of the guide wire in the wrong renal artery. The mode of target vessel loss in this patient was intraoperative difficulty.

Patient 5 - Target vessel threatened

This 80 year-old patient presented with a 73 mm aortic aneurysm that was unsuitable for standard EVAR because of a short conical infra-renal aortic neck. He underwent FEVAR with an endograft incorporating two small (6 mm) fenestrations and a single scallop for the SMA. Correct orientation was achieved with difficulty due to iliac tortuosity, but both renal arteries were eventually successfully cannulated.

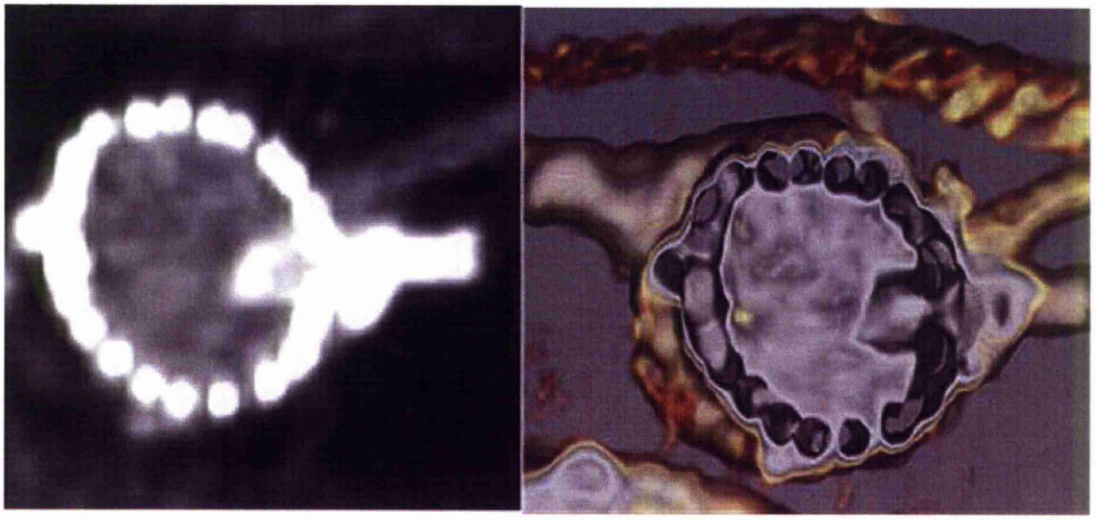

Figure 5.6 Cross sectional images demonstrating the ease with which the left main and accesorry renal arteries could be superimposed.

During subsequent follow up, a precarious connection between the right renal fenestration and target vessel stent was noted (Figure 5.7). This situation had the potential to develop into a type 3 endoleak and also threaten target vessel patency. Core-lab analysis of the pre and post-operative images concluded that axial branching angle of the right renal artery made it difficult to profile the renal artery accurately. Therefore assessing the length of target vessel stent within the aortic lumen was challenging. In this patient, target vessel threat was the result of intraoperative difficulty.

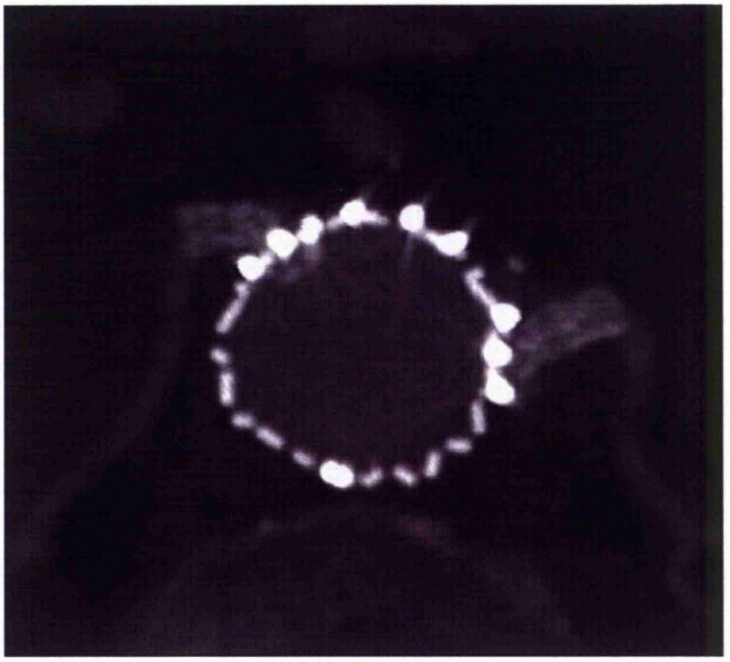

Figure 5.7 Impending dislocation of the right renal target vessel stent arising from difficulty in intra-operative profiling the right renal artery.

Patient 6 – Target vessel threatened

This 69 year old patient with a short infra-renal neck was and a 92 mm aneurysm was treated with a fenestrated stent-graft comprising two fenestrations for the renal arteries and a scallop for the SMA. The renal arteries were stented using 7 mm Atrium stents (Atrium Medical, Rendementsweg, Netherlands). No intraoperative difficulty was reported. At 1 month, the surveillance CT showed misalignment of the SMA scallop, however since the scallop was deployed below the SMA there was no compromise in visceral perfusion (Figure 5.8).

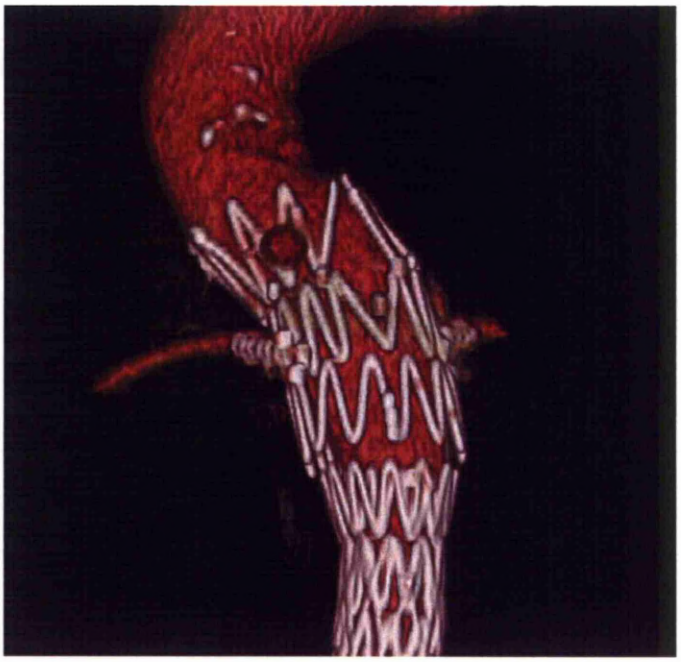

Figure 5.8 SMA scallop misalignment. Since the scallop is below the SMA, there is no compromise in perfusion.

The core-lab analysis did not demonstrate any significant difference between the implanted fenestrated stent-graft design and a new plan based on the original CTA dataset. It was noted however that the morphology of the in situ stent-graft had changed between the immediate post-operative plain x-ray and x-rays at 1 month (Figure 5.9). Further analysis of the surveillance images also showed that the sealing stents may have traversed the angle in the neck of the aorta thereby distorting the aorta. Therefore introduction of the device may have changed the morphology of the aorta. In addition, a large type 2 endoleak arising from the inferior mesenteric artery (IMA) was also noted. This resulted in an increase in the maximal diameter of the aorta and may also have contributed to the post-operative changes and subsequent threat to the target vessels. The panel thus

concluded that target vessel threat in this case was due to a combination of an unforeseen interaction between the stent-graft/ native aorta and post-operative changes in aortic morphology.

Patient 7 - Target vessel threatened (Secondary intervention: right renal stent)

This 70 year old male patient with a 58 mm aortic aneurysm was treated with a stent-graft comprising a single triple width scallop for both the SMA and right renal artery and a small fenestration for the left renal artery. The latter was stented with a 7 mm x 18mm Palmaz Genesis (Cordis, Waterloo, Belgium) uncovered stent. No intra-operative difficulty was reported. Six months following FEVAR, shuttering of the right renal artery was noted on the surveillance CT. Abnormal duplex waveforms were also noted but there was no impairment of renal function. He subsequently had a secondary intervention in the form of additional stenting of his right renal artery to maintain target vessel perfusion (Figure 5.10).

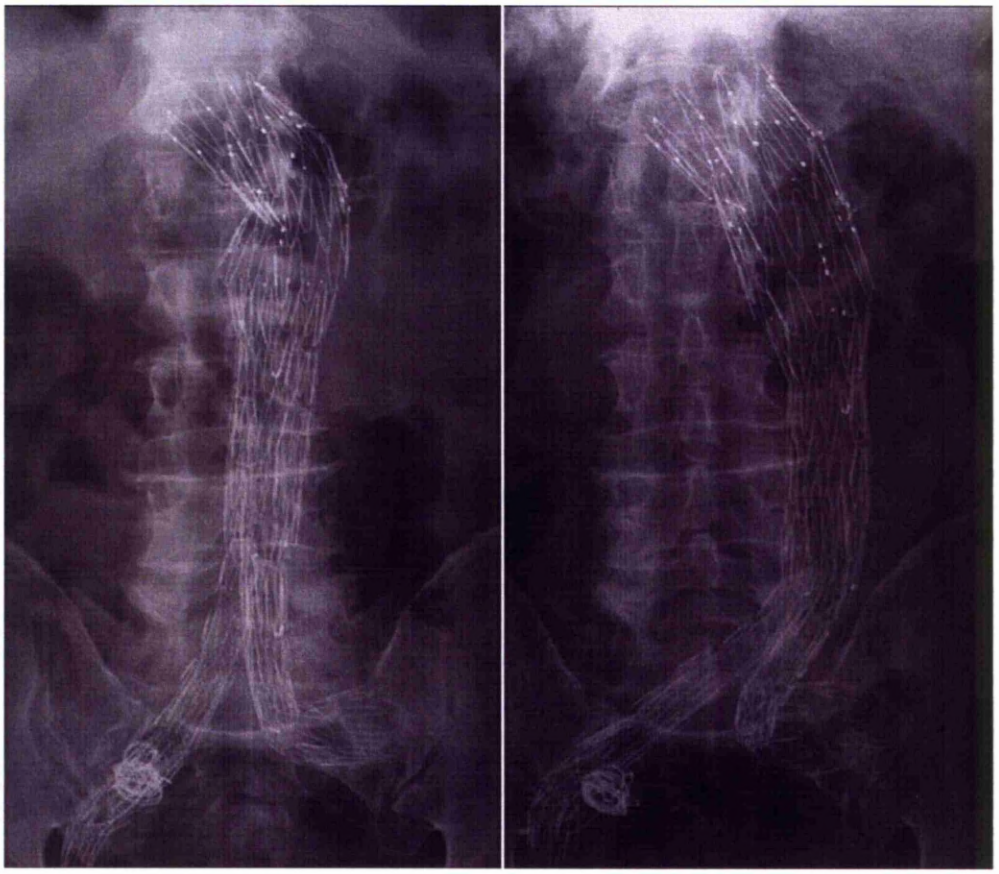

Figure 5.9 Change in angulation of the renal stents due to increase in the aneurysm size as result of a type II endoleak from the IMA.

Core-lab analysis in this patient confirmed that the mode of target vessel threat was circumferential shuttering. This was likely due to migration of the scallop in the circumferential direction as a result of the pulsatile movement of the aorta. Furthermore, although the scallop was designed to be 30 mm wide, the stent-graft was designed with a 20% oversize. This additional excess facilitated repositioning of the sealing stent and thus the scallop during the cardiac cycle. However the major reason for shuttering in this case was a failure to fix the

position of the scallop by using an additional stent for the right renal artery. In this patient target vessel threat was a consequence of planning issues.

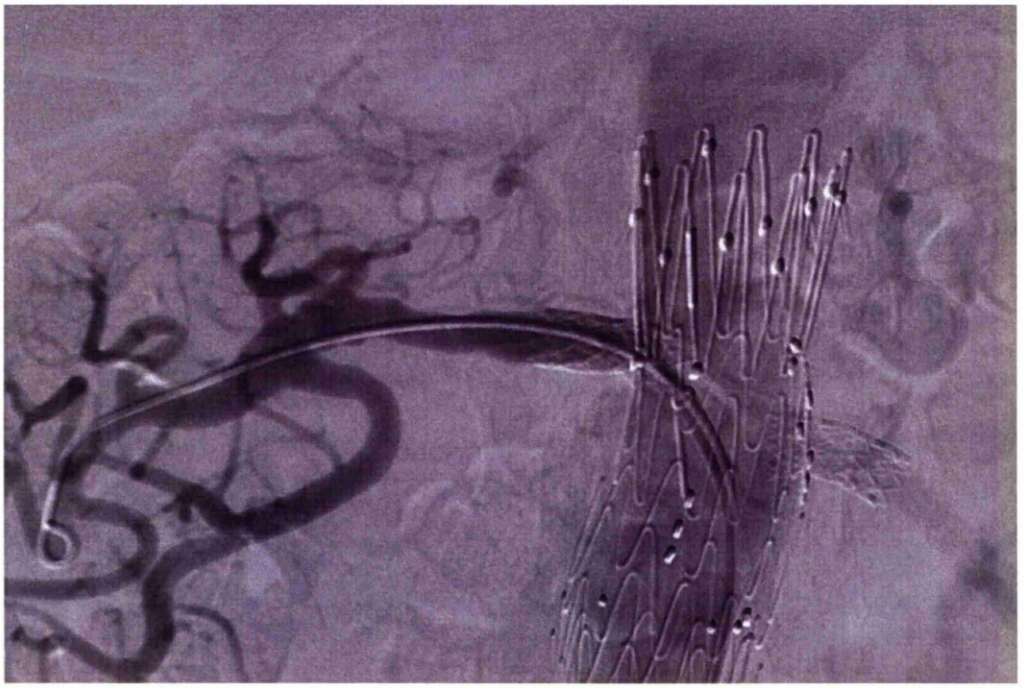

Figure 5.10 Adjunctive stenting of right renal artery to treat thereat to target vessel patency as a result of circumferential shuttering.

Patient 8 - Target vessel threatened

This 66 year old male patient presented with a 60 mm aortic aneurysm. The aortic morphology in this case was not suitable for standard EVAR as a result of a conical infra-renal aortic neck. A stent-graft comprising two small fenestrations for the renal arteries and a large fenestration for the SMA was deployed however the completion angiogram showed a stenosis of the SMA. This was managed by realigning the large fenestration with the SMA ostium using an additional balloon expandable stent. On subsequent surveillance imaging, it was noted that

the right renal stent had been crushed (Figure 5.11 A), but this did not compromise the patient's renal function.

The core-lab analysis of this patient's images revealed that the right renal stent appeared to have been distorted by a longitudinal compressive force. In this patient, the SMA was stented through a large fenestration which is traversed by struts of the Gianturco sealing stent (Figure 5.11 B). Under fluoroscopy it is not possible to determine where the guide wire will emerge within this fenestration. Therefore upon inflation, there may have been a degree of stent-graft movement in the cephalic direction with subsequent crushing of the right renal stent. Distortion of the left renal stent was probably not observed because the considerable hoop strength of stent used; a covered stent Jostent (Abbott, Ill, USA) which resisted the force generated by inflation of the SMA stent. In this patient, target vessel threat was due to intraoperative difficulty.

Patient 9 - Target vessel lost

This 85 year-old patient presented with a 59 mm aortic aneurysm. A large conical infra-renal neck precluded repair with a standard stent-graft so he was treated with a fenestrated stent-graft incorporating two renal fenestrations and a scallop for the SMA. Deployment was successful and no intraoperative difficulty was reported. At one month, his duplex scans showed a potential compromise in renal perfusion however his CT surveillance images revealed a patent target vessel and no endoleak. On this basis, a conservative approach was adopted. Three months following his procedure, the patient presented with left loin pain. A CT scan at this point confirmed occlusion of the left renal stent (Figure 5.12)

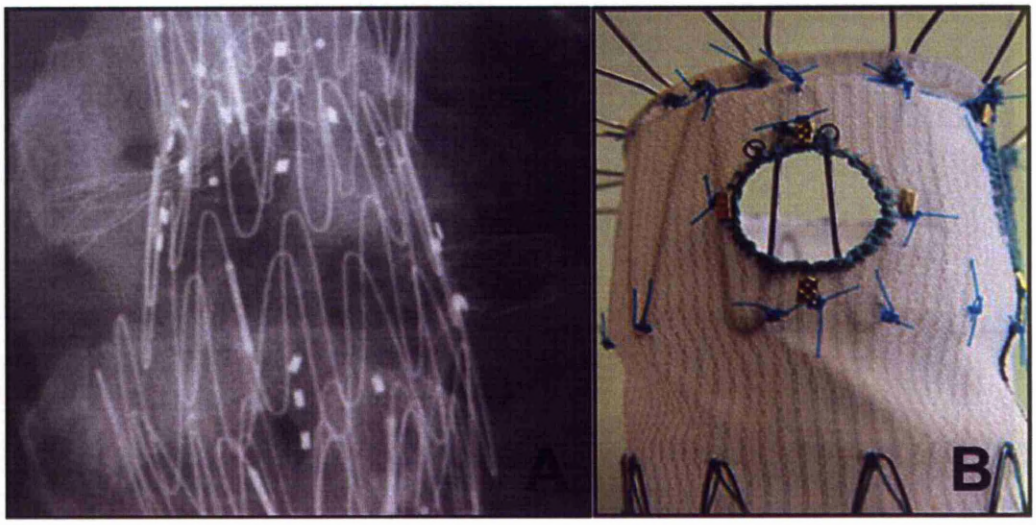

Figure 5.11 (A) Crushed right renal stent following placement of a balloon expandable stent in the SMA fenestration in order to treat a stenosis. (B) Sealing stent in a large fenestration. The gaps between the sealing stent struts are not visible under fluoroscopy and as such a target vessel stent may emerge from any of the three interstices in this fenestration.

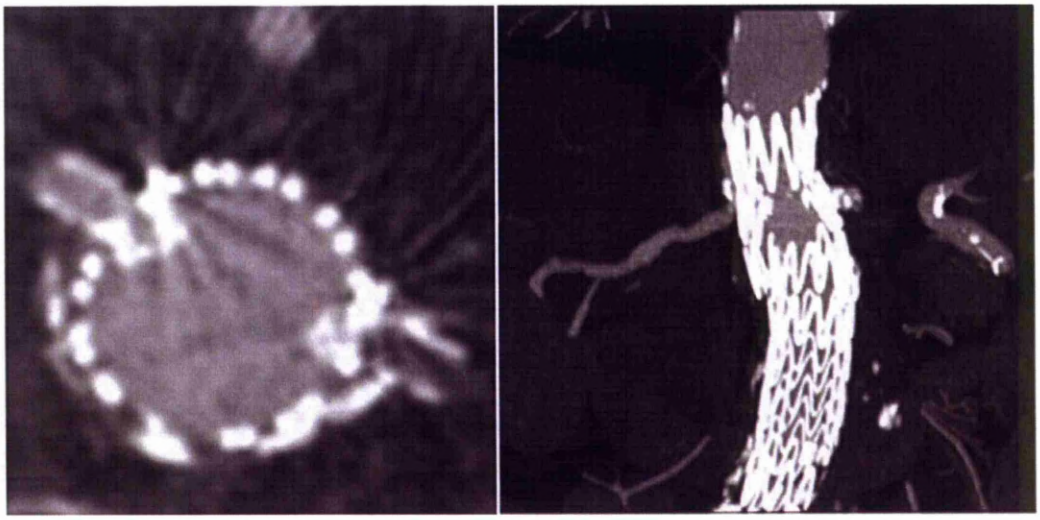

Figure 5.12 Loss of left renal artery stent at 3 months.

Core-lab analysis began by measuring the target vessel separation from the pre-operative CTA dataset for this patient and comparing these measurements with those used in construction of the fenestrated stent-graft. The difference in inter-

renal separation ranged between 2 and 7mm dependent upon the observer and workstation used in the measurement process. Anatomical features thought to contribute to this discrepancy included large renal ostia, calcification at the level of the renal arteries and the branching angle between the renal arteries and the aorta.

The mechanism for target vessel occlusion in this patient is not clear. Surveillance duplex in the first month had shown increased velocities in the left renal artery, but in view of the normal appearances on CT no action was taken. This suggests a dynamic cause that could not be replicated on the static CT images. Potentially discrepancy between the native anatomy and the fenestrated stent-graft may have resulted in unpredictable forces being transmitted through the stent to the renal artery leading to damage to the intima and possibly progressive intimal hyperplasia. In this patient, planning issues and unforeseen interaction between the stent-graft and native aorta lead to target vessel loss.

Patient 10 - Target vessel lost

This 65 year old patient presented with a 71 mm para-anastomotic aneurysm that had developed following previous infra-renal surgical repair. This made his aneurysm unsuitable for standard repair and the combination of a hostile abdomen and ASA score of 3 made him a high risk candidate for open repair.

His aneurysm was treated with a fenestrated cuff comprising a single scallop for the SMA. There were no renal fenestrations as the patient was dialysis dependent prior to his procedure. Intraoperatively, there was difficulty aligning the scallop

with the target vessel because of the tortuosity of the iliac arteries which limited the torque that could be transmitted to the stent-graft. In addition the confined space within the existing surgical graft also limited the ability to position the fenestrated cuff. Misalignment between the scallop and the SMA was noted during the procedure (Figure 5.13); however attempts to correct this problem were not successful and the SMA occluded on the 3rd postoperative day. Target vessel loss in this patient was due to intraoperative difficulty. Fortunately collateral circulation from his coeliac artery obviated the need for surgical reconstruction of the arterial supply to his gut.

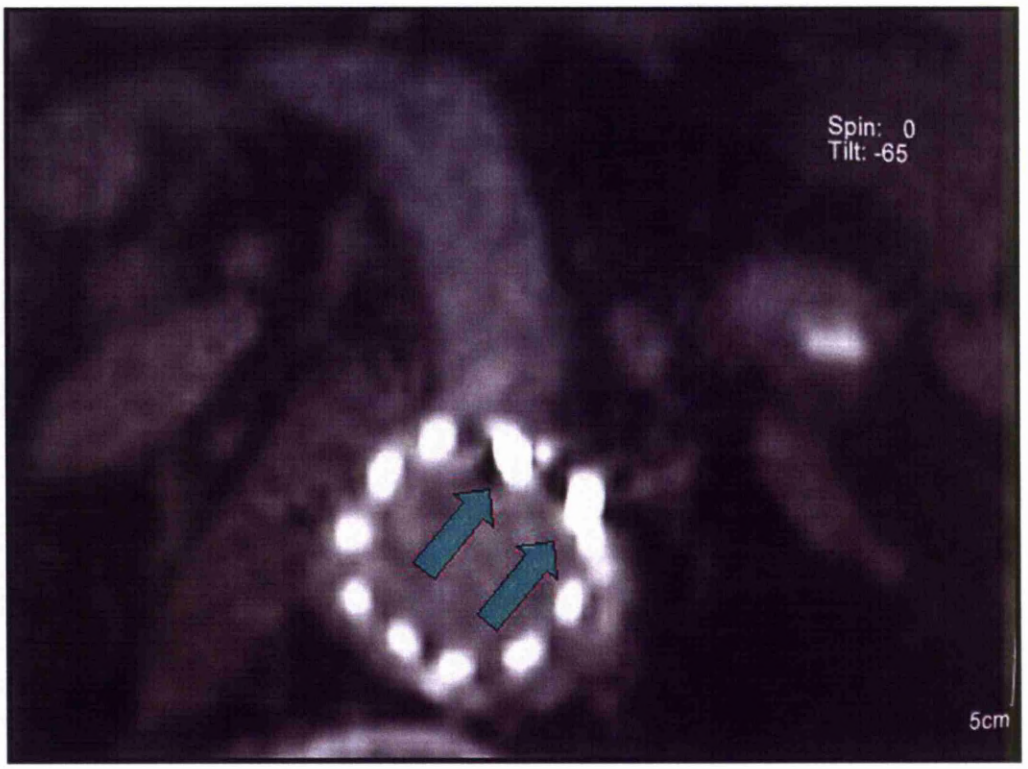

Figure 5.13 Misalignment of the SMA scallop (indicated by arrows) due to tortuous iliac anatomy and restricted space within a pre-existing surgical graft.

Patient	Outcome	Timing	Mode	Mechanism
1	TV threat	15 days	Shuttering	Planning, stent-graft/aorta interaction
2	TV threat	Intra op	Shuttering	Stent-graft/aorta interaction
3	TV threat	3 months	Distortion	Operative difficulty
4	TV loss	1 month	Trauma	Operative difficulty
5	TV threat	6 months	Stent separation	Operative difficulty
6	TV threat	1 month	Shuttering	Stent-graft/aorta interaction
7	TV threat	6 months	Shuttering	Planning
8	TV threat	1 month	Distortion	Operative difficulty
9	TV loss	3 months	Unknown	Planning, stent-graft/aorta interaction
10	TV loss	Intra op	Shuttering	Operative difficulty

Table 5.14 Summary of modes and mechanisms of target vessel loss.

5.4 Discussion

In the absence of an adequate infra-renal aortic neck, fenestrated stent-grafts provide an effective alternative to open surgery thereby increasing the therapeutic indications for endovascular aneurysm repair. However in addition to freedom from endoleak, limb occlusion and migration, long-term patency of target vessels is an important determinant of the durability of FEVAR. This study shows that in the medium term, threat to target vessel patency may arise as a consequence of several mechanisms, though progression to target vessel loss is rare.

At 60 months follow up, overall target vessel patency (both primary and assisted) was 95.3% and is in keeping with published literature (Mohabbat et al., 2009). All target vessel problems were identified within the first year of surveillance and perhaps reflects the observation that in half the threatened vessels, the mechanism of target vessel threat was intra-operative difficulty. Target vessel threat as a consequence of procedural difficulty tended to occur early in the Unit's FEVAR experience and may represent negotiation of the learning curve for FEVAR. This seems to be supported by the observation that target vessel loss was also concentrated in the Unit's early experience of FEVAR.

The long-term durability of stents in the renal arteries is difficult to predict. Late threat to target vessel patency may occur as a result of biological processes occurring at the stent/lumen interface or as a consequence of the complex dynamic interaction between the between the stent-graft complex and the native vasculature. Primary patency rates of 90% at 5 years have been reported after renal stenting (Henry et al., 1999) and is perhaps encouraging when one considers the indication for renal artery stenting is atherosclerotic disease. In this situation deployment of a renal stent results in plaque rupture thereby generating an inflammatory response which may ultimately lead to intimal hyperplasia. In FEVAR, renal stents are deployed in order to maintain alignment between the fenestrations and the target vessel ostia. These vessels are not usually diseased therefore luminal injury and elastic recoil are unlikely to be major risks to target vessel patency. Furthermore, bare metal stents are frequently used in renal artery stenting whereas there is emerging evidence of the benefit of covered stents in

FEVAR. Therefore the presence of the renal stent itself is unlikely to be the root cause of late target vessel occlusion.

Long-term durability of target vessel stents is more likely a function of their interaction with the proximal main body and native aorta. It is interesting to note that stent fracture is rare following FEVAR whereas it is more common in other locations such as the femoral artery where stents are also exposed to dynamic forces. In fact stents used to treat atherosclerotic disease of the superficial femoral artery frequently fail as a result of metal fatigue and subsequent fracture (Nikanorov et al., 2008, Pelton et al., 2008). Problems relating to the target vessel stent (dislocation and distortion) are often noted a few months after the initial procedure and is perhaps indicative of long-term failure modes.

Since acute target vessel loss is usually a consequence of shuttering and frequently occurs within the first year of surveillance, a modified surveillance protocol after FEVAR with emphasis on frequent imaging in the first year of follow up may help minimize threat to target vessel patency. More frequent scanning potentially increases the overall burden of ionizing radiation and surveillance cost however this could be mitigated by identifying patients that are at higher risk of late target vessel occlusion.

5.5 Summary

Target vessel related issues will affect a proportion of patients undergoing FEVAR, although occlusion of target vessels that result in clinically significant complications is rare up to mid-term follow-up. The mechanisms leading to target vessel threat are diverse and elucidation of each requires detailed analysis, but is expected to lead to improvements in target vessel patency.

Chapter 6

Intra and inter-observer variability of target vessel measurement for fenestrated endovascular aneurysm repair (FEVAR)

6.1 Introduction

Endovascular aneurysm repair (EVAR) has been an established alternative to open surgical repair (Prinssen et al., 2004a, UK EVAR trial 1 participants, 2005) for some time, yet unfavourable anatomy of the aneurysm neck is the most frequent reason for unsuitability for EVAR (Diehm et al., 2008); in particular the short aortic neck. In such instances, open surgical repair is associated with a substantial risk of peri-operative complications since a proportion of these patients require suprarenal aortic cross clamping in order to effect aneurysm repair (Sarac et al., 2002a, Faggioli et al., 1998a). Fenestrated endovascular aneurysm repair (FEVAR) overcomes the limitations of standard EVAR by extending the proximal seal zone into the visceral segment of the aorta whilst maintaining end organ perfusion via accurately placed fenestrations.

Accurate measurement of the aortic anatomy is a prerequisite for successful FEVAR. Longitudinal separation between aortic side-branches (target vessels)

and circumferential orientation of the target vessel ostia upon the orthogonal aortic cross section, called 'clock face position' are the two most important measurements required to construct a stent-graft main body that allows target vessel perfusion while achieving aneurysm exclusion. Errors in these measurements will lead to mismatch between the stent-graft and native anatomy, which may in turn result in intra-operative difficulty with stent-graft deployment and/or delayed target vessel occlusion. Measurement for fenestrated stent-graft planning is predominantly performed by three dimensional analyses of computerised tomographic angiography (CTA) images. The effect of observer or of the technique used upon measurement variability has not been previously analysed.

The purpose of this study was to evaluate the intra and inter-observer agreement of target vessel measurements and to compare two measuring techniques commonly utilised in FEVAR planning; namely multi planar reformat (MPR) and semi-automated central luminal line (CLL) measurement.

6.2 Methods

6.2.1 *Material*

Material was selected from a cohort of 64 consecutive patients in whom fenestrated EVAR was performed at a single institution between 1999 and 2009. In order to standardise the measurement protocols and result sets, only patients that required the construction of stent-grafts incorporating a scallop for the

superior mesenteric artery (SMA) and fenestrations for both the left and right renal arteries were considered. A proportion of CT datasets were of poor quality and would have compromised subsequent data analysis, leaving 40 datasets of which 25 patients were selected at random and their CTA datasets retrieved.

6.2.2 *Image analysis*

Two observers (*Olufemi Oshin*- Research Fellow and *Andrew England*- Lecturer) performed image analyses independently according to a set protocol. Two different workstations were used, Aquarius (TeraRecon, CA, USA) and Leonardo (Siemens Medical Solutions Inc, Erlangen, Germany). Both observers had prior training in the use of these workstations and are experienced in using them. Each observer performed measurements twice on separate occasions for each data set. A period of four weeks was allowed to elapse before the repeat measurement.

The technique used to measure longitudinal vessel separation was different for each workstation and reflected the best practice for each of these workstations. With the Aquarius workstation, a semi-automated central luminal line was created by placing seed points above the level of the celiac axis and below the lowermost renal artery. The centreline generated by the workstation was never manually altered. A "stretch view" was then generated from which the longitudinal vessel separation was manually measured using the bottom of the celiac axis ostium as the reference point. The stretch view image was rotated on its centreline axis to identify the optimal view of the midpoint of each target

vessel ostium. With the Leonardo workstation, multi planar reconstructions were created along the visually perceived luminal axis of the visceral segment of the aorta. Although the thickness of the maximal intensity projections (MIP) was kept to a minimum this was neither controlled nor recorded between observers or observations. From these reconstructions, the longitudinal separation of the target vessels was measured, again using the bottom of the celiac axis as the point of reference. Renal separation was defined as the difference between the measured distances from bottom of the celiac axis to the midpoint of each renal artery ostia. Each set of measurement consisted of celiac axis to upper renal ostium and celiac axis to lower renal ostium rounded to the nearest mm.

The circumferential position of the target vessel ostia in a plane orthogonal to the visceral aorta was assigned using a 'clock face' protractor with 12 hour gradations over 360^0 to the nearest 15 minutes (equivalent to 7.50) according to the planning instructions for fenestrated devices issued by the manufacturers Cook® (Bloomington, IN, USA). In the case of both workstations this was achieved by multi planar reconstruction.

6.2.3 *Statistical analysis*

Numeric data representing continuous variables (intra and inter observer differences in measurement) were converted to categorical variables according to set criteria, both for analysis and for descriptive purposes; specifically a discrepancies exceeding 3mm in longitudinal vessel separation and 30 minutes in clock-face measurement were considered significant. Proportions of binary

variables were expressed as percentages. Statistical analysis was performed using SPSS software (SPSS v 16.0, SPSS Inc, Ill). Chi-square analysis was utilised for dichotomous outcomes. Intra and inter-observer variability was measured by calculating the repeatability coefficient given by the mean differences between repeated measures according to Bland and Altman (Bland and Altman, 1986). Three-way repeated measures analysis of variance (ANOVA) was utilised to analyse the individual and combined effects of observer, workstation and time on measurement variability.

Since the reference point for assigning clock positions for the target vessel ostia may vary between observers, the relative positions in minutes was calculated and used to determine observer agreement. A clock position discrepancy of 30 minutes or more for the position of target vessel ostia was considered significant.

6.3 Results

***Inter-renal separation*:** In total, 100 paired sets of CTA measurements were generated, falling into four groups. Intra-observer and workstation specific repeatability coefficients (RC) varied between 3.9 and 4.9 mm (Figure 6.1). The mean difference between repeat observations was less than 1mm in all instances within each group. When this data is examined qualitatively however, 8% of the repeat measurements differed by more than 3mm (a magnitude considered clinically significant) compared to the first measurement of the same observer.

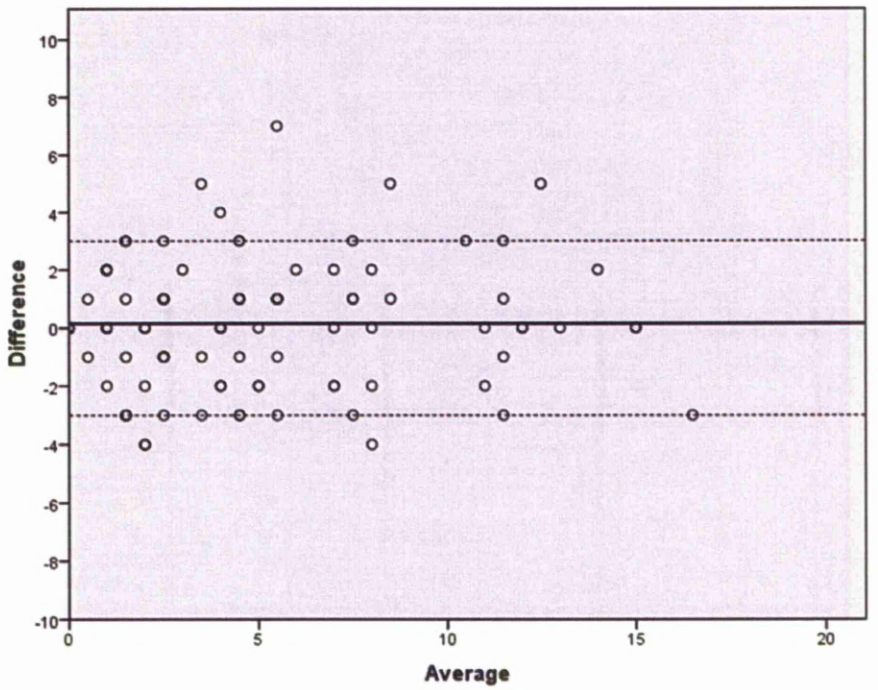

Figure 6.1 Intra-observer variability. Dotted line represents upper and lower limits of agreement.

Data relating to inter-observer variability is given in Figure 6.2. Inter-observer variability was greater with observer and workstation specific RC varying between 5.6 and 7.4mm. There was a tendency towards more consistent measurement between observers using multi-planar reformatting techniques to measure vessel separation. The overall mean difference between the observations of the two observers (inter-observer variability) was also less than 1mm with no significant difference in paired measurements. Qualitative analysis showed that there were more discrepancies between individual measurements with a difference of 3mm or more noted in 18% of paired measurements. However this was not statistically significant compared with intra-observer discrepancy (Chi-square, P = 0.056).

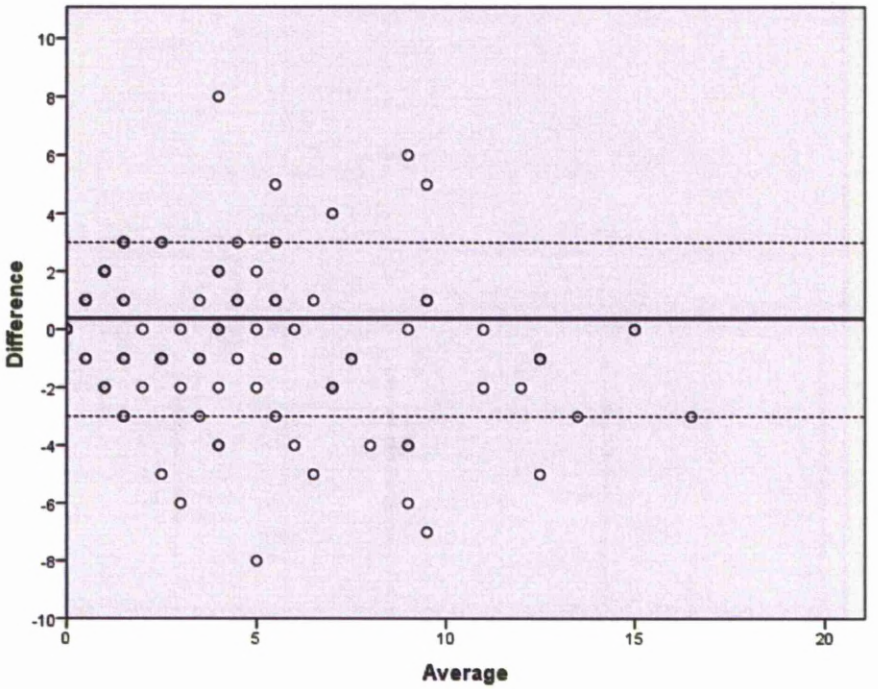

Figure 6.2 Inter-observer variability. Dotted line represents upper and lower limits of agreement.

The results of the 3-way repeated measures ANOVA are given in Table 6.1. The main effect of observer, type of workstation or when the observations were performed (time) on the inter-renal separation was not significant. There was a significant interaction between all three factors (P = 0.022) and by sub-group analysis, the interaction between observer and time was significant (P = 0.031) but statistical significance was not observed between workstation type and time (P = 0.799) or workstation and observer (P = 0.585).

Factor	dF	F	P
Observer	1	0.784	0.385
Workstation	1	0.584	0.452
Time	1	0.783	0.385
Observer * Workstation	1	0.306	0.585
Observer* Time	1	5.240	0.031§
Workstation * Time	1	0.066	0.799
Observer * Workstation * Time	1	6.021	0.022§

Table 6.1 Two-way ANOVA of factors influencing observer variability. § Indicate factors that are statistically significant.

***Clock-face position of target vessels*:** There was no significant intra-observer variation in clock-face measurements. Inter-observer variability was noted with 30 minutes of discrepancy or greater in 17 occasions of which 11 (65%) related to the right renal artery position and 6 (35%) of the left renal artery. When analysed by workstation (Table 6.2), a discrepancy in inter-observer clock-face target vessel position was noted in 12% with Aquarius and in 6% with Leonardo, but this difference did not reach statistical significance (P = 0.19, Chi-square).

	Aquarius		Leonardo	
Intra-observer	Observer 1	Observer 2	Observer 1	Observer 2
Right renal	0	0	0	0
Left renal	0	0	0	0
Inter-observer	Observation 1	Observation 2	Observation 1	Observation 2
Right renal	3	2	2	3
Left renal	3	3	0	0

Table 6.2 Intra and inter-observer variability of target vessel clock position

6.4 Discussion

Accurate assessment of vascular anatomy is of particular importance with fenestrated stent-grafts since errors may lead to serious consequences. Fenestrated and side-branched devices are tailored based on measurements of both the orientation and separation of target vessels. Image analysis workstations are designed to carry out measurements of vascular anatomy and landmarks. There are different workstations available for this purpose with varying, but validated software (Isokangas et al., 2003). Measurement of anatomy, even when performed according to a predetermined protocol, may remain subject to observer interpretation and potentially compounded by variations in workstation software. The resulting inter and intra-observer variation of target vessel

measurements for fenestrated stent-graft planning has not been reported previously.

In addition to standard quantitative analyses available to examine variance, additional qualitative analysis of the data was also considered important to avoid the possibility of clinically insignificant discrepancies resulting in a statistically significant result or vice versa. For these purposes, a discrepancy of >3mm in longitudinal vessel separation and of >30 min in clock face measurement were considered significant. These arbitrary limits were chosen by the authors since lesser degrees of measurement errors were considered unlikely to create serious consequences due to a degree of tolerance within the proximal main body of the stent-graft system that incorporates the fenestrations.

The observers in this study have both received training in using both the workstations and are experienced in using workstations. Qualitative analysis suggests that intra and inter observer variation to the extent considered clinically significant occurs with measurement for fenestrated EVAR. When data is examined within workstation and observer specific sets for variation, the mean difference in repeat measurements was less than 1mm in all instances. This coupled with the fact that the majority of the repeat measurements were within qualitatively acceptable limits of the initial measurement is reassuring. There are however examples of significant measurement discrepancies both on quantitative (repeatability coefficients that exceeded arbitrary limits set for clinical significance) and qualitative analyses. This suggests that some measurements are likely to have been significantly inaccurate. This is true for both longitudinal

separation and of clock-face assignment. In common with many other studies of image analyses, inter-observer variation is greater than intra-observer variation. Furthermore by 3-way ANOVA, it would appear that this is not a function of the type of workstation / technique used, but rather a result of the interaction between observer and time (repeat measurement). This suggests that despite predefined criteria and protocols, interpretation of vascular landmarks remains subjective.

Unique anatomical features such as angulation within aorta and the trajectory, tortuosity and non-planarity of target vessels likely influence observer interpretation of target vessel position in both longitudinal and cross-sectional orientation. The majority of clock position discrepancies between the observers relate to the right renal artery, a vessel whose course takes a circuitous route behind the inferior vena cava. A higher incidence of target vessel occlusion has been reported with this artery and has been attributed to a higher probability of the renal stent kinking due to the curvature of this vessel (Mohabbat et al., 2009). Errors in assigning clock position of the right renal artery could also be a contributory factor.

In addition to the inherently subjective nature of the task, there are factors that could have potentially influenced the results. Slice thickness of CTA data acquisition, quality of arterial contrast enhancement, unique anatomical features of aorta and its branches, distortion from anisotropic voxels in some CTA datasets and even the hardware used for image acquisition may all have

potentially influenced subsequent image analysis. Since a number of CTA have been acquired at different hospitals and referred to our institution for FEVAR, it was not possible to reduce heterogeneity of these aspects. Certain functions of workstation, in particular semi-automated CLL generation is influenced by the degree of contrast enhancement (Wyss et al., 2009) and may therefore be responsible for the trend towards consistency when MPR, a technique that relies solely on observer manipulation of the images, was used.

It might not be possible to completely eliminate measurement errors or discrepancies. Furthermore it should also be recognised that native anatomy may be distorted intra-operatively due to the insertion of rigid stent-graft systems and contribute to difficulties in target vessel cannulation, in addition to measurement errors. Although encouraging technical success rates are reported (Sun et al., 2006), intra-operative difficulties that may ensue from distorted anatomy or device mismatch are seldom reported. It would therefore appear that fenestrated stent-grafts have a degree of tolerance to mismatch with native anatomy. Indeed the ability to incorporate fenestrations that are larger than the target vessel ostium and flexibility within the proximal main body are two features that contribute to this. Innovations that provide greater tolerance would compensate for measurement errors and also lead to a reduced need for customisation.

6.5 Summary

This study shows that measurements performed for planning fenestrated EVAR are prone to significant intra and inter observer discrepancy in a small proportion of patients. Further study is warranted to identify factors that predispose to measurement discrepancies and to develop consensus regarding image interpretation. Stent-graft systems that would allow safe and effective transluminal revascularisation of target vessels without relying heavily upon accurate measurement of native anatomy would also be beneficial.

Chapter 7

FEVAR planning: Anatomical factors influencing observer error

---

7.1 Introduction

Accurate assessment of patient anatomy is required for the design of fenestrated stent-grafts, however direct measurement of the circumferential position and relative distance between the side branches of the abdominal aorta is not possible. This problem is further compounded by the fact that assessment of the abdominal aorta and its branches requires varying degrees of image manipulation in order to fully appreciate the relationship between the visceral branches, thereby introducing additional subjectivity to the measurement process. As observer error (accuracy) cannot be measured in this situation, the variability of repeat measurements is frequently used as an indirect marker of accuracy. Variability describes how clustered or disperse a data set is and is an inevitable consequence of measurement or the measurement process itself; it is therefore possible to generate consistent but erroneous results. However the relationship between the morphology of the aorta and observer error has not been studied previously.

7.2 Aim

The aim of this study was to determine the anatomical features and characteristics that promote significant observer error and variability.

7.3 Methods

Phantoms depicting pathological vascular anatomy consisting of the human aorta with its side branches (two renal arteries, SMA and Coeliac axis) were created with a combination of specific predetermined anatomical features that included selected combinations of variation in a predetermined and controlled manner of the following features:

1. Antero-posterior angulation of the aortic neck (coronal plane- 20, 40 and 60 degrees)
2. Lateral angulation of the aortic neck (sagittal plane- 20, 40 and 60 degrees)
3. Longitudinal inter-renal separation
4. Longitudinal renal artery branching angle in the coronal plane (90, 120 and 140 degrees)
5. Clock-face orientation
    a. Left renal (2, 3 and 4 o'clock)
    b. Right renal (8, 9 and 11 o'clock)
6. Axial branching angles renal arteries(-60, 0 and 60 degrees)

The resulting rapid-prototyped phantoms were then subjected to CT scans. All CT scans were performed according to a standard protocol that included arterial phase scanning with a slice thickness of 2mm, using a 16 detector scanner (SOMATOM Sensation, Siemens Medical Solutions, Erlangen, Germany). Subsequently a panel of observers (*Mathew Bown*- Consultant Vascular Surgeon, *John Brennan*- Consultant Vascular Surgeon, *Robert Fisher*- Consultant Vascular Surgeon, *Geoffrey Gilling-Smith*- Consultant Vascular Surgeon and *Srinivasa Vallabhaneni*- Consultant Vascular Surgeon) measured the inter-vessel separation and clock position of the aortic side branches once using a Leonardo workstation (Siemens medical solutions, Erlangen, Germany).

7.3.1 *Phantom design*

In the interest of both simplicity and the financial outlay for this study, construction of the phantoms was limited to the visceral segment of the aorta (i.e. segment incorporating the branch vessels) only and therefore represented by a tube. The overall length of the tubes was variable in order to allow the variation in the position and geometric position of the aortic side branches. The inner aortic diameter for the phantoms was set at 20mm with a thickness of 1.5mm

The phantoms were designed using Pro-Engineer, a parametric computer aided design (CAD) software package. A central "skeleton" depicting the long axis of the aorta was first created in either the coronal or sagittal plane dependent on the desired direction of the angulation in the long axis of the aorta. In order to produce a phantom which is as faithful a representation of human anatomy as

possible, the transition at the point of angulation was smoothed using a standard radius of curvature of 10mm.

Following this the phantom was "fleshed out" by generating a 20mm tube along the desired trajectory. Axial datum planes were then created along the course of the tubular phantom at specific points in order to mark the level at which the side branches would be created. In the section of the phantom where the trajectory was angulated, the axial datum plane was adjusted so that it was perpendicular to the trajectory of the phantom's long axis. For the purposes of clock-face position, the undisplaced sagittal plane was used to represent 12 o'clock. From this adjustments to the position of subsequent planes were made to represent desired clock-face positions.

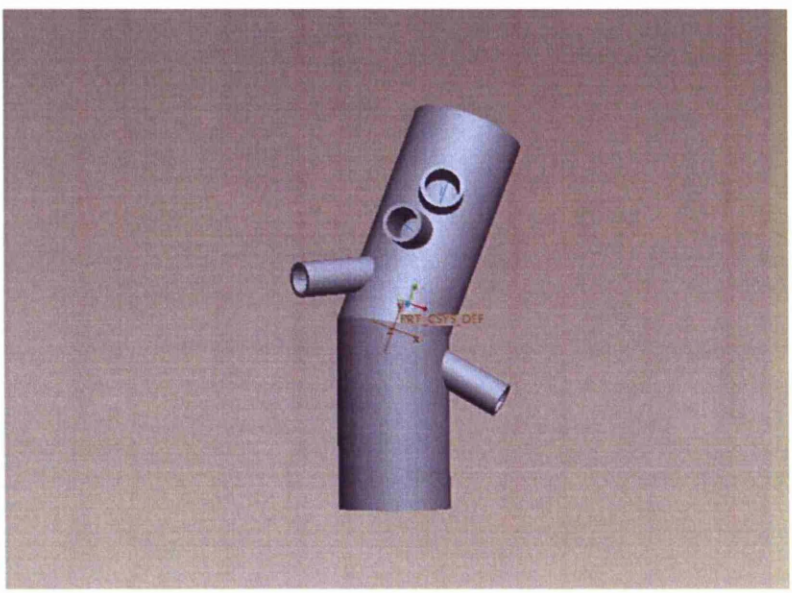

Figure 7.1 Phantom created in Pro-Engineer

Within each of the planes assigned for the Coeliac, SMA, and both renal arteries trajectories were plotted corresponding to the intended path of the side branches of the aorta. A similar process to "flesh out" these vessels was undertaken. Here the coeliac and SMA inner diameters were set at 10mm with a vessel wall thickness of 1mm. For the renal vessels, the inner diameter was set at 6mm with a wall thickness of 1mm.

The final phantom design was saved as an STL file. Cone height and angle were set to maximise the resolution of the complete image. Rapid prototypes of the phantoms were created using a 3D printer (Stratasys Dimension Elite, Dimension Inc. Minnesota, USA). Following fabrication, the separation between the side branches and the SMA each phantom was manually validated by direct measurement using digital callipers. In total, nine phantoms were created with the anatomical characteristics shown in Table 7.1.

Each phantom was filled with a mixture of gelatine and intravenous contrast material. In order to determine the quantity of contrast needed for the gelatine mixture, a random sample of Hounsfield unit measurements were taken from a CTA dataset (Figure 7.2). Subsequently gelatine mixtures composed of varying concentrations of contrast were created according to the protocol described below:

Protocol for the creation 100 ml 12% (weight/volume) gelatine solution

1. Measure 98 ml of water into a beaker
2. Measure 11.2 grams of gelatine into a container
3. Bring water to boil and allow to cool for 5 minutes

4. Add gelatine slowly to water whilst string briskly. Continue stirring until all gelatine powder has been incorporated into solution.

To create a 2% (by volume) solution with iodinated contrast, 4ml of iodixanol (270 mg/mL) contrast agent (Visipaque^{TM}) was added to 16 ml of 12% gelatine solution.

These samples were then subjected to CT scanning and the sample with an average Hounsfield unit that was closest to the intraluminal value used.

7.3.2 *Statistical analysis*

The inter-renal separation for each phantom was calculated by subtracting the measured distances from the mid-point each renal artery. Since the inter-renal separation varied between the phantoms, measurement error was standardised by expressing it as a fractional error of the true inter-renal separation.

$$Fractional\ error = \frac{(Inter\ renal\ separation_T - Inter\ renal\ separation_O)}{Inter\ renal\ separation_T}$$

Where:

T = *true*

O = *observed*

The pooled average fractional error of all the observers for each model is subsequently presented as the median with range in parentheses. Non-parametric tests using SPSS statistical software (SPSS Inc., Chicago Ill) were performed. The Kruskall-Wallis test was utilised to determine if there were any significant

differences average fractional error between the phantoms whilst the Mann-Whitney test was used to identify morphological characteristics that were associated with significant accuracy using phantom 9 as the comparator.

7.4 Results

The Hounsfield measurements for the various gelatine mixtures are shown in Figure 7.3. The average value for intraluminal contrast was 300 Hounsfield units and was best modelled by a 2% (by volume) concentration of contrast (Figure 7.2). All six observers successfully measured the target vessel separation of the phantoms. One phantom was of poor quality (ostium of the SMA was not well visualised) and was therefore discarded from further analysis. The median fractional error for each phantom is presented in Table 7.2. A visual representation of the recorded positions of the target vessels in relation to the true positions as measured by direct measurement is presented in figures 1 to 8. Analysis using Kruskall-Wallis demonstrated a statistically significant difference between the groups ($p = 0.004$). Subsequent analysis using the Mann-Whitney U test (Table 7.4) to compare the median fractional error of each phantom with phantom 9 showed that significant error was present in phantoms 2 (40 degree coronal angulation of aorta) and 5 (20 degree coronal angulation of aorta).

Model ID	Configuration	Distance from Mid SMA (mm)		Clock-face position (Hrs:mins)		
		R Renal	**L Renal**	**SMA**	**R Renal**	**L Renal**
[01]	Aorta- 40° degree sagittal, no renal angulation	20mm	10mm	12.00	9.00	3.00
[02]	Aorta- 40° degree coronal, no renal angulation	20mm	10mm	12.00	9.00	3.00
[03]	Aorta- straight vessel , 40° degree RRA angulation	30mm	20mm	12.00	9.00	3.00
[04]	Aorta- straight vessel, 60° degree RRA angulation	30mm	20mm	12.00	9.00	3.00
[05]	Aorta-20° degree coronal, no renal angulation	27mm	20mm	12.15	9.00	3.00
[06]	Aorta- 20° degree sagittal, no renal anglulation	30mm	20mm	12.00	9.00	3.00
[07]	Aorta- 60° coronal, no renal anglulation	30mm	20mm	12.15	9.00	3.00
[08]	Aorta- 60° sagittal, no renal anglulation	30mm	20mm	12.00	9.00	3.00
[09]	Aorta- straight vessel, no renal anglulation	30mm	20mm	12.00	9.00	3.00

Table 7.1 Anatomical characteristics of the phantoms investigated in this study

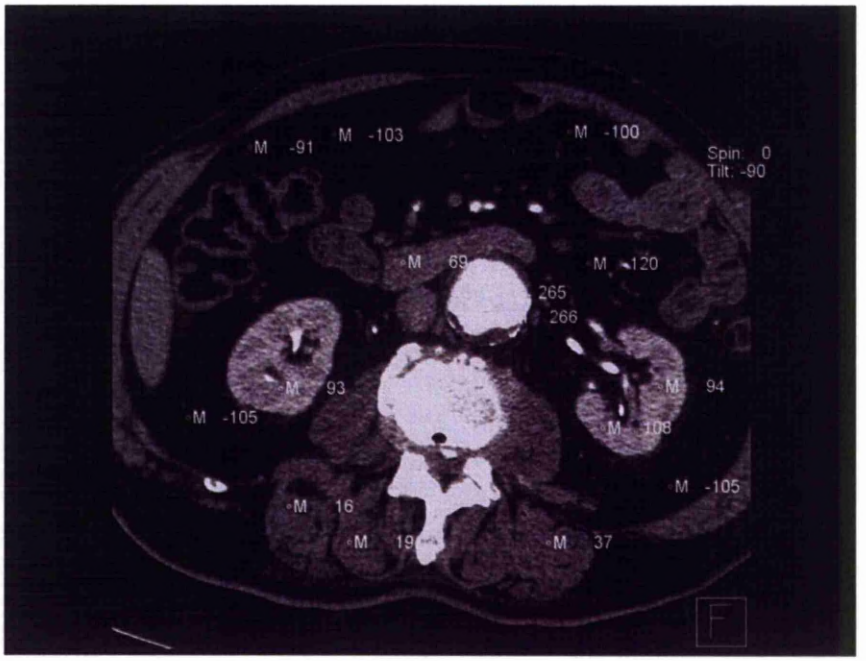

Figure 7.2. Hounsfield units for various tissue types within the abdomen.

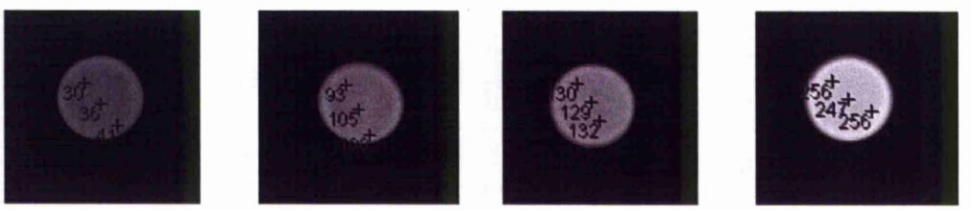

Figure 7.2 Hounsfield units for the various gelatine compositions.

Phantom	Median fractional error in mm (range)
1	0.06 (0-0.7)
2	0.7 (0-0.8)
3	0.02 (0-0.1)
4	0.03 (0-0.1)
5	0.28 (0-0.7)
6	0.09 (0-0.1)
7	0.03 (0-0.3)
8	0 (0-0.02)

Table 7.3 Median fractional error of target vessel measurements for each phantom.

Phantom combination	p Value
1 vs 9	0.052
2 vs 9	0.008*
3 vs 9	0.264
4 vs 9	0.219
5 vs 9	0.008*
6 vs 9	0.052
7 vs 9	0.22

Table 7.4 Results of Mann-Whitney U tests comparing straight phantom with angulated phantoms. * Siginificant 0.05 level.

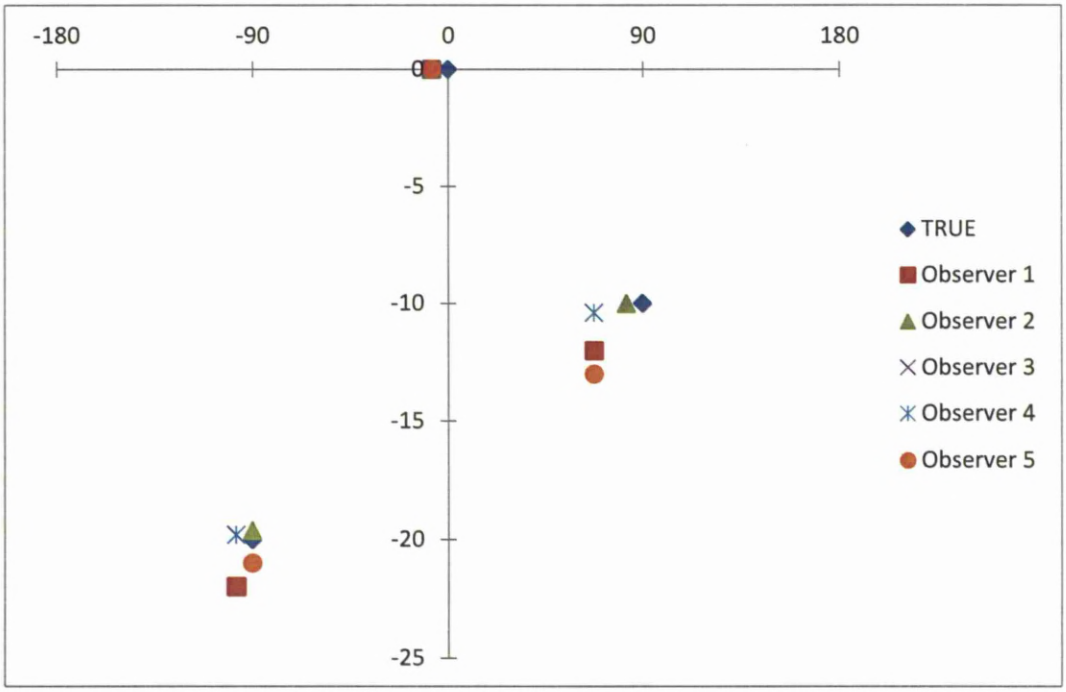

Figure 7.5 Visual representation of Phantom 1 measurements.

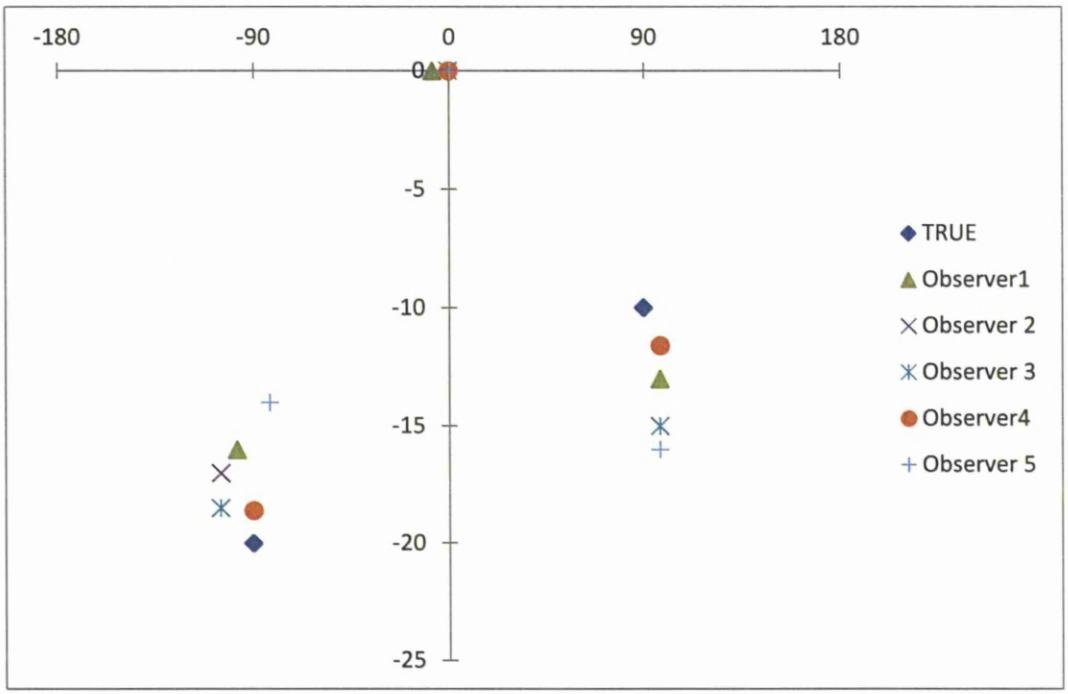

Figure 7.6 Phantom 2.

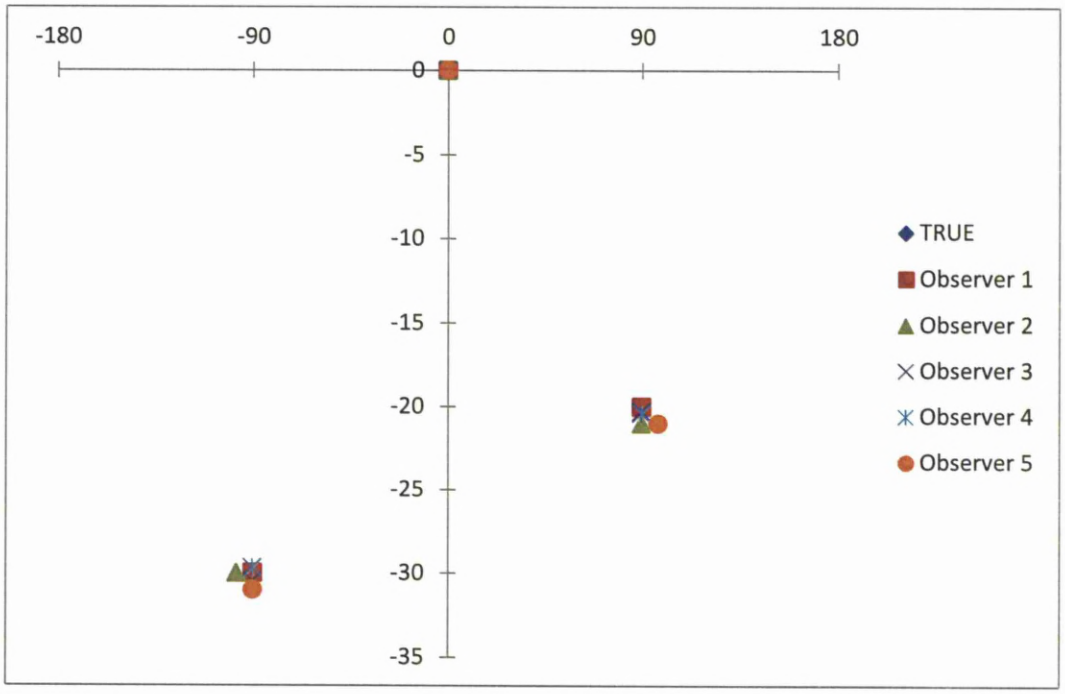

Figure 7.7 Phantom 3.

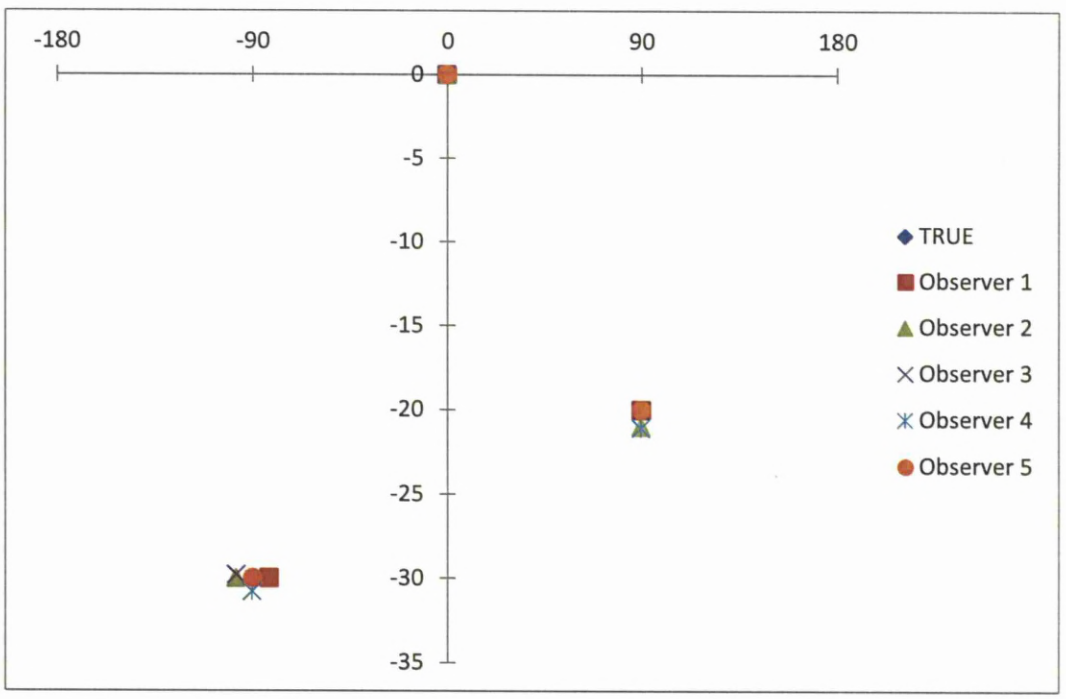

Figure 7.8 Phantom 4.

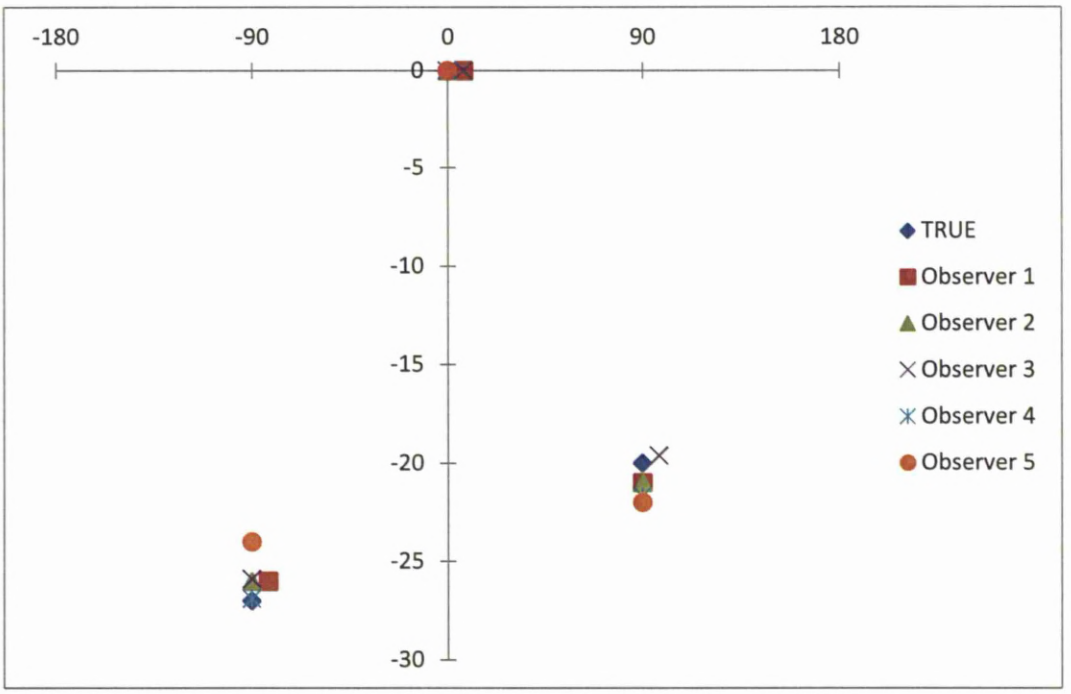

Figure 7. 9 Phantom 5.

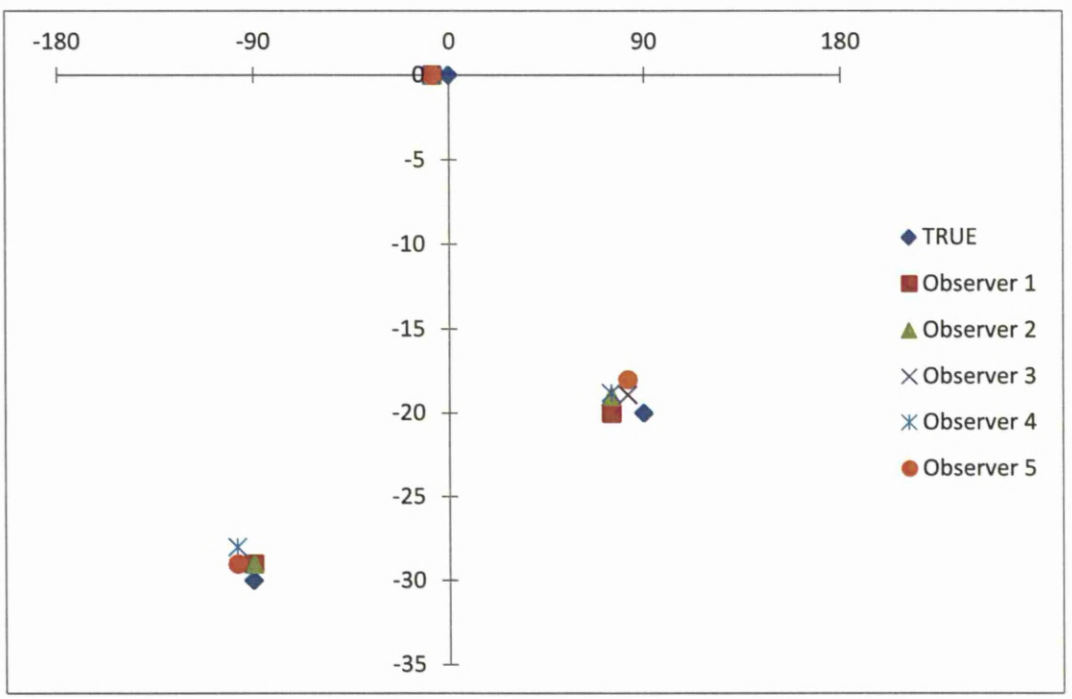

Figure 7.10 Phantom 6.

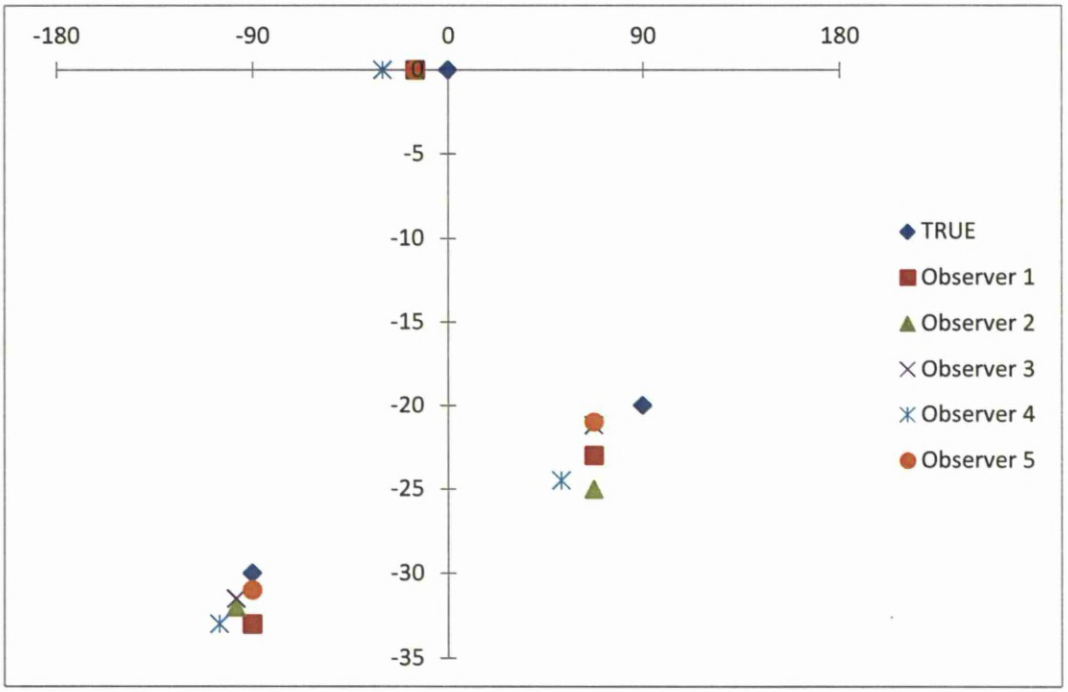

Figure 7.11 Phantom 7.

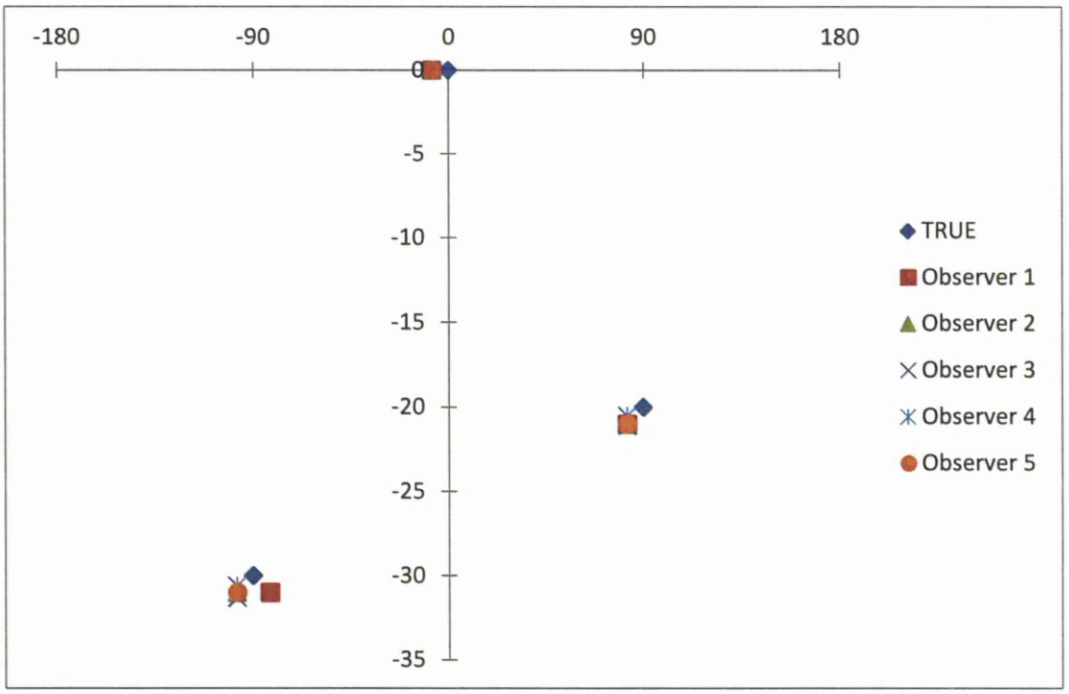

Figure 7.12 Phantom 9.

7.5 Discussion

Assessment of aortic morphology is a critical process in fenestrated endovascular aneurysm repair of aortic aneurysms since fenestrated stent-grafts are designed to exactly fit individual patient anatomy. Measurement software designed to facilitate this process have been developed and validated however the results of the previous chapter demonstrates an inherent subjectivity in the measurement of the human aorta. As yet, the anatomical characteristics that lead to measurement error have received little attention in scientific literature.

The results of this study suggest that the coronal angulation between the target vessels has a significant influence on both the reproducibility and accuracy of target vessel measurement. It was not possible to identify a correlation between the magnitude of coronal angulation and median fractional error as the results of the phantom with 60 degree coronal angulation had to be discarded. This relationship has been previously identified by Sun et al (Sun et al., 2006) and arises if the target vessel position is not measured perpendicular to the long axis of the aorta. Although all the observers in this study were experienced in planning endovascular stent-grafts, the technique used to measure vessel separation may have contributed to the measurement error.

There was a tendency to underestimate target vessel separation when there was concomitant coronal angulation of the aorta as displayed by the cluster pattern of target vessel measurements (Figures 7.5 and 7.8) however this was not replicated

with the angulation of the aorta in the sagittal plane. In this study, multi-planar reconstruction was used to measure the target vessel separation. As such a degree of observer discretion is required when reconstructing the images. When measuring target vessel separation, both renal vessels need to be visualised and are often best viewed on a coronal image slice. If the renal vessels appear to be angulated in this plane, then interpretation of their relative position may be more subjective, leading to inaccurate measurement. Sagittal angulation on the other hand does not create apparent angulation of the renal vessels and as such has little effect upon measurement error. Arguably, more standardised and perhaps more accurate reconstructions may have been obtained by using an automated centreline of flow (CFL) measuring technique particularly as the phantoms were not irregular in shape. Indeed semi-automated CFL have been shown to be very accurate when measuring phantoms in vitro (Isokangas et al 2003). However not all observers participating in this study were sufficiently experienced in the use of this technique to generate results that were not subject to bias.

The maximum fractional error in this study was 0.7 (Phantom 2). Compared with other validation studies using phantoms, this value is significantly higher. In their 2003 study, Isokangas et al report a mean fractional error of 0.017 and 0.009 for diameter and length measurements respectively. However, the phantoms created for this study depict idealised pathological aortic anatomy designed to test the hypothesis that some morphological features influence the accuracy of target vessel measurements. In practice, it is very unlikely that patients with significant coronal angulation between the renal arteries would be considered for fenestrated aneurysm repair; indeed such anatomy is infrequently encountered.

Of greater clinical relevance is the effect of the longitudinal renal branching angle on measurement accuracy. In this study, the longitudinal branching angle of the renal arteries was varied but did not result in significant measurement error. The maximum fractional error for these phantoms (0.03) compares well with the mean fractional error from the study by Isokangas and would support a definite relationship between coronal angulation of the aorta and measurement error. It is impossible to validate this result clinically since the morphology of the aorta cannot be directly measured.

Limitations

A major limitation of this study is the fact that a limited number of phantoms were created. The phantoms utilised in this study were chosen in order to investigate the basic morphological characteristics in isolation. Ideally a combination of these characteristics would be more representative of anatomy likely to be encountered in clinical practice. In order to exhaustively investigate the morphological characteristics chosen for this study, 8748 different phantoms would have been required. It was therefore neither financially viable nor practical to create and investigate all these phantoms.

In addition, each phantom in this study had a regular shape. Although it was possible to introduce an element of irregularity, it would have been difficult to control this feature in a quantitative manner in order to draw clinical comparisons Furthermore it was not possible to introduce artefacts such as variations in

contrast representative of flow disturbances or mural atheroma sometimes seen in the aorta. It is unclear how much influence these additional features would have had on observer variability, however it follows that simple phantoms are more likely to generate more consistent measurements between observers.

7.6 Summary

The accuracy of target vessel measurements for fenestrated endovascular aneurysm repair is significantly reduced by angulation of the aorta in the coronal plane. Accuracy may be improved by using centre line of flow measurements however it is unlikely that this is a clinically significant finding since such anatomy are not usually considered suitable for endovascular repair.

Chapter 8

Tolerance of the Zenith Cook™ Fenestrated Endovascular Aortic Stent-Graft

---

8.1 Introduction

The devices used for fenestrated endovascular aneurysm repair are custom-made stent-grafts designed with the intention to exactly fit the native anatomy of the visceral aorta. Planning and subsequent construction of these devices relies on an accurate assessment of both the circumferential and longitudinal position of the target vessels in order to create fenestrations in the stent-graft fabric which permit continued perfusion of the viscera. The measurement of aortic anatomy is subject to both intra and inter-observer variability (Oshin et al., 2010a). Such variability has the potential to introduce mismatch between native anatomy and stent-graft design which has implications on several factors including achieving seal.

8.2 Aim

The aim of this study was to examine the effect of varying mismatch between fenestrated stent-grafts and native anatomy on proximal seal.

8.3 Methods

This study was a bench–top experiment using a single 36mm fenestrated proximal main body incorporating two fenestrations for the renal vessels and a scallop for the SMA. This stent-graft was then deployed into a series of phantoms depicting the visceral aorta using a standard deployment protocol. The phantoms were created from transparent acrylic tubes with a luminal diameter of 30mm, thus giving an effective oversize of 20% with using the 36mm fenestrated main body. In total seven phantoms were produced, representing varying mismatch between the phantoms and the proximal main body by incremental changes in the position of the left renal target vessel in both the longitudinal (n=3) and circumferential direction (n=4). The configurations of the phantoms studied is summarised in Table 8.1.

8.3.1 Deployment of phantoms

The deployment process began with preparation of the stent-graft. First the diameter reducing ties were engaged using a trigger wire then the proximal bare-metal stents were constrained using sutures (Figure 8.1). Thus when the stent-graft was placed within the phantom being investigated, it represented a fully

unsheathed proximal main body with the "top cap" still in place as one would find in situ (Figure 8.2).

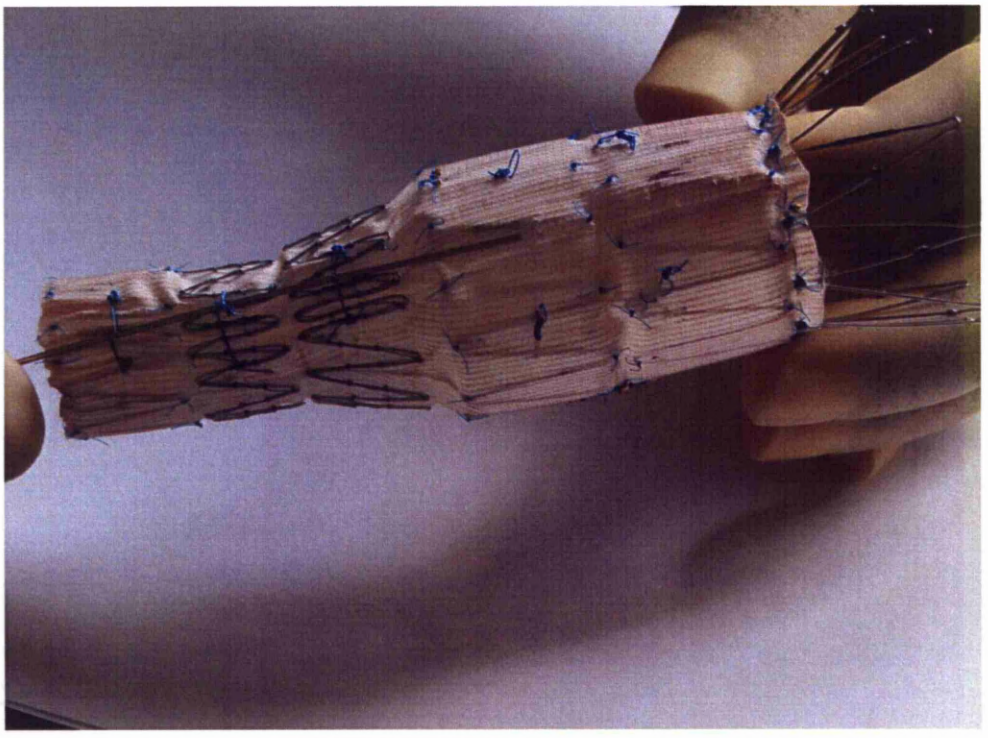

Figure 8.1 Engagement of the diameter reducing ties

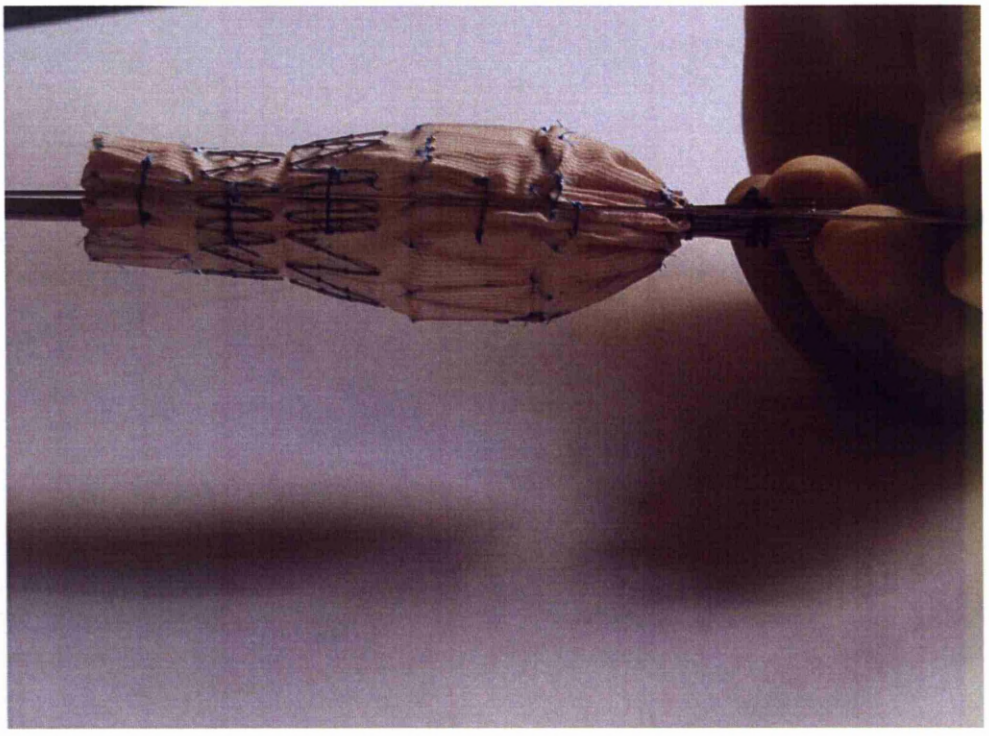

Figure 8.2 Proximal sealing stent constrained

Each target vessel (left and right renal vessels) was then cannulated sequentially using a cobra guiding catheter. For practical reasons this was performed without fluoroscopy under direct vision and necessitated retrograde cannulation of the stent-graft (Figure 8.3). Once wire access to the target vessels was achieved, large sheaths were placed into the target vessels (Figure 8.4) to permit delivery of the target vessel stents. The deployment process was then completed by releasing the diameter reducing ties and cutting the sutures constraining the proximal bare metal stents. Finally balloon expandable stents (Atrium (Atrium Medical, Rendementsweg, Netherlands)) were placed in the target vessels and ballooned into place with flaring of the luminal segment.

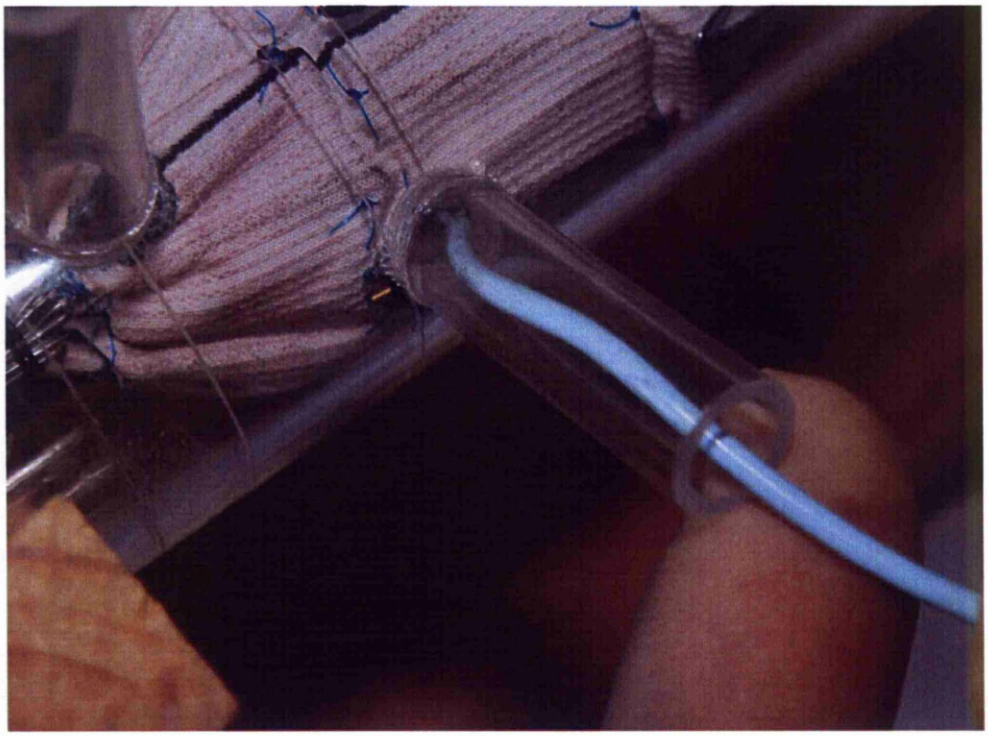

Figure 8.3 Sequential retrograde cannulation of each target vessel

8.3.2 *Analysis*

Seal was defined as fabric lumen apposition. The effect of mismatch on seal was qualitatively assessed using visual inspection and an analysis on a 3D workstation (Aquarius TeraRecon) of the CT images of each phantom. In addition potential target vessel problems arising from mismatch as a result of either shuttering or proximal main body distortion was also noted.

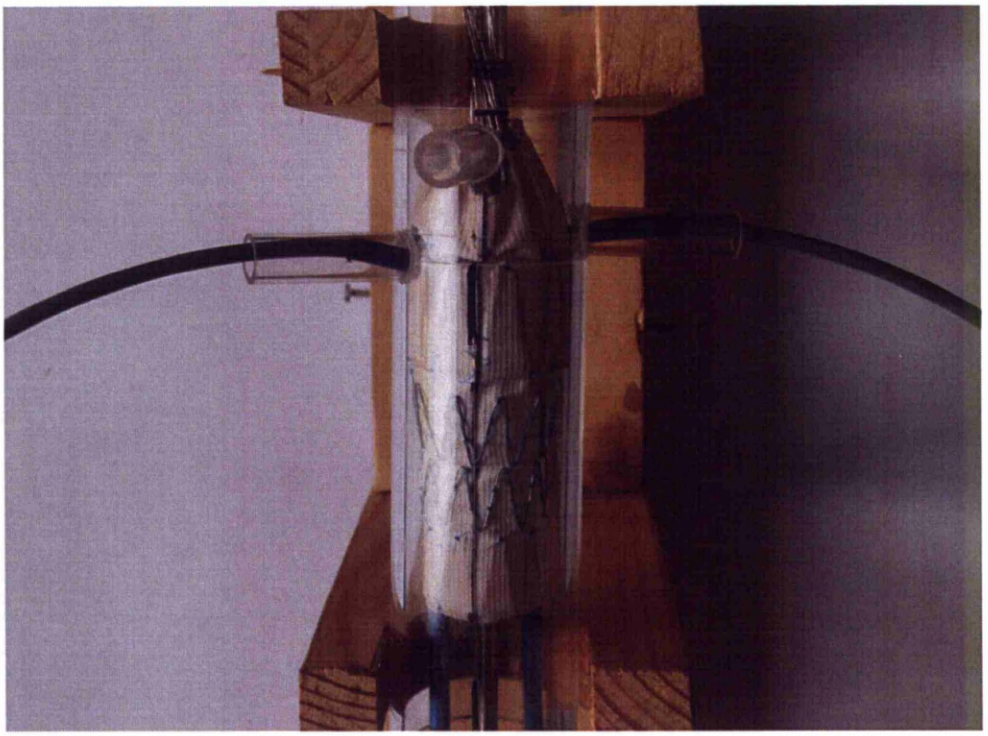

Figure 8.4 Sheaths placed in target vessels

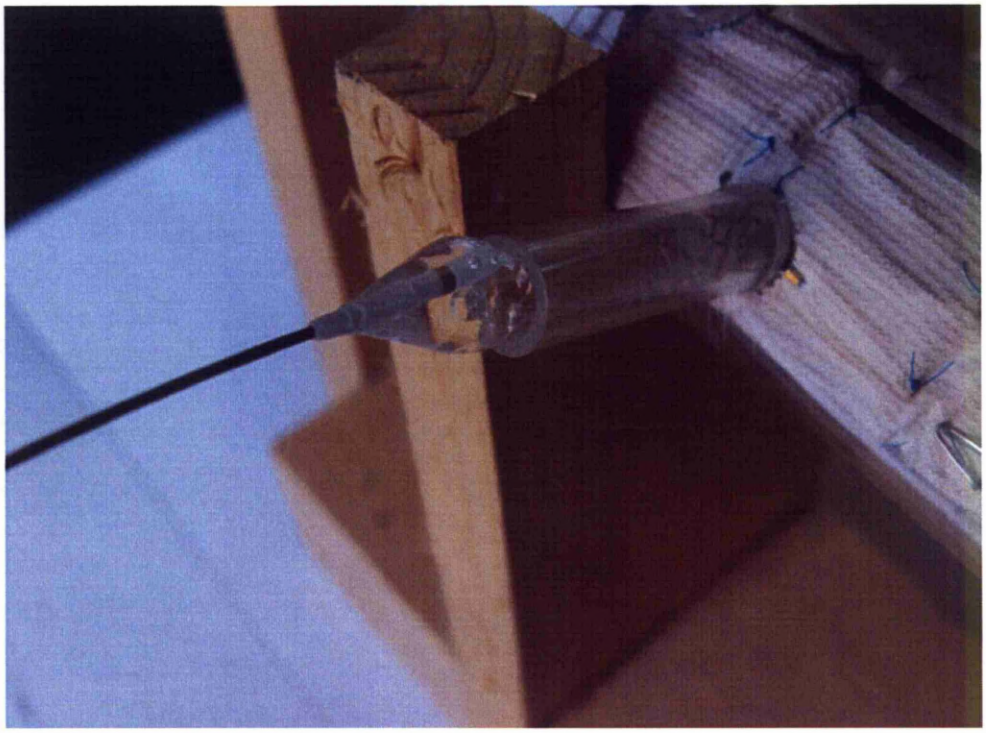

Figure 8.5 Inflation of balloon expandable stent in target vessel

8.4 Results

At 15 degrees discrepancy (equivalent to 30 minutes by clock-face position) visual inspection showed that fabric to lumen apposition (seal) was maintained. There was no compromise to target vessel patency, and on the CTA images there is no evidence of separation between the metal component of the stents and the lumen of the phantoms. This finding was also repeated with 30° discrepancy. When a discrepancy increased to 45° (equivalent to 90 minutes by clock-face position) fabric to lumen apposition was maintained however the minor degree of misalignment between the scallop and the SMA target vessel was observed. The encroachment of the scallop fabric on the SMA target vessel ostium did not result in shuttering.

At 90° discrepancy, alignment between the two renal fenestrations was a possible but visual inspection demonstrated completed misalignment between the scallop and the SMA target vessel that resulted in complete shuttering. This finding was also demonstrated on of radiological assessment of this the phantom. The SMA shuttering could be corrected using balloon expandable stents however with an open cell stent, continued patency of the SMA was compromised due to a combination of stent deformation (Fig. 8.6 A) and encroachment of the stent-graft fabric between the interstices of the stent (Fig. 8.6 B). A further consequence of correcting the SMA shuttering was the loss of fabric/lumen apposition (seal). This was clearly evident on visual inspection and the reconstructed CTA images (Fig 8.7 A and B) clearly show that the metallic components of the stent-graft are no longer in contact with the inner surface of the phantom.

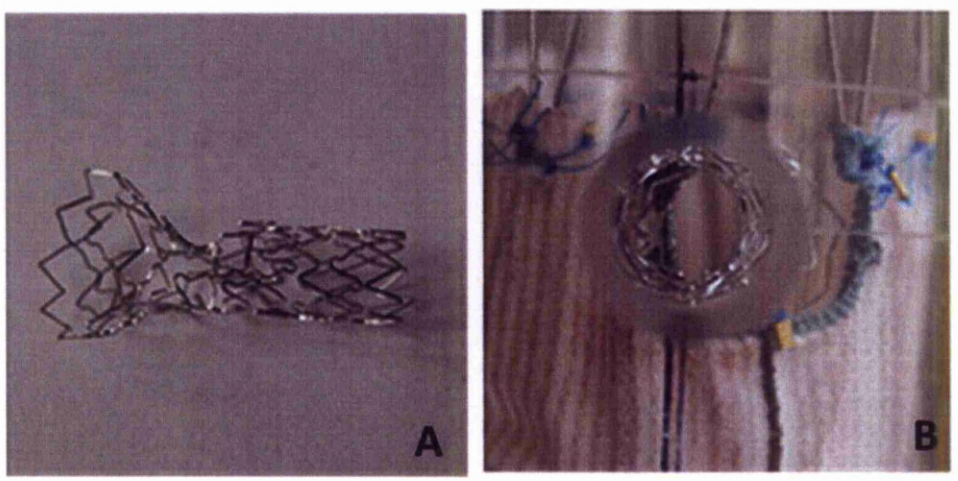

Figure 8.6 (A) Deformation of open cell stent and (B) encroachment of fabric between interstices of open cell stent.

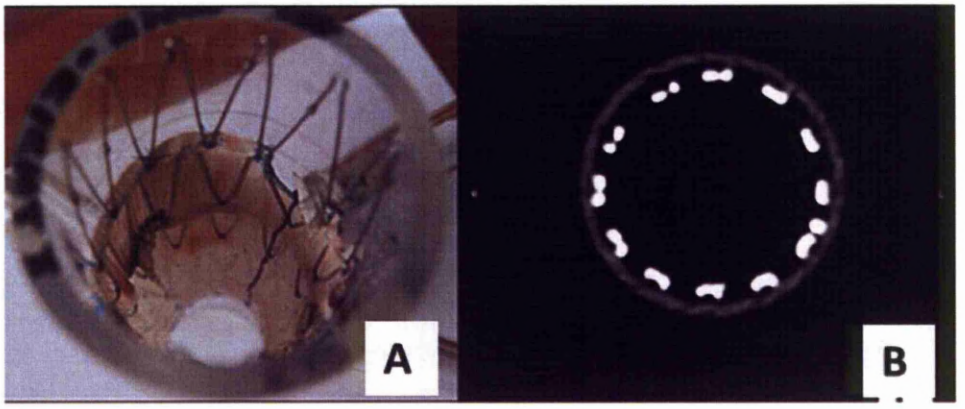

Figure 8.7 (A) Loss of seal on visual inspection and (B) on cross sectional imaging.

In the longitudinal direction extreme mismatch i.e. discrepancies exceeding 5 mm, created challenges in target vessel cannulation however this could be overcome without obvious compromise of target vessel patency (Fig 8.8).

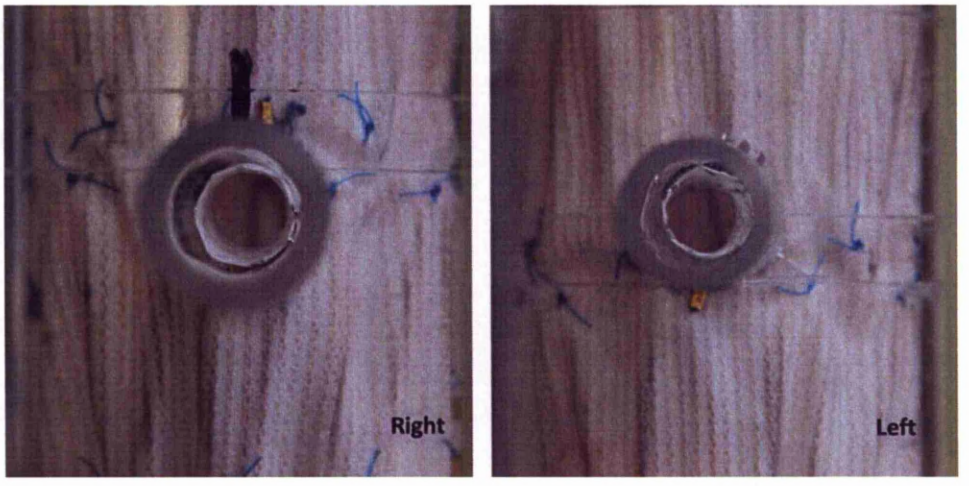

Figure 8.8 Right and left target vessel stent integrity maintained despite mismatch of 5mm or more in the longitudinal direction.

8.5 Discussion

Maintaining proximal and distal seal is an important principle in endovascular aneurysm repair since this ensures that the aneurysm remains isolated from systemic circulation. Furthermore, when the infra-renal aortic neck is inadequate and extension of the proximal sealing zone into the visceral aorta is required, additional consideration must also be given to the geometrical relationship between the target vessels to create fenestrations in the stent-graft fabric which permit both visceral and renal perfusion. However quantifying this relationship is prone to both observer error and variability.

Intra and inter-observer variability when measuring human anatomy is well documented and is often expressed using repeatability coefficients derived from Bland-Altman analysis of repeated measurements. However this is a statistical value that identifies the limits of agreement between two observers measuring the same object but does not indicate whether the observed variability in measurement is significant. In clinical practice, acceptable limits of agreement between repeat measurements when designing fenestrated stent-grafts is based on arbitrary values derived from the clinical judgement of experienced observers rather than objective evidence. This study has shown that a single proximal fenestrated main-body stent-graft may be deployed into a series of phantoms with mismatch in the position of the intended target vessel position of up to 8 mm in the longitudinal direction and 45° in the circumferential orientation without compromise of seal or target vessel patency.

The capacity of fenestrated stent-grafts to tolerate a wide degree of mismatch is perhaps not surprising when one considers the fact that the design of fenestrated stent-grafts are based upon static images of the abdominal aorta. It is therefore not possible to take into consideration the unpredictable changes in aortic morphology which the stent-graft will encounter given the dynamic nature of the cardiovascular system. Indeed, even the introduction of the delivery system itself alters the relationship between the target vessels particularly in patients where there is a degree of aortic neck angulation. However despite variable and potentially inaccurate target vessel measurements due to changes that occur in aortic morphology, only a small proportion of target vessels are lost at mid-term follow-up suggesting that a degree of mismatch between the fenestrated stent-graft and the native aorta may be tolerated.

The ability to tolerate mismatch in the circumferential direction whilst maintaining seal is probably attributable to the practice of oversizing the circumference endovascular stent-grafts. Most manufacturers recommend oversizing a stent-graft by a factor of 20% in order to allow continued contact between the fabric of the stent-graft and the walls of the aorta during the cardiac cycle. In the case of the Cook fenestrated stent-graft, this is further augmented by constraint of the Gianturco Z-stents which promote continued apposition by virtue of the radial force they exert on the walls of the aorta. Therefore in theory seal can only be compromised when the fabric between the fenestrations is less than the circumferential distance between the target vessels.

However such a calculation fails to take into account the effect of misalignment between the scallop and position of the SMA ostium, the degree of which may be variable as a result of an irregularly shaped aorta. Furthermore attempts to correct this problem compromised seal when extreme circular mismatch was encounter. This suggests that the interaction that occurs when more than two fenestrations are misaligned is complex and can affect seal in unpredictable ways.

In the longitudinal direction tolerance of the fenestrated stent-graft is more reliant on the material properties of the Dacron fabric. When the distance between the target vessels is over estimated, alignment between the fenestrations and the target vessel ostia is achieved by compressing the fabric of the stent-graft. This may result in infolding of the stent-graft fabric and potentially threaten seal, however infolding was not observed in this study. In the converse situation where the distance between the target vessels is underestimated giving rise to a shorter distance between the fenestrations on the stent-graft than the inter-renal separation of the native aorta, the ability of the proximal main body to tolerate mismatch is dependent on the tensile forces acting on the fabric of the stent graft.

The choice is stents used to correct misalignment also appears to be important. In this study, both open cell and closed cell on expandable stents were used to correct scallop misalignment. However with the open cell stent, significant distortion was observed. This may be related to the type of material the stent was composed from since this has the direct bearing on its hoop stress. Another

reason for the greater degree of defamation observed with an open cell stent is that the design of the stents may make them more prone crushing because the stent mesh is unlinked. Whilst this has the advantage of allowing open-cell stents to be more flexible however it is also makes it possible for the stent-graft fabric to slip between the interstices is of the stents thereby threatening target vessel patency.

For the purposes of this study, practical considerations necessitated cannulation of the phantom under direct vision. *In vivo*, the ability to cannulate target vessels successfully when mismatch occurs is a major concern since prolonged attempts at cannulation lengthens the procedure and has implications on factors such as limb ischaemia time, radiation exposure and increased use of contrast media. Target vessel cannulation is complex process involving tactile feedback from the guide wire and guiding catheter as well as an appreciation of the relationship between the 2-dimensional fluoroscopy images and the 3-dimensional position of the target vessel ostia. Often vessels with larger ostia are easier to cannulate than those with smaller ostia therefore target vessel shuttering increases cannulation difficulty by effectively reducing the size of the target vessel ostium which in turn demands a higher degree of accuracy when positioning the guiding catheter to allow passage of the guide wire and sheaths. This problem is further compounded when there is close proximity between the proximal main body of the stent-graft and the aortic wall. The fact that successful cannulation is achievable when extreme mismatch is encountered (albeit under direct vision) suggests that refinement of cannulation techniques may be necessary.

There is anecdotal evidence from published fenestrated EVAR series that use of double diameter reducing ties aid correct orientation of the proximal main body stent-graft when difficult anatomy such as an angulated aortic neck anatomy and tortuous iliac arteries are encountered (Scurr et al., 2008a). The double diameter reducing ties reduce the profile of the delivery system thus facilitating its manipulation *in situ*. This reduction in profile may also be advantageous when attempting to cannulate target vessels since additional space is created between the stent-graft and the luminal wall of the aorta within the proximal sealing zone. Manipulation of the guiding catheters could then take place in the "peri-graft" space, perhaps with the aid of pre-loaded guide wires. In such a situation, the choice of catheter to achieve the right shape for cannulation and profiling of the target vessel are crucial steps however the feasibility of such techniques are beyond the scope of this study and merit further investigation.

Limitations

A major limitation of this study is that it was not performed under dynamic conditions. Therefore one might postulate that the expansion of the aorta with systole may in fact result in compromised seal. Dynamic morphology studies of patients with abdominal aortic aneurysms suitable for EVAR (van Herwaarden et al., 2006) et al have shown aortic significant changes in the diameter of the aortic neck (defined as the region 1 cm below and 3cm above the lowermost renal artery) during the cardiac cycle. This demonstrated a change in diameter of up to 11.5% and an increase in aortic area of up to 15.8%, however this was unaffected by the insertion of an endograft. Furthermore it has also been observed that aortic

expansion is not isometric and there is a tendency for elliptical expansion which changes in direction depending on the segment of aorta being examined. For example at the suprarenal level, elliptical expansion tends toward the right anterior direction whilst at the infrarenal level there is a tendency towards maximal expansion left-anterior direction. Indeed an increase of up to 30% in has been reported. Applying these results to the outcomes of this study would therefore suggest that a discrepancy of 15 degrees (30 minutes) may be tolerated before seal is compromised. As a consequence, if there are discrepancies with repeated measurements of clock face position, one may wish to err on the side of caution and accept the measurement which results in greater separation of the target vessels in order to mitigate the effect of asymmetrical expansion

However such extrapolation may be of limited value for several reasons. First studies using dynamic MRA report the extreme variation in aortic diameter *throughout* the cardiac cycle. However the static CTA images used to design fenestrated stent-grafts may be representative of the vascular anatomy at any point during the cardiac cycle. Second the interaction between the stent-graft and the aortic wall may alter the stiffness and therefore ability of the aorta to distend with the cardiac cycle. Indeed movement of the aorta after EVAR remains controversial as some authors have shown reduced pulsatile wall motion after the implantation of endografts.

Dynamic MRA studies assessing the interaction between the aorta and endovascular grafts are limited to patients who do not have grafts with ferromagnetic properties such as the Cook Zenith platform which uses stainless

steel Z-stents. It is reasonable to assume that standard Cook stent-grafts behave in a manner similar to that reported with other stent-graft designs. However extension of the stent-graft fabric into the visceral aorta requires the placement of balloon expandable stents into the target vessels. The effect of the interaction between these stents, the proximal main body and aorta has not been studied and is therefore unknown. What is known is that the presence of target vessel stents reduces the movement of the renal arteries by at least 300% and that their presence also enhances migration resistance. Conceivably they may also increase the stiffness of the aorta/stent-graft complex and thus limit expansion.

8.6 Summary

Recently there has been increasing interest in the concept of "off-the-shelf" fenestrated stent-grafts which has the advantage of potentially eliminating the inevitable manufacturing delay associated with the construction of custom-made devices. A further advantage is also the potential to broaden the applicability of the fenestrated technology to emergency procedures. Published studies examining this concept have made arbitrary assumptions about the tolerance of fenestrated stent-grafts based on the personal experience the authors. These assumptions are largely driven by potential difficulty in cannulation when extreme mismatch occurs.

Chapter 9

Magnitude of the forces acting upon target vessel stents after fenestrated endovascular aneurysm repair

9.1 Introduction

Endovascular aneurysm repair in juxta-renal aortic aneurysms or aneurysms with short infra renal necks are primary indications for the use of fenestrated-stent grafts. These fenestrations may be large or small and whilst the customised nature of these stent grafts demand accurate assessment of aortic morphology, the continued patency of the visceral vessels is dependent on perfect alignment between the fenestrations and target vessel ostia. Early clinical experience with fenestrated stent grafts has shown that target vessel patency is best preserved by maintaining alignment between target vessels and fenestrations with balloon expandable stents (Muhs et al., 2006b), thus avoiding potential shuttering of target vessel ostia as a result of measurement error or the dynamic interaction between the native aorta and fenestrated stent-graft complex.

A degree of mismatch may be tolerated by fenestrated endografts without compromising seal. However this is mainly reliant on the ability of the balloon

expandable stents used to maintain alignment between fenestrations and target vessel ostia resisting both the rotational and longitudinal forces generated by the stent-graft/native aorta mismatch. What remains unclear is the degree of misalignment that may be tolerated by the target vessel stents without subsequent compromise of target vessel perfusion.

9.2 Aims

The aim of this study was to determine the magnitude of the forces acting on target vessel stents when there is misalignment between stent-graft fenestrations and the target vessel ostium.

9.3 Methods

9.3.1 *Experimental design*

The stent-graft/aorta complex is essentially a laminar composite comprising aorta, stent-graft fabric (Dacron) and the metal of the sealing stent (Figure 9.1). The forces acting on the target vessel stent therefore arises as a net result of the forces that each individual component of this composite structure is subjected to. For the purposes of this study, a two-fenestration 36mm Cook Zenith stent-graft designed for deployment into an a 30mm diameter aorta was considered. The intended target vessels for the fenestrations were anterior branches of the aorta located at the same level (inter-renal separation of zero) with "clock-face" position of 2 and 10 o'clock respectively (Figure 9.2). The net force on the target vessel stent as a result of progressive mismatch between the aorta and stent-graft

was calculated for systole and diastole. For simplicity, the effect of friction between the stent-graft and lumen of the aorta was not considered in this model and the forces calculated were those acting in the direction circumferential and parallel to the long axis of the stent-graft.

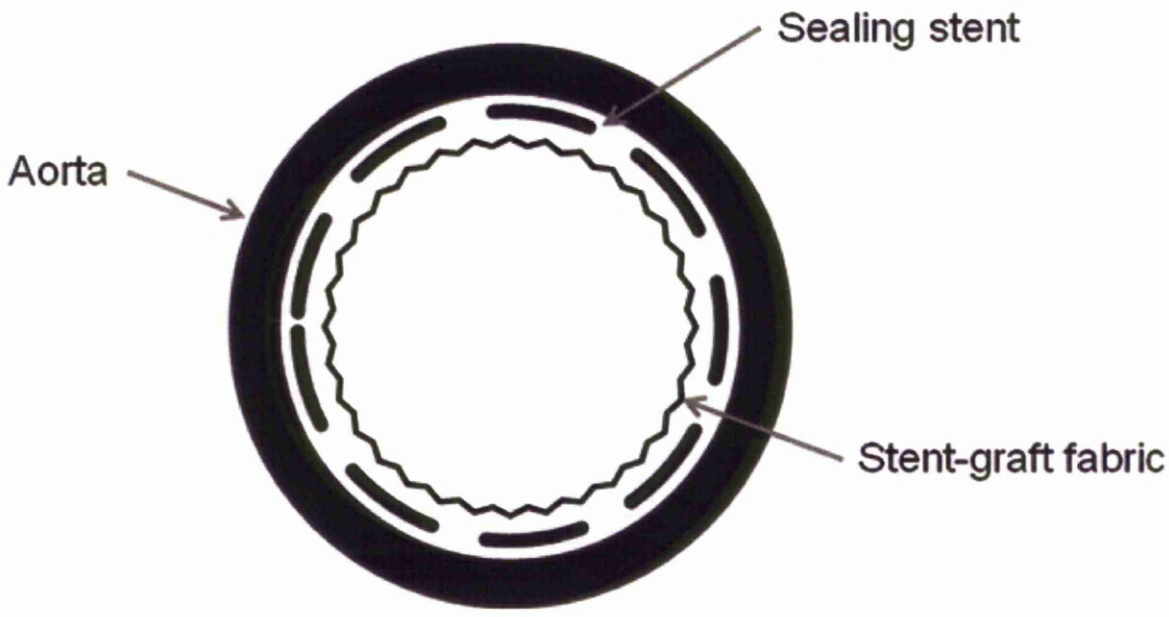

Figure 9.1 Stent-graft/aorta laminar complex

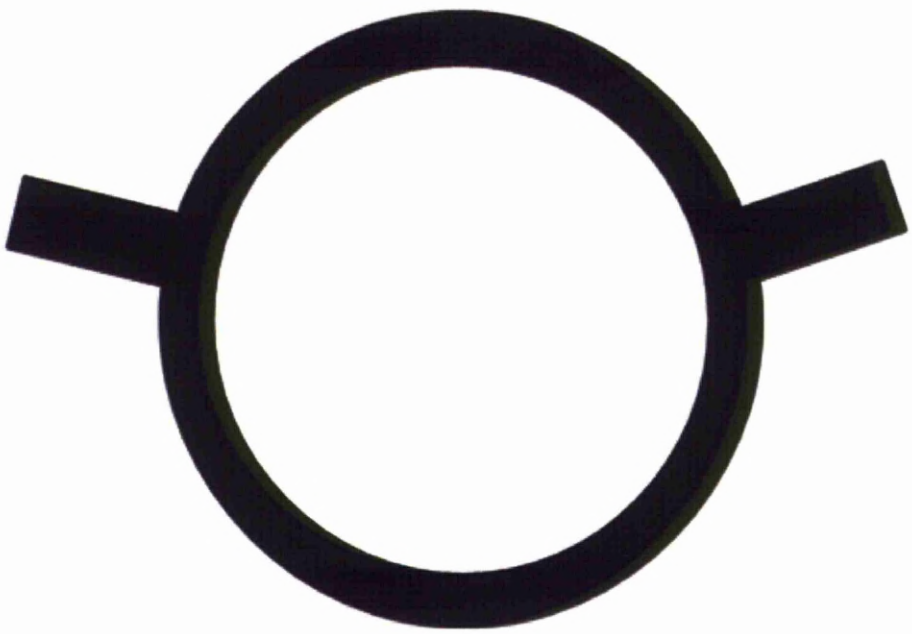

Figure 9.2 Schematic representation of aortic morphology

9.3.2 *Circumferential forces*

The aortic cross section changes throughout the cardiac cycle as the shock wave created by left ventricular ejection passes through. For the purpose of this study, contraction of the aortic lumen was called the diastolic phase and the enlargement of the aortic cross section was the systolic phase.

As a consequence of oversizing, the sealing stent as a whole is compressed, therefore the majority of the circumferential compressive force acting upon the target vessel stent is the net force generated by the anterior and posterior sections of the sealing stent (Fig. 9.3). Since the sealing stent behaves in an elastic manner, the magnitude of these forces is proportional to the arc length of the anterior and posterior sections of the sealing stent and can be determined from experimental measurements using Hooke's law.

Hooke's law describes the behaviour of elastic materials under stress whereby the increasing load (tension) results in an increase in the overall length of the material. This principle also applies to springs where the tension in the spring is proportional to its length. Hooke's spring constant κ therefore relates to the stiffness of the material in question.

$$\sigma = K\varepsilon$$

Where σ = load (N) and ε = displacement (m)

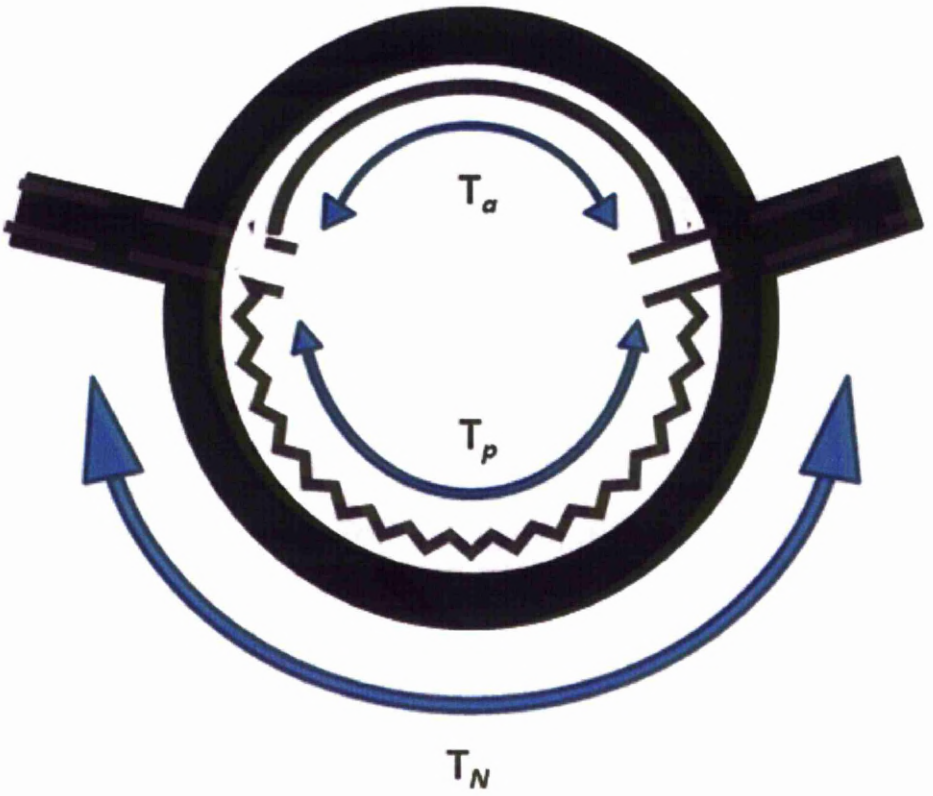

Figure 9.3 Net compressive force T_N acting upon the target vessel stents is determined by the relative tension in the anterior and posterior section of the sealing stent (T_A and T_B).

In systole, the stent-graft fabric is put under stretch if the oversizing is insufficient to permit full expansion of the aorta. This is most likely to occur in the anterior section of the stent-graft if the distance between the target vessel ostia has been underestimated. Since the stiffness and tensile strength of Dacron is higher than that of human aorta, (Salacinski et al., 2001, Sarkar et al., 2006) this will lead to the target ostia being displaced anteriorly in order to accommodate the diameter change of the aorta during systole (Fig. 9.4). This displacement is equivalent to the difference between the anterior circumferential separation of the fenestrations when the stent-graft is at full stretch and the true distance between the target vessel ostia. The resulting compressive force acting

upon the target vessel stents is the force required to align the target vessel ostia and fenestrations by stretching the posterior section of the aorta.

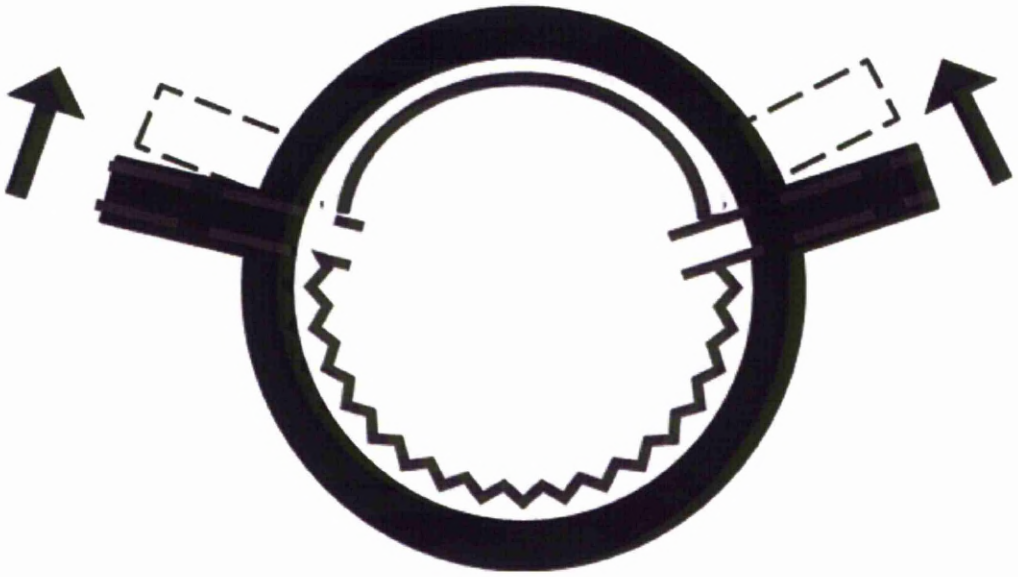

Figure 9.4 Underestimation of anterior target vessel separation is, the stent-graft fabric limits expansion during systole. In order to maintain target vessel/ostia alignment, translation of the target vessel ostia in the direction indicated by the arrows occurs.

9.3.3 *Longitudinal forces*

The forces acting in parallel to the long axis of the stent-graft are determined primarily by the material properties of the graft fabric and the aorta. If the inter-vessel separation is underestimated additional force is required to align the ostia and fenestration. This is again dependent on the relative material properties of the aorta and Dacron as discussed previously. On the other hand if inter-vessel separation is overestimated, infolding is likely to occur as Dacron has no columnar strength. Therefore in this situation, it is unlikely that the target vessel stent is subject to any additional force.

9.3.4 *Materials testing*

9.3.4.1 *Aorta*

Porcine aorta was used to model human aorta and subjected to tensile testing. All adherent non-vascular tissue was removed by a sharp dissection. The aorta was divided along its ventral border in order to incorporate its anterior branches. Each aorta was then divided into specimens measuring 120 mm by 35 mm. The specimens were divided as distal as possible in order to ensure that as much of the specimen was derived from the abdominal section as possible. This also had the added benefits of reducing the variation in specimen thickness since there was a marked change in bulk the abdominal aorta it came continuous with the thoracic aorta.

The thickness of the aortic specimens was determined by placing the specimen between two glass slides. This prevented indentation of the specimens by the callipers. The thickness of the specimen was therefore determined by subtracting the combined thickness of the glass slides and the specimen from the thickness of the two glass slides. These measurements were taken at random points in order to determine whether or not there was a significant variability between the specimens been tested. Finally, a 6 mm diameter fenestration representing a side branch ostium was created using a manual for punching device after which the specimens were stored in normal saline solution at room temperature. All tensile tests were conducted within 4 hours of the acquisition of the aortas from the abattoir.

9.3.4.2 *Tensile testing*

The specimens were mounted onto a specially created jig (Figure 9.5) designed to administer varying degrees of strain in both the circumferential and longitudinal direction. For the purposes of this study 10 and 20% strain were applied in the circumferential and longitudinal directions respectively. The jaws of the jig were lined with abrasive paper in order to prevent slippage of the specimen during testing.

A computerised material testing machine (Nene Instruments Ltd) fitted with a 50 N load cell was used to test the specimens. Attached to the 50 N load cell was steel hook which was placed through the fenestration in the specimen been tested (Figure 9.6). The apparatus was calibrated such that the rate of deformation was set to 10 mm per minute with a maximum of displacement of 10 mm. Load/displacement data was recorded at intervals of 1/100 second was recorded for subsequent analysis. The tests were performed once on each specimen at room temperature in both the longitudinal and circumferential direction. Since the duration of each test cycle was limited to 1 minute, the risk of specimen desiccation was not considered significant. Each specimen was inspected after testing. The tensile test results were discarded in specimens where slippage had occurred or where there was evidence that the fenestration had been torn by the hook.

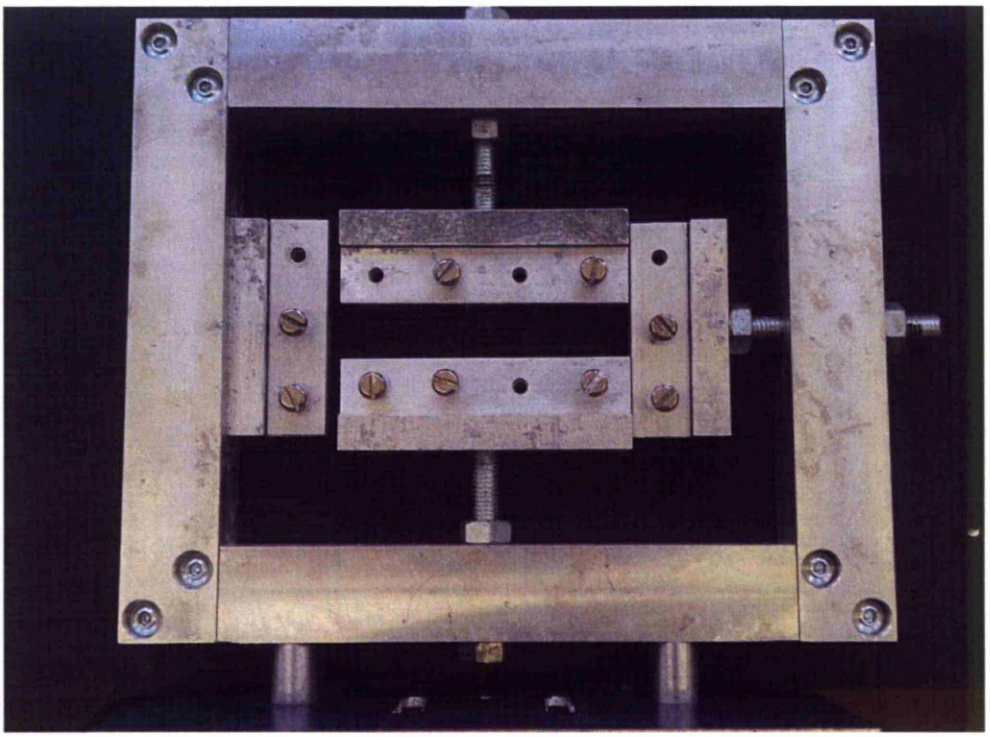

Figure 9.5 Tensile testing jig

9.3.4.3 *Z stent spring constant*

In order to determine the tension in the sealing stents when mismatch occurs, the sealing stents were subjected to tensile testing. This sealing stents were removed from the stent-graft and divided into "V" shaped segments which represented the smallest individual units of a Gianturco Z-stent. 10 segments were obtained from one sealing stent. The segments were mounted onto the tensile testing machine (Nene Instruments Ltd) and held in place with pneumatic grips (Figure 9.7). A 50N load cell was utilised and the gauge length (initial length of the sample) was set at 9 mm with a cross-head displacement speed of 10 mm per minute. Maximum displacement was set at 5 mm. Data were recorded at 1/100 second intervals from which a load displacement curve was generated. Each

segment was tested twice and the average the recorded values was used to determine the spring constant of the Z-stent.

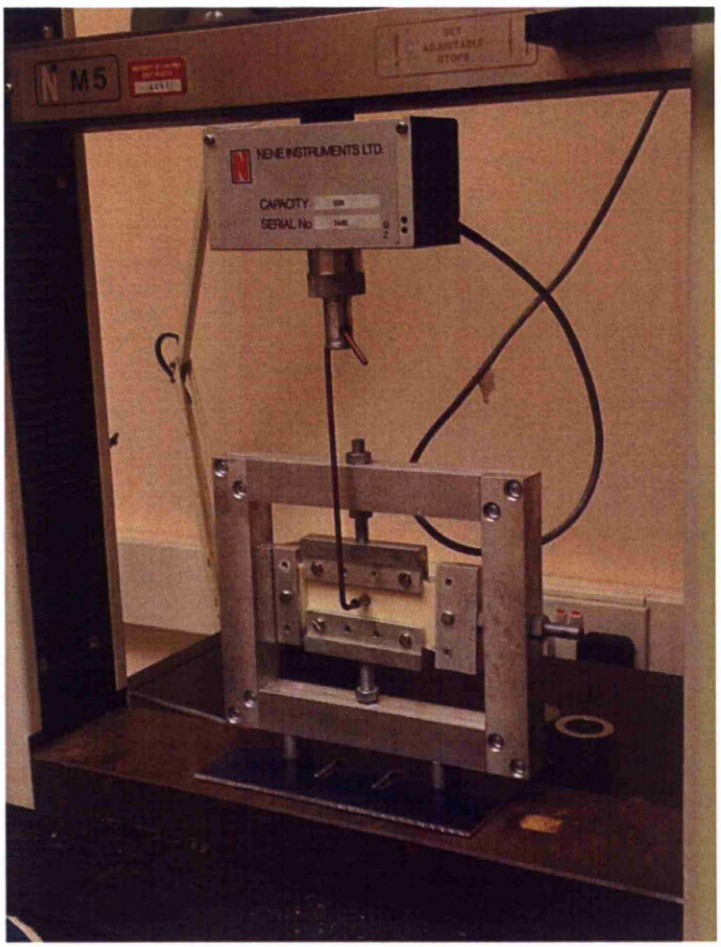

Figure 9.6 Tensile testing of porcine aorta specimen

9.3.4.4. *Stent-graft fabric (Dacron)*

In order to verify the initial assumptions of this model, the material properties of Dacron were determined by tensile testing. The Dacron was obtained from a Cook main body stent-graft and was divided in to specimens measuring 20 mm by 75 mm. The thickness of the Dacron graft was determined by digital callipers and measured 0.17mm.

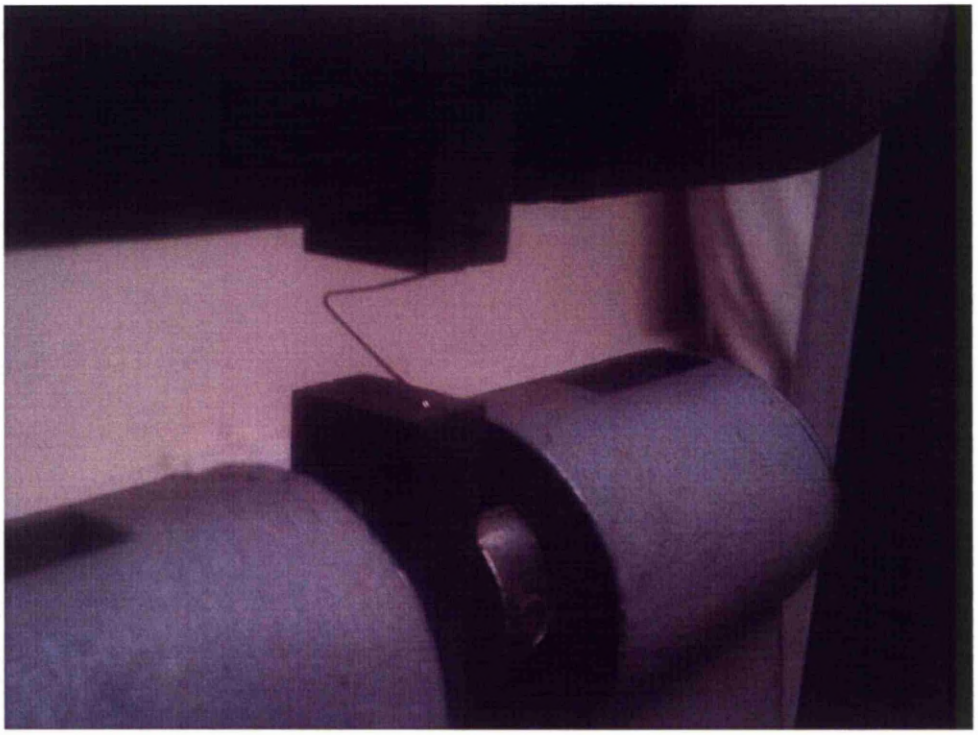

Figure 9.7 Tensile testing of sealing stent

A 500 N load cell was used. The gauge length was set at 50 mm and maximum displacement at 75 mm. The test speed was measured according to the movement of the cross head which was set at 10 mm per minute. Each specimen was tested to failure and from the load displacement graph maximum load and Ultimate tensile strength, Young's modulus and strain at failure was calculated.

9.4 Results

9.4.1 *Tensile tests*

A total of 20 aortic specimens were subjected to tensile testing (n=10 longitudinal and n=10 circumferential). There was evidence of a torn fenestration

in 1 longitudinal specimen and slippage/ tearing occurred in 4 of the circumferential specimens. The results of these 5 tests were discarded leaving 15 results eligible for analysis.

The median force required to displace the fenestration by 10mm in the circumferential direction (at an initial strain of 10%) was 3.97 N (interquartile range: 0.81 N) and in the longitudinal direction (at an initial strain of 20%), 6.1 N (interquartile range: 1.6 N). The load displacement curves for the aortic specimens in the circumferential and longitudinal direction are given in figures 9.8 and 9.9.

The sealing stent of a fenestrated graft was tested to determine the spring constant of a Gianturco Z-stent for a given wire gauge. The diameter of the sealing stent wire was 0.45mm and the length of each leg was 22mm. Six "V" shaped segments from the sealing stent were tested twice. At 5mm displacement, the average maximum load on the sealing stent section was 2 N (interquartile range 0.4 N) giving a spring constant of 0.4 N/mm.

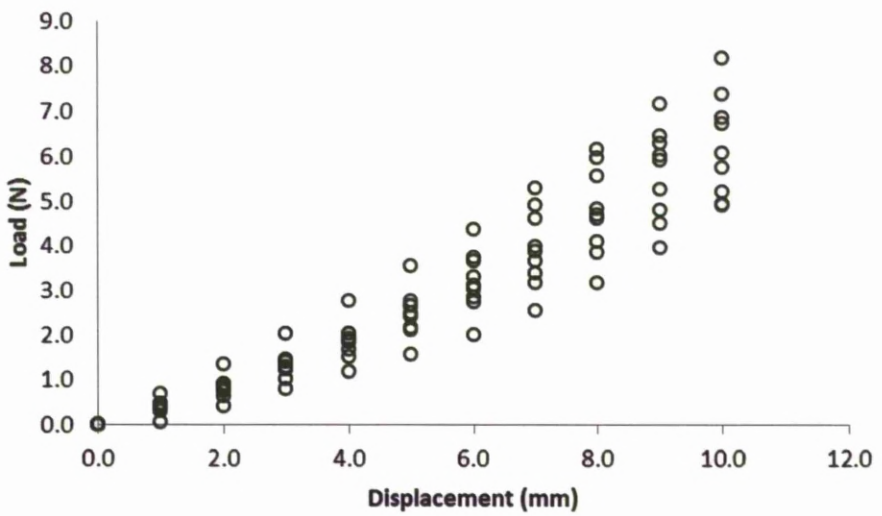

Figure 9.8 Longitudinal load/displacement scatter plot for porcine aorta

Eight Dacron samples were obtained from the stent-graft. Three were discarded because of significant damage to the samples (frayed edges, large stitch holes) which would have compromised the results of the tensile tests. A load displacement curve depicting the median values for the samples tested is given in Figure 9.10 and raw data from the tensile tests are given in appendix xx. The median (interquartile range) values for the mechanical properties of the stent-graft fabric were as follows: maximum load at failure 211N (22.6 N), maximum strain at failure 0.22 (0.02), Ultimate Tensile Strength 62.05 x 10^6 N/m^2 and Young's modulus 282.04 x 10^6 N/m^2. Since the stiffness of the stent-graft fabric is significantly larger than that of aortic tissue, subsequent calculations of the forces acting on the target vessel stents are based on the assumption that the stent-graft fabric does not deform.

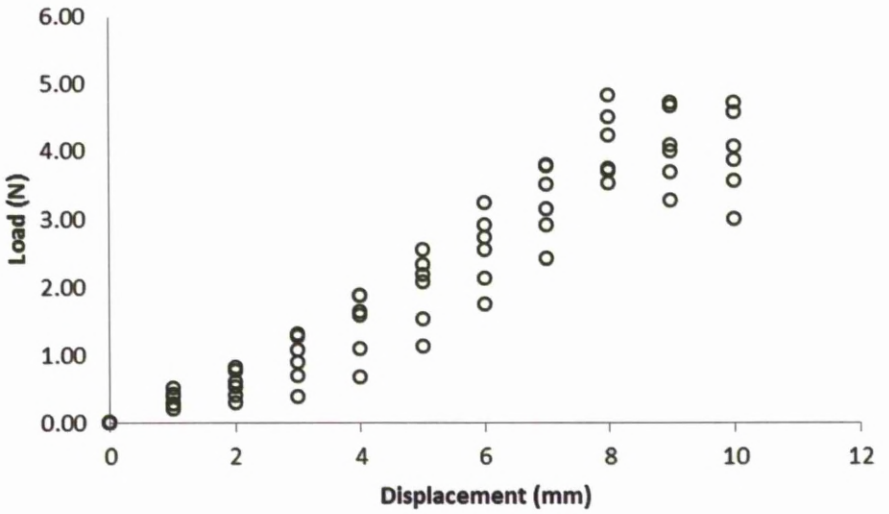

Figure 9.9 Circumferential load/displacement scatter plot for porcine aorta

9.4.2 *Forces acting upon target vessel stents*

In the circumferential direction, the calculated anterior and posterior separation of the target vessel ostia and the fenestrations is given in table 9.11. Under diastolic conditions, when target vessel separation is underestimated by 30 minutes (15^0), 45 minutes (22.5^0) and 60 minutes (30^0), a net force of 0.6 N, 0.8 N and 1.1 N is generated by the sealing stent for each respective gradation of discrepancy. If target vessel position is overestimated, each gradation of discrepancy results in a net force on the stent of 0.3 N, 0.6 N and 0.9 N respectively.

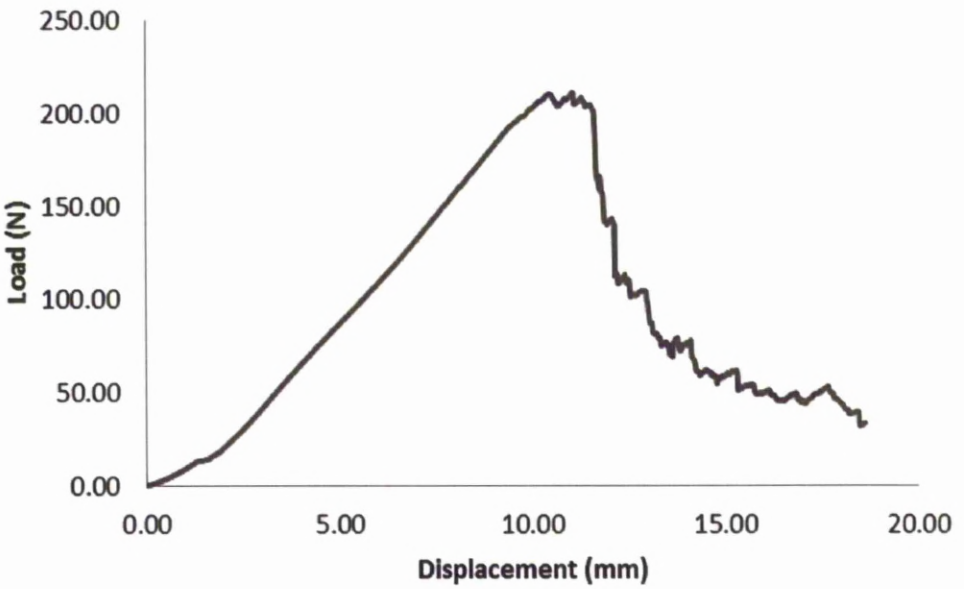

Figure 9.10 Load/displacement curve for Dacron

During systole, the potential difference between the centre of the fenestrations and the target vessel ostia when intra luminal diameter expands by 4, 8 and 12% is given in tables 9.12, 9.13 and 9.14 for each gradation of target

vessel/fenestration mismatch. The greatest mismatch occurs with a combined of underestimation target vessel separation of 60 minutes (30^0) and an increase in aortic diameter due to systole of 12%. This results in a discrepancy between the target vessel ostia and fenestrations of the stent-graft of 6.32 mm and is equivalent to a median force of 2.81 N (interquartile range 0.61N). The magnitude of the longitudinal forces acting on the target vessel stent may be derived the load/displacement curve of the aortic specimens (Figures 9.8 and 9.9).

Total discrepancy	**Arc length (mm)**				**Effective oversize (%)**		**Stent tension (N)**		**Net force(N)**
	Lumen		**Graft**						
Degrees (minutes)	**A**	**P**	**A**	**P**	**A**	**P**	**A**	**P**	
Nil	31.4	62.8	37.7	75.3	20.1	19.9	-0.6	-0.6	0.0
15 (30)	35.3	58.9	37.7	75.3	6.8	27.8	-0.2	-0.8	0.6
22.5 (45)	37.3	56.9	37.7	75.3	1.1	32.3	0.0	-0.9	0.8
30 (60)	39.3	54.9	37.7	75.3	-4.1	37.2	0.2	-1.0	1.1
- 15(30)	29.4	64.8	37.7	75.3	28.2	16.2	-0.8	-0.5	-0.3
- 22.5 (45)	27.4	66.8	37.7	75.3	37.6	12.7	-1.0	-0.4	-0.6
- 30(60)	25.4	68.8	37.7	75.3	48.4	9.4	-1.2	-0.3	-0.9

Table 9.11 Summary of the net force generated by discrepancy between the target vessel ostia and stent-graft fenestration using diastolic model. A (anterior), P (posterior).

Circumferential discrepancy Degrees (minutes)	Stent-graft/aorta mismatch (mm)		Total ostia translation (mm)	Tension due to mismatch (N)
	A	P		
0 (0)	5.0	10.0	0.0	0
- 15 (30)	1.0	14.0	0.0	0.0
- 22.5 (45)	-1.1	16.1	1.1	0.35
- 30 (60)	-3.2	18.2	3.2	1.11

Table 9.12 Summary of data for systolic model at 4% change in diameter. A (anterior), P (posterior)

Circumferential discrepancy Degrees (minutes)	Stent-graft/aorta mismatch (mm)		total ostia translation (mm)	Tension due to mismatch (N)
	A	P		
0 (0)	3.80	7.50	0.0	0
- 15 (30)	-0.42	11.69	0.4	0.15
- 22.5 (45)	-2.58	13.85	2.6	0.77
- 30 (60)	-4.74	16.01	4.7	2.01

Table 9.13 Summary of data for systolic model at 8% change in diameter. A (anterior), P (posterior)

Circumferential discrepancy Degrees (minutes)	Stent-graft/aorta mismatch (mm)		total ostia translation (mm)	Tension due to mismatch (N)
	A	P		
0 (0)	2.50	5.00	0.0	0
15 (30)	-1.84	9.33	1.8	0.51
22.5 (45)	-4.08	11.57	4.0	1.61
30 (60)	-6.32	13.81	6.3	2.81

Table 9.14 Summary of data for systolic model at 12% change in diameter. A (anterior), P (posterior)

9.5 Discussion

Accurate assessment of aortic morphology is essential in the design of fenestrated grafts however these measurements are subject to both intra and inter-observer variability. Thus by inference a degree of mismatch between patient anatomy and the design of fenestrated grafts may be tolerated without target vessel compromise. Since mismatch requires enforced alignment between the stent-graft fenestration and the target vessel ostia, the limits of stent-graft aorta mismatch (continued target vessel patency) is determined by the structural integrity of the target vessel stent. The potential forces to which target vessel stents are subjected have not been reported previously.

The results of this study show that the range of mismatch conditions investigated may potentially generate forces that could reduce the cross-sectional area of commonly used target vessel stents, however in no stent does the this reduction generate a stenosis greater than 15% (Scurr et al., 2008b). Since a flow limiting renal stenosis is defined as a reduction in cross-sectional area of at least 60% (Hansen et al., 1990, Kohler et al., 1986, Taylor et al., 1988), it appears a considerable degree of mismatch may be tolerated without compromising renal perfusion. The ability to resist deformation is a desirable feature in target vessel stents particularly at the level of the fenestration/target vessel ostia. However in the context of complex renal artery movement due to the cardiac cycle and respiration (Draney et al., 2005, Kaandorp et al., 2000, Muhs et al., 2006a), stiffer target vessel stents such as the Jostent (though better able to resist deformation and thus cross-sectional area reduction) may create a new fulcrum

for this movement at the transition between the stent and distal native artery with a risk of neointimal hyperplasia and subsequent occlusion.

Theoretical discrepancies in circumferential target vessel position of up to 60 minutes (30^0) were considered in this study. In practice discrepancies in circumferential target vessel position rarely exceed 30 minutes (15^0) between different observers, however differences in perceived longitudinal target vessel separation is more common (Oshin et al., 2010a). Determining whether this observed difference is significant is often based on an arbitrary figure informed by the size of the target vessel fenestration which does not take into account the possibility that either the stent-graft or the aorta may deform in order to maintain alignment between the fenestration and target vessel ostia. Since the stent-graft fabric is much stiffer than aortic tissue, underestimation of target vessel separation results in additional tension on the aortic wall in order to maintain alignment. As such displacement of up to 10mm is possible with the stents commonly used in fenestrated EVAR without creating a flow limiting stenosis.

This analysis of longitudinal resistance to crushing does not take into account the hemodynamic forces acting on the graft (in particular those acting at the aortic bifurcation) that are often the root cause of caudal migration however it is unlikely that these additional forces contribute significantly to the forces acting on the target vessel stents due to unique design characteristics of the Cook fenestrated stent-graft. First, the modular design of the fenestrated stent-graft minimises transmission of the force acting on the flow divider of the distal body. This results in modular distraction instead of caudal migration of the proximal

main body. Second, in the preceding study where the aorta was modelled as a rigid structure, the fenestrated main body accommodated an additional 8mm increase in longitudinal separation without any apparent distortion of the target vessel stent (Advanta V12). This suggests that the proximal main body of a fenestrated stent-graft in fact has a remarkable degree of flexibility which allows it to conform to variations in native anatomy. As such the magnitude of the forces calculated in this study are probably an overestimation of the compressive forces acting upon the target vessel stent when mismatch occurs.

Limitations

Calculation of the force acting on the target vessel stent in the circumferential direction relied on the assumption that aortic expansion is symmetrical in all directions. However ECG-gated MRA studies have shown that this is not the case due to the proximity of the vertebral column posteriorly. The mean change in aortic diameter is 8% however in some directions an increase in diameter of up to 22% has been reported (van Herwaarden et al., 2006, van Prehn et al., 2009). The applicability of this observation to general practice is unknown since fenestrated stent-grafts are usually designed from computer-aided tomographic angiogram (CTA) images that may be taken from any point within the cardiac cycle. An increase in diameter in some directions of this magnitude is not in its own right since this is also accompanied by modest expansion in other directions. Furthermore analyses following EVAR show that the stent-graft conforms to the elliptical shape that the aortic neck adopts during systole. However since the target vessel stents effectively fixes the fenestrated stent-graft to specific points on the aortic wall, the distension of the aorta is limited thus the ability of the

fenestrated stent-graft to conform to changes in the aorta may be compromised and potentially result in loss of fabric apposition and the development of a type 1 endoleak.

Friction between the stent-graft and the aortic wall was not considered in order to simplify the boundary conditions of this model however it is more likely to have a significant role where circumferential mismatch is concerned particularly during the diastolic phase. During the systolic phase, the wall of the aorta stretches and is accommodated by the excess fabric of the stent-graft oversize. In diastole, the aorta remains still whilst the metal component of the stent-graft attempts to return to equilibrium. It is this movement that is resisted by friction however this force only serves to maintain alignment between the fenestrations and target vessel ostia.

9.6 Summary

It may not be possible to eliminate errors or discrepancies between observers when designing fenestrated stent-grafts. This study shows that forces generated by stent-grafts when mismatch occurs can be tolerated by the target vessel stents without significant compromise to end organ perfusion. However the complex movement of the target vessels highlights the fact that at present an ideal target vessel stent for fenestrated repair does not exist. Innovative stent designs able to resist dynamic forces at the interface between the stent-graft and aorta whilst allowing free movement of the distal artery would be beneficial.

Chapter 10

General discussion, implications of findings and suggestion for future study

---

Endovascular aneurysm repair is an effective alternative to open surgery in patients with anatomy suitable for treatment with a standard endograft. In the absence of an adequate infra-renal aortic neck, endovascular repair using fenestrated stent-grafts necessitates extension of the proximal sealing stent into the visceral aorta in order to create seal. However, the role of fenestrated stent-grafts in endovascular repair of complex aneurysms is still being evaluated since the familiar complications of standard EVAR (endoleak, migration and limb occlusion) are further compounded by the potential risk of target vessel loss.

In the short to medium term, target vessel loss is an event that usually occurs within the first 12 months of intervention and is frequently a consequence of intra-operative difficulty particularly when tortuous access vessels are encountered. A proportion of these problems may be attributed to negotiation of the learning curve for this complex technique; it is now known that certain stent designs are more suitable for use as target vessel stents and the use of double diameter-reducing ties is now encouraged when difficult access vessels are encountered. However, the fact that target vessel loss also occurs as a result of unforeseen interaction between native anatomy and the stent-graft complex

suggests an important relationship between pre-operative assessment, the design of fenestrated stent-grafts and subsequent threat to target vessel patency.

Measurement is a crucial step when planning a fenestrated stent-graft and since it is designed to exactly fit the native anatomy, it would follow that accuracy is essential. These measurements require knowledge of the relative circumferential and longitudinal positions of the visceral branches of the aorta. Accuracy requires an appreciation of potential measurement error; however since the visceral aorta cannot be measured directly, it is not possible to quantify the magnitude of observer error that occurs during the measurement process.

Potentially, the degree of intra and inter-observer variability may be used as a proxy for accuracy and quality control since target vessel measurements are either repeated by the same observer or checked by another prior to stent-graft construction. It would appear that angulation of the aorta in the coronal plane may be associated with a tendency towards increased observer variability and potentially observer error. However, categorising the morphology of the native aorta in a manner that permits reproducible analysis is difficult given the potential geometrical complexity of the aorta and its branches. As such the exact nature of the relationship between morphology and observer variability is yet to be elucidated and is an area for future study.

It may not be possible to eliminate error or discrepancies between observers when designing fenestrated stent-grafts. Indeed a disadvantage of using variability as a proxy for accuracy is the fact that it is possible for erroneous measurements to be consistent. Furthermore, the fact that most target vessels remain patent during follow up despite the existence of intra and inter-observer

variability implies that a degree of mismatch is permissible between native anatomy and the stent-graft complex. In addition, it is likely that in practice completely accurate target vessel measurement is probably not achieved when designing fenestrated stent-grafts. Therefore accuracy may not be an absolute requirement for successful fenestrated endovascular repair.

Some authors have acknowledged the possibility of tolerance within the stent-graft complex; however, the limits of mismatch have so far been based upon expert opinion. The remarkable ability of stent-grafts to tolerate considerable mismatch without compromising seal has now been demonstrated in vitro and subsequent studies have also shown that theoretically under dynamic conditions, the compressive force acting upon target vessel stents when mismatch occurs can be resisted without compromising perfusion of visceral organs. However, the complex movement of the stent-graft complex when mismatch occurs highlight deficiencies in the stents currently used to maintain target vessel alignment with stent-graft fenestrations. As such innovations in stent-graft materials and designs able to resist these forces are areas for future study.

The parameters used to calculate the forces acting upon target vessel stents are a limitation of this study in this study. Future studies could focus on refining these parameters by characterisation of both aortic anatomy and the mechanical properties of the stent-graft and delivery system. This would permit the development of computer simulations to assess the deployment of fenestrated devices in complex anatomy.

These findings lead to the conclusion that successful fenestrated endovascular aneurysm repair is possible within the limits of intra and inter-observer variability identified in this study. This has implications for broadening the application of fenestrated EVAR from the elective setting to emergent intervention and potentially the development of "of-the-shelf" fenestrated stent-grafts. However, such use must be tempered with caution since the long-term consequences of fenestrated stent-graft/ aorta mismatch are as yet unknown.

References

ANDERSON, J. L., BERCE, M. & HARTLEY, D. E. 2001. Endoluminal aortic grafting with renal and superior mesenteric artery incorporation by graft fenestration. *Journal of endovascular therapy : an official journal of the International Society of Endovascular Specialists,* 8, 3-15.

ANJUM, A. & POWELL, J. T. 2012. Is the incidence of abdominal aortic aneurysm declining in the 21st century? Mortality and hospital admissions for England & Wales and Scotland. *Eur J Vasc Endovasc Surg,* 43, 161-6.

ARMON, M. P., YUSUF, S. W., LATIEF, K., WHITAKER, S. C., GREGSON, R. H., WENHAM, P. W. & HOPKINSON, B. R. 1997. Anatomical suitability of abdominal aortic aneurysms for endovascular repair. *Br J Surg,* 84, 178-80.

ASHTON, H. A., BUXTON, M. J., DAY, N. E., KIM, L. G., MARTEAU, T. M., SCOTT, R. A., THOMPSON, S. G. & WALKER, N. M. 2002. The Multicentre Aneurysm Screening Study (MASS) into the effect of abdominal aortic aneurysm screening on mortality in men: a randomised controlled trial. *Lancet,* 360, 1531-9.

BASHEIN G, D. P. (ed.) 1994. *Centroid of a polygon,* New York, NY: Academic press.

BECQUEMIN, J. P. 2009. The ACE trial: a randomized comparison of open versus endovascular repair in good risk patients with abdominal aortic aneurysm. *J Vasc Surg,* 50, 222-4; discussion 224.

BECQUEMIN, J. P., KELLEY, L., ZUBILEWICZ, T., DESGRANGES, P., LAPEYRE, M. & KOBEITER, H. 2004. Outcomes of secondary interventions after abdominal aortic aneurysm endovascular repair. *J Vasc Surg,* 39, 298-305.

BEEMAN, B. R., DOCTOR, L. M., DOERR, K., MCAFEE-BENNETT, S., DOUGHERTY, M. J. & CALLIGARO, K. D. 2009. Duplex ultrasound imaging alone is sufficient for midterm endovascular aneurysm repair surveillance: a cost analysis study and prospective comparison with computed tomography scan. *J Vasc Surg,* 50, 1019-24.

BLACK, S. A., CARRELL, T. W., BELL, R. E., WALTHAM, M., REIDY, J. & TAYLOR, P. R. 2009. Long-term surveillance with computed tomography after endovascular aneurysm repair may not be justified. *Br J Surg,* 96, 1280-3.

BLAND, J. M. & ALTMAN, D. G. 1986. Statistical methods for assessing agreement between two methods of clinical measurement. *Lancet,* 1, 307-10.

BRADY, A. R., THOMPSON, S. G., FOWKES, F. G., GREENHALGH, R. M. & POWELL, J. T. 2004. Abdominal aortic aneurysm expansion: risk factors and time intervals for surveillance. *Circulation,* 110, 16-21.

BRENNER, D. J. & HALL, E. J. 2007. Computed tomography--an increasing source of radiation exposure. *N Engl J Med,* 357, 2277-84.

BRUNKWALL, J., HAUKSSON, H., BENGTSSON, H., BERGQVIST, D., TAKOLANDER, R. & BERGENTZ, S. E. 1989. Solitary aneurysms of the iliac arterial system: an estimate of their frequency of occurrence. *J Vasc Surg,* 10, 381-4.

CARPENTER, J. P., BAUM, R. A., BARKER, C. F., GOLDEN, M. A., MITCHELL, M. E., VELAZQUEZ, O. C. & FAIRMAN, R. M. 2001. Impact of exclusion criteria on patient selection for endovascular abdominal aortic aneurysm repair. *J Vasc Surg,* 34, 1050-4.

CARRAFIELLO, G., RECALDINI, C., LAGANA, D., PIFFARETTI, G. & FUGAZZOLA, C. 2008. Endoleak detection and classification after endovascular treatment of abdominal aortic aneurysm: value of CEUS over CTA. *Abdom Imaging,* 33, 357-62.

CARROCCIO, A., FARIES, P. L., MORRISSEY, N. J., TEODORESCU, V., BURKS, J. A., GRAVEREAUX, E. C., HOLLIER, L. H. & MARIN, M. L. 2002. Predicting iliac limb occlusions after bifurcated aortic stent grafting: anatomic and device-related causes. *J Vasc Surg,* 36, 679-84.

CHAER, R. A., GUSHCHIN, A., RHEE, R., MARONE, L., CHO, J. S., LEERS, S. & MAKAROUN, M. S. 2009. Duplex ultrasound as the sole long-term surveillance method post-endovascular aneurysm repair: a safe alternative for stable aneurysms. *J Vasc Surg,* 49, 845-9; discussion 849-50.

COCHENNEC, F., BECQUEMIN, J. P., DESGRANGES, P., ALLAIRE, E., KOBEITER, H. & ROUDOT-THORAVAL, F. 2007. Limb graft occlusion following EVAR: clinical pattern, outcomes and predictive factors of occurrence. *Eur J Vasc Endovasc Surg,* 34, 59-65.

CONNER, M. S., 3RD, STERNBERGH, W. C., 3RD, CARTER, G., TONNESSEN, B. H., YOSELEVITZ, M. & MONEY, S. R. 2002. Secondary procedures after endovascular aortic aneurysm repair. *J Vasc Surg,* 36, 992-6.

CONRAD, M. F., ADAMS, A. B., GUEST, J. M., PARUCHURI, V., BREWSTER, D. C., LAMURAGLIA, G. M. & CAMBRIA, R. P. 2009. Secondary intervention after endovascular abdominal aortic aneurysm repair. *Ann Surg,* 250, 383-9.

COSTIN, J. A., WATSON, D. R., DUFF, S. B., EDMONSON-HOLT, A., SHAFFER, L. & BLOSSOM, G. B. 2006. Evaluation of the complexity of open abdominal aneurysm repair in the era of endovascular stent grafting. *Journal of vascular surgery : official publication, the Society for Vascular Surgery [and] International Society for Cardiovascular Surgery, North American Chapter,* 43, 915-20; discussion 920.

CRAFOORD, C. 1947. The surgical treatment of coarctation of the aorta. *Surgery,* 21, 146.

CREECH, O., JR. 1966. Endo-aneurysmorrhaphy and treatment of aortic aneurysm. *Ann Surg,* 164, 935-46.

CREECH, O., JR., DEBAKEY, M. E. & MORRIS, G. C., JR. 1956. Aneurysm of thoracoabdominal aorta involving the celiac, superior mesenteric, and renal arteries; report of four cases treated by resection and homograft replacement. *Ann Surg,* 144, 549-73.

CURCI, J. A., PETRINEC, D., LIAO, S., GOLUB, L. M. & THOMPSON, R. W. 1998. Pharmacologic suppression of experimental abdominal aortic aneurysms: acomparison of doxycycline and four chemically modified tetracyclines. *J Vasc Surg,* 28, 1082-93.

DAWSON, J., COCKERILL, G., CHOKE, E., LOFTUS, I. & THOMPSON, M. M. 2006. Circulating cytokines in patients with abdominal aortic aneurysms. *Ann N Y Acad Sci,* 1085, 324-6.

DIAS, N. V., RESCH, T., MALINA, M., LINDBLAD, B. & IVANCEV, K. 2001. Intraoperative proximal endoleaks during AAA stent-graft repair: evaluation of risk factors and treatment with Palmaz stents. *J Endovasc Ther,* 8, 268-73.

DIAS, N. V., RIVA, L., IVANCEV, K., RESCH, T., SONESSON, B. & MALINA, M. 2009a. Is there a benefit of frequent CT follow-up after EVAR? *Eur J Vasc Endovasc Surg,* 37, 425-30.

DIAS, N. V., RIVA, L., IVANCEV, K., RESCH, T., SONESSON, B. & MALINA, M. 2009b. Is there a benefit of frequent CT follow-up after EVAR? *European journal of vascular and endovascular surgery : the official journal of the European Society for Vascular Surgery,* 37, 425-30.

DIEHM, N., BAUM, S. & BENENATI, J. F. 2008. Fenestrated and branched endografts: why we need them now. *J Vasc Interv Radiol,* 19, S63-7.

DONAS, K. P., TORSELLO, G., PITOULIAS, G. A., AUSTERMANN, M. & PAPADIMITRIOU, D. K. 2011. Surgical versus endovascular repair by iliac branch device of aneurysms involving the iliac bifurcation. *Journal of vascular surgery : official publication, the Society for Vascular Surgery [and] International Society for Cardiovascular Surgery, North American Chapter,* 53, 1223-9.

DRANEY, M. T., ZARINS, C. K. & TAYLOR, C. A. 2005. Three-dimensional analysis of renal artery bending motion during respiration. *J Endovasc Ther,* 12, 380-6.

DUBOST, C., ALLARY, M. & OECONOMOS, N. 1952. Resection of an aneurysm of the abdominal aorta: reestablishment of the continuity by a

preserved human arterial graft, with result after five months. *AMA Arch Surg,* 64, 405-8.

FAGGIOLI, G., STELLA, A., FREYRIE, A., GARGIULO, M., TARANTINI, S., RODIO, M., PILATO, A. & D'ADDATO, M. 1998a. Early and long-term results in the surgical treatment of juxtarenal and pararenal aortic aneurysms. *Eur J Vasc Endovasc Surg,* 15, 205-11.

FAGGIOLI, G., STELLA, A., FREYRIE, A., GARGIULO, M., TARANTINI, S., RODIO, M., PILATO, A. & D'ADDATO, M. 1998b. Early and long-term results in the surgical treatment of juxtarenal and pararenal aortic aneurysms. *European journal of vascular and endovascular surgery : the official journal of the European Society for Vascular Surgery,* 15, 205-11.

FAIRMAN, R. M., BAUM, R. A., CARPENTER, J. P., DEATON, D. H., MAKAROUN, M. S. & VELAZQUEZ, O. C. 2002. Limb interventions in patients undergoing treatment with an unsupported bifurcated aortic endograft system: a review of the Phase II EVT Trial. *J Vasc Surg,* 36, 118-26.

FOWKES, F. G., MACINTYRE, C. C. & RUCKLEY, C. V. 1989. Increasing incidence of aortic aneurysms in England and Wales. *BMJ,* 298, 33-5.

FRANSEN, G. A., VALLABHANENI, S. R., SR., VAN MARREWIJK, C. J., LAHEIJ, R. J., HARRIS, P. L. & BUTH, J. 2003. Rupture of infra-renal aortic aneurysm after endovascular repair: a series from EUROSTAR registry. *Eur J Vasc Endovasc Surg,* 26, 487-93.

FRIEDMAN, S. G. & FRIEDMAN, M. S. 1989. Matas, Antyllus, and endoaneurysmorrhaphy. *Surgery,* 105, 761-3.

GALLAND, R. B. 2007. Popliteal aneurysms: from John Hunter to the 21st century. *Ann R Coll Surg Engl,* 89, 466-71.

GREEN, R. M., RICOTTA, J. J., OURIEL, K. & DEWEESE, J. A. 1989. Results of supraceliac aortic clamping in the difficult elective resection of infrarenal abdominal aortic aneurysm. *Journal of vascular surgery : official publication, the Society for Vascular Surgery [and] International Society for Cardiovascular Surgery, North American Chapter,* 9, 124-34.

GREENBERG, R. K., TURC, A., HAULON, S., SRIVASTAVA, S. D., SARAC, T. P., O'HARA, P. J., LYDEN, S. P. & OURIEL, K. 2004. Stent-graft migration: a reappraisal of analysis methods and proposed revised definition. *J Endovasc Ther,* 11, 353-63.

HANNAWA, K. K., ELIASON, J. L. & UPCHURCH, G. R., JR. 2009. Gender differences in abdominal aortic aneurysms. *Vascular,* 17 Suppl 1, S30-9.

HANSEN, K. J., TRIBBLE, R. W., REAVIS, S. W., CANZANELLO, V. J., CRAVEN, T. E., PLONK, G. W., JR. & DEAN, R. H. 1990. Renal duplex sonography: evaluation of clinical utility. *J Vasc Surg,* 12, 227-36.

HARRISON, G. J., OSHIN, O. A., VALLABHANENI, S. R., BRENNAN, J. A., FISHER, R. K. & MCWILLIAMS, R. G. 2011. Surveillance after EVAR Based on Duplex Ultrasound and Abdominal Radiography. *European journal of vascular and endovascular surgery : the official journal of the European Society for Vascular Surgery.*

HEIKKINEN, M. A., ALSAC, J. M., ARKO, F. R., METSANOJA, R., ZVAIGZNE, A. & ZARINS, C. K. 2006. The importance of iliac fixation in prevention of stent graft migration. *J Vasc Surg,* 43, 1130-7; discussion 1137.

HENRY, M., AMOR, M., HENRY, I., ETHEVENOT, G., TZVETANOV, K., COURVOISIER, A., MENTRE, B. & CHATI, Z. 1999. Stents in the treatment of renal artery stenosis: long-term follow-up. *Journal of endovascular surgery : the official journal of the International Society for Endovascular Surgery,* 6, 42-51.

HINCHLIFFE, R. J., ALRIC, P., WENHAM, P. W. & HOPKINSON, B. R. 2003. Durability of femorofemoral bypass grafting after aortouniiliac endovascular aneurysm repair. *J Vasc Surg,* 38, 498-503.

HOBO, R. & BUTH, J. 2006. Secondary interventions following endovascular abdominal aortic aneurysm repair using current endografts. A EUROSTAR report. *J Vasc Surg,* 43, 896-902.

ISOKANGAS, J. M., HIETALA, R., PERALA, J. & TERVONEN, O. 2003. Accuracy of computer-aided measurements in endovascular stent-graft planning: an experimental study with two phantoms. *Invest Radiol,* 38, 164-70.

JOHANSEN, K. & KOEPSELL, T. 1986. Familial tendency for abdominal aortic aneurysms. *JAMA,* 256, 1934-6.

JONES, J. E., ATKINS, M. D., BREWSTER, D. C., CHUNG, T. K., KWOLEK, C. J., LAMURAGLIA, G. M., HODGMAN, T. M. & CAMBRIA, R. P. 2007. Persistent type 2 endoleak after endovascular repair of abdominal aortic aneurysm is associated with adverse late outcomes. *J Vasc Surg,* 46, 1-8.

JONGKIND, V., YEUNG, K. K., AKKERSDIJK, G. J., HEIDSIECK, D., REITSMA, J. B., TANGELDER, G. J. & WISSELINK, W. 2010. Juxtarenal aortic aneurysm repair. *Journal of vascular surgery : official*

publication, the Society for Vascular Surgery [and] International Society for Cardiovascular Surgery, North American Chapter, 52, 760-7.

KAANDORP, D. W., VASBINDER, G. B., DE HAAN, M. W., KEMERINK, G. J. & VAN ENGELSHOVEN, J. M. 2000. Motion of the proximal renal artery during the cardiac cycle. *J Magn Reson Imaging,* 12, 924-8.

KATZ, D. J., STANLEY, J. C. & ZELENOCK, G. B. 1997. Gender differences in abdominal aortic aneurysm prevalence, treatment, and outcome. *J Vasc Surg,* 25, 561-8.

KNOTT, A. W., KALRA, M., DUNCAN, A. A., REED, N. R., BOWER, T. C., HOSKIN, T. L., ODERICH, G. S. & GLOVICZKI, P. 2008. Open repair of juxtarenal aortic aneurysms (JAA) remains a safe option in the era of fenestrated endografts. *Journal of vascular surgery : official publication, the Society for Vascular Surgery [and] International Society for Cardiovascular Surgery, North American Chapter,* 47, 695-701.

KOCH, A. E., HAINES, G. K., RIZZO, R. J., RADOSEVICH, J. A., POPE, R. M., ROBINSON, P. G. & PEARCE, W. H. 1990. Human abdominal aortic aneurysms. Immunophenotypic analysis suggesting an immune-mediated response. *Am J Pathol,* 137, 1199-213.

KOHLER, T. R., ZIERLER, R. E., MARTIN, R. L., NICHOLLS, S. C., BERGELIN, R. O., KAZMERS, A., BEACH, K. W. & STRANDNESS, D. E., JR. 1986. Noninvasive diagnosis of renal artery stenosis by ultrasonic duplex scanning. *J Vasc Surg,* 4, 450-6.

KRAJCER, Z., GILBERT, J. H., DOUGHERTY, K., MORTAZAVI, A. & STRICKMAN, N. 2002. Successful treatment of aortic endograft thrombosis with rheolytic thrombectomy. *J Endovasc Ther,* 9, 756-64.

LAHEIJ, R. J., BUTH, J., HARRIS, P. L., MOLL, F. L., STELTER, W. J. & VERHOEVEN, E. L. 2000. Need for secondary interventions after endovascular repair of abdominal aortic aneurysms. Intermediate-term follow-up results of a European collaborative registry (EUROSTAR). *Br J Surg,* 87, 1666-73.

LALKA, S., DALSING, M., CIKRIT, D., SAWCHUK, A., SHAFIQUE, S., NACHREINER, R. & PANDURANGI, K. 2005. Secondary interventions after endovascular abdominal aortic aneurysm repair. *Am J Surg,* 190, 787-94.

LEDERLE, F. A., FREISCHLAG, J. A., KYRIAKIDES, T. C., PADBERG, F. T., JR., MATSUMURA, J. S., KOHLER, T. R., LIN, P. H., JEAN-CLAUDE, J. M., CIKRIT, D. F., SWANSON, K. M. & PEDUZZI, P. N. 2009. Outcomes following endovascular vs open repair of abdominal aortic aneurysm: a randomized trial. *JAMA,* 302, 1535-42.

LEDERLE, F. A., JOHNSON, G. R. & WILSON, S. E. 2001. Abdominal aortic aneurysm in women. *J Vasc Surg,* 34, 122-6.

LEDERLE, F. A., WILSON, S. E., JOHNSON, G. R., REINKE, D. B., LITTOOY, F. N., ACHER, C. W., BALLARD, D. J., MESSINA, L. M., GORDON, I. L., CHUTE, E. P., KRUPSKI, W. C., BUSUTTIL, S. J., BARONE, G. W., SPARKS, S., GRAHAM, L. M., RAPP, J. H., MAKAROUN, M. S., MONETA, G. L., CAMBRIA, R. A., MAKHOUL, R. G., ETON, D., ANSEL, H. J., FREISCHLAG, J. A. & BANDYK, D. 2002. Immediate repair compared with surveillance of small abdominal aortic aneurysms. *N Engl J Med,* 346, 1437-44.

LEE, W. A., HIRNEISE, C. M., TAYYARAH, M., HUBER, T. S. & SEEGER, J. M. 2004. Impact of endovascular repair on early outcomes of ruptured abdominal aortic aneurysms. *J Vasc Surg,* 40, 211-5.

LIFELINE REGISTRY OF ENDOVASCULAR ANEURYSM REPAIR STEERING COMMITTEE 2001. Lifeline Registry: collaborative evaluation of endovascular aneurysm repair. *J Vasc Surg,* 34, 1139-46.

MALINA, M., LINDBLAD, B., IVANCEV, K., LINDH, M., MALINA, J. & BRUNKWALL, J. 1998. Endovascular AAA exclusion: will stents with hooks and barbs prevent stent-graft migration? *J Endovasc Surg,* 5, 310-7.

MAY, J., WHITE, G. H., WAUGH, R., STEPHEN, M. S., CHAUFOUR, X., ARULCHELVAM, M. & HARRIS, J. P. 2000. Comparison of first- and second-generation prostheses for endoluminal repair of abdominal aortic aneurysms: a 6-year study with life table analysis. *J Vasc Surg,* 32, 124-9.

MOHABBAT, W., GREENBERG, R. K., MASTRACCI, T. M., CURY, M., MORALES, J. P. & HERNANDEZ, A. V. 2009. Revised duplex criteria and outcomes for renal stents and stent grafts following endovascular repair of juxtarenal and thoracoabdominal aneurysms. *J Vasc Surg,* 49, 827-37; discussion 837.

MOHAN, I. V., HARRIS, P. L., VAN MARREWIJK, C. J., LAHEIJ, R. J. & HOW, T. V. 2002. Factors and forces influencing stent-graft migration after endovascular aortic aneurysm repair. *Journal of endovascular therapy : an official journal of the International Society of Endovascular Specialists,* 9, 748-55.

MOSORIN, M., JUVONEN, J., BIANCARI, F., SATTA, J., SURCEL, H. M., LEINONEN, M., SAIKKU, P. & JUVONEN, T. 2001. Use of doxycycline to decrease the growth rate of abdominal aortic aneurysms: a randomized, double-blind, placebo-controlled pilot study. *J Vasc Surg,* 34, 606-10.

MUHS, B. E., TEUTELINK, A., PROKOP, M., VINCKEN, K. L., MOLL, F. L. & VERHAGEN, H. J. 2006a. Endovascular aneurysm repair alters renal artery movement: a preliminary evaluation using dynamic CTA. *J Endovasc Ther,* 13, 476-80.

MUHS, B. E., VERHOEVEN, E. L., ZEEBREGTS, C. J., TIELLIU, I. F., PRINS, T. R., VERHAGEN, H. J. & VAN DEN DUNGEN, J. J. 2006b. Mid-term results of endovascular aneurysm repair with branched and fenestrated endografts. *J Vasc Surg,* 44, 9-15.

MULTICENTER ANEURYSM SCREENING STUDY GROUP 2002. Multicentre aneurysm screening study (MASS): cost effectiveness analysis of screening for abdominal aortic aneurysms based on four year results from randomised controlled trial. *BMJ,* 325, 1135.

MURPHY, E. H., JOHNSON, E. D. & ARKO, F. R. 2007. Device-specific resistance to in vivo displacement of stent-grafts implanted with maximum iliac fixation. *J Endovasc Ther,* 14, 585-92.

NEWMAN, K. M., JEAN-CLAUDE, J., LI, H., RAMEY, W. G. & TILSON, M. D. 1994. Cytokines that activate proteolysis are increased in abdominal aortic aneurysms. *Circulation,* 90, II224-7.

NIKANOROV, A., SMOUSE, H. B., OSMAN, K., BIALAS, M., SHRIVASTAVA, S. & SCHWARTZ, L. B. 2008. Fracture of self-

expanding nitinol stents stressed in vitro under simulated intravascular conditions. *J Vasc Surg,* 48, 435-40.

NORDON, I. M., HINCHLIFFE, R. J., HOLT, P. J., LOFTUS, I. M. & THOMPSON, M. M. 2009a. Modern treatment of juxtarenal abdominal aortic aneurysms with fenestrated endografting and open repair--a systematic review. *European journal of vascular and endovascular surgery : the official journal of the European Society for Vascular Surgery,* 38, 35-41.

NORDON, I. M., KARTHIKESALINGAM, A., HINCHLIFFE, R. J., HOLT, P. J., LOFTUS, I. M. & THOMPSON, M. M. 2009b. Secondary Interventions Following Endovascular Aneurysm Repair (EVAR) and the Enduring Value of Graft Surveillance. *Eur J Vasc Endovasc Surg.*

OCKERT, S., SCHUMACHER, H., BOCKLER, D., MALCHEREK, K., HANSMANN, J. & ALLENBERG, J. 2007. Comparative early and midterm results of open juxtarenal and infrarenal aneurysm repair. *Langenbeck's archives of surgery / Deutsche Gesellschaft fur Chirurgie,* 392, 725-30.

ORR, W. M. & DAVIES, M. 1974. Simplified repair of abdominal aortic aneurysms using non-bifurcated (straight) inlay prostheses. *Br J Surg,* 61, 847-9.

OSHIN, O. A., ENGLAND, A., MCWILLIAMS, R. G., BRENNAN, J. A., FISHER, R. K. & VALLABHANENI, S. R. 2010a. Intra- and interobserver variability of target vessel measurement for fenestrated endovascular aneurysm repair. *J Endovasc Ther,* 17, 402-7.

OSHIN, O. A., FISHER, R. K., WILLIAMS, L. A., BRENNAN, J. A., GILLING-SMITH, G. L., VALLABHANENI, S. R. & MCWILLIAMS, R. G. 2010b. Adjunctive iliac stents reduce the risk of stent-graft limb occlusion following endovascular aneurysm repair with the Zenith stent-graft. *Journal of endovascular therapy : an official journal of the International Society of Endovascular Specialists,* 17, 108-14.

PARODI, J. C., PALMAZ, J. C. & BARONE, H. D. 1991. Transfemoral intraluminal graft implantation for abdominal aortic aneurysms. *Ann Vasc Surg,* 5, 491-9.

PEARCE, W. H. 2009. *Abdominal Aortic Aneurysm* [Online]. E-medicine. Available: http://emedicine.medscape.com/article/463354-overview.

PELTON, A. R., SCHROEDER, V., MITCHELL, M. R., GONG, X. Y., BARNEY, M. & ROBERTSON, S. W. 2008. Fatigue and durability of Nitinol stents. *J Mech Behav Biomed Mater,* 1, 153-64.

PETERSEN, E., BOMAN, J., WAGBERG, F. & ANGQUIST, K. A. 2002. Presence of Chlamydia pneumoniae in abdominal aortic aneurysms is not associated with increased activity of matrix metalloproteinases. *Eur J Vasc Endovasc Surg,* 24, 365-9.

PETRIK, P. V. & MOORE, W. S. 2001. Endoleaks following endovascular repair of abdominal aortic aneurysm: the predictive value of preoperative anatomic factors--a review of 100 cases. *J Vasc Surg,* 33, 739-44.

PETRINEC, D., LIAO, S., HOLMES, D. R., REILLY, J. M., PARKS, W. C. & THOMPSON, R. W. 1996. Doxycycline inhibition of aneurysmal degeneration in an elastase-induced rat model of abdominal aortic

aneurysm: preservation of aortic elastin associated with suppressed production of 92 kD gelatinase. *J Vasc Surg,* 23, 336-46.

PITTON, M. B., SCHESCHKOWSKI, T., RING, M., HERBER, S., OBERHOLZER, K., LEICHER-DUBER, A., NEUFANG, A., SCHMIEDT, W. & DUBER, C. 2009. Ten-year follow-up of endovascular aneurysm treatment with Talent stent-grafts. *Cardiovasc Intervent Radiol,* 32, 906-17.

PRAUSE, G., RATZENHOFER-COMENDA, B., PIERER, G., SMOLLE-JUTTNER, F., GLANZER, H. & SMOLLE, J. 1997. Can ASA grade or Goldman's cardiac risk index predict peri-operative mortality? A study of 16,227 patients. *Anaesthesia,* 52, 203-6.

PRINSSEN, M., VERHOEVEN, E. L., BUTH, J., CUYPERS, P. W., VAN SAMBEEK, M. R., BALM, R., BUSKENS, E., GROBBEE, D. E. & BLANKENSTEIJN, J. D. 2004a. A randomized trial comparing conventional and endovascular repair of abdominal aortic aneurysms. *N Engl J Med,* 351, 1607-18.

PRINSSEN, M., WIXON, C. L., BUSKENS, E. & BLANKENSTEIJN, J. D. 2004b. Surveillance after endovascular aneurysm repair: diagnostics, complications, and associated costs. *Ann Vasc Surg,* 18, 421-7.

PYO, R., LEE, J. K., SHIPLEY, J. M., CURCI, J. A., MAO, D., ZIPORIN, S. J., ENNIS, T. L., SHAPIRO, S. D., SENIOR, R. M. & THOMPSON, R. W. 2000. Targeted gene disruption of matrix metalloproteinase-9 (gelatinase B) suppresses development of experimental abdominal aortic aneurysms. *J Clin Invest,* 105, 1641-9.

REED, D., REED, C., STEMMERMANN, G. & HAYASHI, T. 1992. Are aortic aneurysms caused by atherosclerosis? *Circulation,* 85, 205-11.

RESCH, T., MALINA, M., LINDBLAD, B. & IVANCEV, K. 2001. The impact of stent-graft development on outcome of AAA repair--a 7-year experience. *Eur J Vasc Endovasc Surg,* 22, 57-61.

RESCH, T., MALINA, M., LINDBLAD, B., MALINA, J., BRUNKWALL, J. & IVANCEV, K. 2000. The impact of stent design on proximal stent-graft fixation in the abdominal aorta: an experimental study. *Eur J Vasc Endovasc Surg,* 20, 190-5.

RUTHERFORD, R. B. (ed.) 2000. *Vascular Surgery*: W.B. Saunders.

SAKALIHASAN, N., LIMET, R. & DEFAWE, O. D. 2005. Abdominal aortic aneurysm. *Lancet,* 365, 1577-89.

SALACINSKI, H. J., GOLDNER, S., GIUDICEANDREA, A., HAMILTON, G., SEIFALIAN, A. M., EDWARDS, A. & CARSON, R. J. 2001. The mechanical behavior of vascular grafts: a review. *J Biomater Appl,* 15, 241-78.

SAMPAIO, S. M., PANNETON, J. M., MOZES, G. I., ANDREWS, J. C., BOWER, T. C., KARLA, M., NOEL, A. A., CHERRY, K. J., SULLIVAN, T. & GLOVICZKI, P. 2004. Proximal type I endoleak after endovascular abdominal aortic aneurysm repair: predictive factors. *Ann Vasc Surg,* 18, 621-8.

SARAC, T. P., CLAIR, D. G., HERTZER, N. R., GREENBERG, R. K., KRAJEWSKI, L. P., O'HARA, P. J. & OURIEL, K. 2002a. Contemporary results of juxtarenal aneurysm repair. *J Vasc Surg,* 36, 1104-11.

SARAC, T. P., CLAIR, D. G., HERTZER, N. R., GREENBERG, R. K., KRAJEWSKI, L. P., O'HARA, P. J. & OURIEL, K. 2002b. Contemporary results of juxtarenal aneurysm repair. *Journal of vascular surgery : official publication, the Society for Vascular Surgery [and] International Society for Cardiovascular Surgery, North American Chapter,* 36, 1104-11.

SARKAR, S., SALACINSKI, H. J., HAMILTON, G. & SEIFALIAN, A. M. 2006. The mechanical properties of infrainguinal vascular bypass grafts: their role in influencing patency. *Eur J Vasc Endovasc Surg,* 31, 627-36.

SCHMIEDER, G. C., STOUT, C. L., STOKES, G. K., PARENT, F. N. & PANNETON, J. M. 2009a. Endoleak after endovascular aneurysm repair: duplex ultrasound imaging is better than computed tomography at determining the need for intervention. *J Vasc Surg,* 50, 1012-7; discussion 1017-8.

SCHMIEDER, G. C., STOUT, C. L., STOKES, G. K., PARENT, F. N. & PANNETON, J. M. 2009b. Endoleak after endovascular aneurysm repair: duplex ultrasound imaging is better than computed tomography at determining the need for intervention. *Journal of vascular surgery : official publication, the Society for Vascular Surgery [and] International Society for Cardiovascular Surgery, North American Chapter,* 50, 1012-7; discussion 1017-8.

SCHURINK, G. W., AARTS, N. J., VAN BAALEN, J. M., SCHULTZE KOOL, L. J. & VAN BOCKEL, J. H. 1999. Stent attachment site-related endoleakage after stent graft treatment: An in vitro study of the effects of

graft size, stent type, and atherosclerotic wall changes. *J Vasc Surg,* 30, 658-67.

SCOTT, R. A., BRIDGEWATER, S. G. & ASHTON, H. A. 2002. Randomized clinical trial of screening for abdominal aortic aneurysm in women. *Br J Surg,* 89, 283-5.

SCOTT, R. A., VARDULAKI, K. A., WALKER, N. M., DAY, N. E., DUFFY, S. W. & ASHTON, H. A. 2001. The long-term benefits of a single scan for abdominal aortic aneurysm (AAA) at age 65. *Eur J Vasc Endovasc Surg,* 21, 535-40.

SCURR, J. R., BRENNAN, J. A., GILLING-SMITH, G. L., HARRIS, P. L., VALLABHANENI, S. R. & MCWILLIAMS, R. G. 2008a. Fenestrated endovascular repair for juxtarenal aortic aneurysm. *The British journal of surgery,* 95, 326-32.

SCURR, J. R., HOW, T. V., MCWILLIAMS, R. G., LANE, S. & GILLING-SMITH, G. L. 2008b. Fenestrated stent-graft repair: which stent should be used to secure target vessel fenestrations? *J Endovasc Ther,* 15, 344-8.

SENIOR, R. M., GRIFFIN, G. L., FLISZAR, C. J., SHAPIRO, S. D., GOLDBERG, G. I. & WELGUS, H. G. 1991. Human 92- and 72-kilodalton type IV collagenases are elastases. *J Biol Chem,* 266, 7870-5.

SIVAMURTHY, N., SCHNEIDER, D. B., REILLY, L. M., RAPP, J. H., SKOVOBOGATYY, H. & CHUTER, T. A. 2006. Adjunctive primary stenting of Zenith endograft limbs during endovascular abdominal aortic aneurysm repair: implications for limb patency. *J Vasc Surg,* 43, 662-70.

SPRONK, S., VAN KEMPEN, B. J., BOLL, A. P., JORGENSEN, J. J., HUNINK, M. G. & KRISTIANSEN, I. S. 2011. Cost-effectiveness of

screening for abdominal aortic aneurysm in the Netherlands and Norway. *Br J Surg,* 98, 1546-55.

SUN, Z., MWIPATAYI, B. P., SEMMENS, J. B. & LAWRENCE-BROWN, M. M. 2006. Short to midterm outcomes of fenestrated endovascular grafts in the treatment of abdominal aortic aneurysms: a systematic review. *J Endovasc Ther,* 13, 747-53.

TANG, T. Y., WALSH, S. R., FANSHAWE, T. R., SEPPI, V., SADAT, U., HAYES, P. D., VARTY, K., GAUNT, M. E. & BOYLE, J. R. 2007. Comparison of risk-scoring methods in predicting the immediate outcome after elective open abdominal aortic aneurysm surgery. *Eur J Vasc Endovasc Surg,* 34, 505-13.

TAYLOR, D. C., KETTLER, M. D., MONETA, G. L., KOHLER, T. R., KAZMERS, A., BEACH, K. W. & STRANDNESS, D. E., JR. 1988. Duplex ultrasound scanning in the diagnosis of renal artery stenosis: a prospective evaluation. *J Vasc Surg,* 7, 363-9.

THE UK SMALL ANEURYSM TRIAL PARTICIPANTS 1998. Mortality results for randomised controlled trial of early elective surgery or ultrasonographic surveillance for small abdominal aortic aneurysms. The UK Small Aneurysm Trial Participants. *Lancet,* 352, 1649-55.

TORSELLO, G., TROISI, N., DONAS, K. P. & AUSTERMANN, M. 2011. Evaluation of the Endurant stent graft under instructions for use vs off-label conditions for endovascular aortic aneurysm repair. *Journal of vascular surgery : official publication, the Society for Vascular Surgery [and] International Society for Cardiovascular Surgery, North American Chapter.*

TREIMAN, G. S., LAWRENCE, P. F., EDWARDS, W. H., JR., GALT, S. W., KRAISS, L. W. & BHIRANGI, K. 1999. An assessment of the current applicability of the EVT endovascular graft for treatment of patients with an infrarenal abdominal aortic aneurysm. *J Vasc Surg,* 30, 68-75.

UK EVAR 2 TRIAL PARTICIPANTS 2005. Endovascular aneurysm repair and outcome in patients unfit for open repair of abdominal aortic aneurysm (EVAR trial 2): randomised controlled trial. *Lancet,* 365, 2187-92.

UK EVAR TRIAL 1 PARTICIPANTS 2005. Endovascular aneurysm repair versus open repair in patients with abdominal aortic aneurysm (EVAR trial 1): randomised controlled trial. *Lancet,* 365, 2179-86.

VAN HERWAARDEN, J. A., BARTELS, L. W., MUHS, B. E., VINCKEN, K. L., LINDEBOOM, M. Y., TEUTELINK, A., MOLL, F. L. & VERHAGEN, H. J. 2006. Dynamic magnetic resonance angiography of the aneurysm neck: conformational changes during the cardiac cycle with possible consequences for endograft sizing and future design. *J Vasc Surg,* 44, 22-8.

VAN PREHN, J., VAN HERWAARDEN, J. A., VINCKEN, K. L., VERHAGEN, H. J., MOLL, F. L. & BARTELS, L. W. 2009. Asymmetric aortic expansion of the aneurysm neck: analysis and visualization of shape changes with electrocardiogram-gated magnetic resonance imaging. *J Vasc Surg,* 49, 1395-402.

VERHOEVEN, E. L., TIELLIU, I. F., PRINS, T. R., ZEEBREGTS, C. J., VAN ANDRINGA DE KEMPENAER, M. G., CINA, C. S. & VAN DEN DUNGEN, J. J. 2004. Frequency and outcome of re-interventions after

endovascular repair for abdominal aortic aneurysm: a prospective cohort study. *Eur J Vasc Endovasc Surg,* 28, 357-64.

VERLOES, A., SAKALIHASAN, N., KOULISCHER, L. & LIMET, R. 1995. Aneurysms of the abdominal aorta: familial and genetic aspects in three hundred thirteen pedigrees. *J Vasc Surg,* 21, 646-55.

VINE, N. & POWELL, J. T. 1991. Metalloproteinases in degenerative aortic disease. *Clin Sci (Lond),* 81, 233-9.

VOLLMAR, J. F., PAES, E., PAUSCHINGER, P., HENZE, E. & FRIESCH, A. 1989. Aortic aneurysms as late sequelae of above-knee amputation. *Lancet,* 2, 834-5.

VOLODOS, N. L., KARPOVICH, I. P., TROYAN, V. I., KALASHNIKOVA YU, V., SHEKHANIN, V. E., TERNYUK, N. E., NEONETA, A. S., USTINOV, N. I. & YAKOVENKO, L. F. 1991. Clinical experience of the use of self-fixing synthetic prostheses for remote endoprosthetics of the thoracic and the abdominal aorta and iliac arteries through the femoral artery and as intraoperative endoprosthesis for aorta reconstruction. *Vasa Suppl,* 33, 93-5.

VON ALLMEN, R. S. & POWELL, J. T. 2012. The management of ruptured abdominal aortic aneurysms: screening for abdominal aortic aneurysm and incidence of rupture. *J Cardiovasc Surg (Torino),* 53, 69-76.

WALSH, S. R., TANG, T. Y. & BOYLE, J. R. 2008. Renal consequences of endovascular abdominal aortic aneurysm repair. *J Endovasc Ther,* 15, 73-82.

WHITE, G. H., YU, W., MAY, J., CHAUFOUR, X. & STEPHEN, M. S. 1997. Endoleak as a complication of endoluminal grafting of abdominal aortic

aneurysms: classification, incidence, diagnosis, and management. *J Endovasc Surg,* 4, 152-68.

WILLS, A., THOMPSON, M. M., CROWTHER, M., SAYERS, R. D. & BELL, P. R. 1996. Pathogenesis of abdominal aortic aneurysms--cellular and biochemical mechanisms. *Eur J Vasc Endovasc Surg,* 12, 391-400.

WILSON, W. R., ANDERTON, M., CHOKE, E. C., DAWSON, J., LOFTUS, I. M. & THOMPSON, M. M. 2008. Elevated plasma MMP1 and MMP9 are associated with abdominal aortic aneurysm rupture. *Eur J Vasc Endovasc Surg,* 35, 580-4.

WOLF, Y. G., FOGARTY, T. J., OLCOTT, C. I., HILL, B. B., HARRIS, E. J., MITCHELL, R. S., MILLER, D. C., DALMAN, R. L. & ZARINS, C. K. 2000. Endovascular repair of abdominal aortic aneurysms: eligibility rate and impact on the rate of open repair. *Journal of vascular surgery : official publication, the Society for Vascular Surgery [and] International Society for Cardiovascular Surgery, North American Chapter,* 32, 519-23.

WYSS, T. R., DICK, F., ENGLAND, A., BROWN, L. C., RODWAY, A. D. & GREENHALGH, R. M. 2009. Three-dimensional imaging core laboratory of the endovascular aneurysm repair trials: validation of methodology. *Eur J Vasc Endovasc Surg,* 38, 724-31.

XU, C., ZARINS, C. K. & GLAGOV, S. 2001. Aneurysmal and occlusive atherosclerosis of the human abdominal aorta. *J Vasc Surg,* 33, 91-6.

YOUNG, E. L., HOLT, P. J., POLONIECKI, J. D., LOFTUS, I. M. & THOMPSON, M. M. 2007. Meta-analysis and systematic review of the

relationship between surgeon annual caseload and mortality for elective open abdominal aortic aneurysm repairs. *J Vasc Surg,* 46**,** 1287-94.

ZARINS, C. K., XU, C. P. & GLAGOV, S. 1992. Aneurysmal enlargement of the aorta during regression of experimental atherosclerosis. *J Vasc Surg,* 15**,** 90-8; discussion 99-101.

ZIEGLER, P., AVGERINOS, E. D., UMSCHEID, T., PERDIKIDES, T. & STELTER, W. J. 2007. Fenestrated endografting for aortic aneurysm repair: a 7-year experience. *Journal of endovascular therapy : an official journal of the International Society of Endovascular Specialists,* 14**,** 609-18.

Intra- and interobserver variability of target vessel measurement for fenestrated endovascular aneurysm repair.

Oshin OA, England A, McWilliams RG, Brennan JA, Fisher RK, Vallabhaneni SR.
J Endovasc Ther. 2010 Jun;17(3):402-7.

Magnitude of the forces acting on target vessel stents as a result of a mismatch between native aortic anatomy and fenestrated stent-grafts.

Oshin OA, How TV, Brennan JA, Fisher RK, McWilliams RG, Vallabhaneni SR.
J Endovasc Ther. 2011 Aug;18(4):569-75.

◆ ISES ENDOVASCULAR RESEARCH COMPETITION, FIRST PLACE ◆

Intra- and Interobserver Variability of Target Vessel Measurement for Fenestrated Endovascular Aneurysm Repair

Olufemi A. Oshin, BEng, MBChB, MRCS; Andrew England, BSc, MSc; Richard G. McWilliams, FRCR; John A. Brennan, MD, FRCS; Robert K. Fisher, MD, FRCS; and S. Rao Vallabhaneni, MD, FRCS

Regional Vascular Unit, Royal Liverpool University Hospital, Liverpool, UK.

Purpose: To evaluate intra- and interobserver agreement of target vessel measured from computed tomography (CT) scans with 2 measuring techniques used in planning fenestrated endovascular aneurysm repairs (FEVAR): multiplanar reconstruction (MPR) and semi-automated central lumen line (CLL).
Methods: CT datasets from 25 FEVAR patients were independently analyzed by 2 experienced observers according to a standardized protocol using the MPR (Leonardo workstation) and CLL (Aquarius workstation) techniques for each patient. Longitudinal vessel separation and clock-face position of the visceral aortic branches were measured twice. The repeatability coefficient (RC) was calculated using the Bland and Altman method to measure intra- and interobserver variability. Differences between groups were examined by paired *t* test (continuous data) or chi-squared analysis (categorical). Clock-face discrepancy >30 minutes was considered significant.
Results: Intraobserver mean difference was insignificant regardless of the measurement technique: the observer and workstation-specific RCs varied between 3.9 and 4.9 mm. Paired measurements differed by >3 mm in 8%. Interobserver variability was greater: observer and workstation-specific RC varied between 5.6 and 7.4 mm, with a tendency toward consistency using MPR, although the mean difference was insignificant. Paired measurements differed by >3 mm in 18%. There was no significant intraobserver variation in clock-face measurement, while interobserver variation was significant in 12% of measurements using the Aquarius workstation and 6% using the Leonardo workstation ($p=0.19$).
Conclusion: Subjective interpretation of anatomical landmarks is more important than measurement techniques or workstations used in the generation of measurement inconsistencies. Introduction of consensus regarding interpretation of anatomical detail and development of fenestrated stent-grafts tolerant of measurement errors might ameliorate some of the problems encountered in FEVAR.
J Endovasc Ther. 2010;17:402–407

Key words: endovascular aneurysm repair, fenestrated stent-graft, target vessel, imaging, computed tomographic angiography, observer variability

The annual ISES Endovascular Research Competition held on March 1, 2010, at International Congress XXIII on Endovascular Interventions (Scottsdale, Arizona, USA) evaluated participants on both their oral and written presentations. ISES congratulates the 2010 winners.

The authors have no commercial, proprietary, or financial interest in any products or companies described in this article.

Address for correspondence and reprints: S. Rao Vallabhaneni, MD, FRCS, Link 8C, Royal Liverpool University Hospital, Prescot Street, Liverpool L7 8XP, UK. E-mail: *fempop@liv.ac.uk*

J ENDOVASC THER
2010;17:402–407

Endovascular aneurysm repair (EVAR) is an established alternative to open surgery,[1,2] yet the unfavorable aneurysm neck anatomy, particularly short length, of juxtarenal aneurysms is the most frequent contraindication to EVAR.[3] In such instances, open surgical repair is associated with a substantial risk of perioperative complications since a proportion of these patients require suprarenal aortic cross clamping.[4,5] Fenestrated endovascular aneurysm repair (FEVAR) overcomes the limitations of standard EVAR by extending the proximal seal zone into the visceral segment of the aorta while maintaining end organ perfusion via accurately placed fenestrations.

Accurate measurement of the aortic anatomy is a prerequisite for successful FEVAR. Longitudinal separation between aortic side branches (target vessels) and circumferential orientation of the target vessel ostia upon the orthogonal aortic cross section, called "clock-face position," are the two most important measurements required to construct a stent-graft main body that allows target vessel perfusion while achieving aneurysm exclusion. Errors in these measurements will lead to mismatch between the stent-graft and native anatomy, which may in turn result in intraoperative difficulty with stent-graft deployment and/or late target vessel occlusion. Measurement for fenestrated stent-graft planning is predominantly performed by 3-dimensional analyses of computed tomographic angiography (CTA) images. The effects that the observer or the measurement technique may have upon measurement variability have not been previously analyzed.

The purpose of this study was to evaluate the intra- and interobserver agreement of target vessel measurements and to compare two measuring techniques commonly utilized in FEVAR planning: multiplanar reconstruction (MPR) and semi-automated central lumen line (CLL) measurement.

METHODS

The records of 64 consecutive patients in whom FEVAR was performed at a single institution between 1999 and 2009 were examined. To standardize the measurement protocols and datasets, only patients who required the construction of stent-grafts incorporating a scallop for the superior mesenteric artery and fenestrations for both the left and right renal arteries were considered. Of these, 25 patients were selected at random, and their CTA datasets were retrieved.

Image Analysis

Two observers (O.A.O. and A.E.) performed image analyses independently according to a set protocol. Two different workstations were used: Aquarius (TeraRecon, San Mateo, CA, USA) and Leonardo (Siemens Medical Solutions Inc, Erlangen, Germany). Both observers had received training in the use of these workstations and were experienced operators. Each observer performed measurements twice on separate occasions (4 weeks apart) for each dataset.

The technique used to measure longitudinal vessel separation was different for each workstation and reflected the best practice for each of these platforms. With the Aquarius workstation, a semi-automated central lumen line was created by placing seed points above the level of the celiac axis and below the lowermost renal artery; the centerline generated by the workstation was never manually altered. A "stretch view" was then generated from which the longitudinal vessel separation was manually measured using the bottom of the celiac axis ostium as the reference point. The stretch view image was rotated on its centerline axis to identify the optimal view of the midpoint of each target vessel ostium.

With the Leonardo workstation, multiplanar reconstructions were created along the visually perceived axis of the aortic lumen in the visceral segment. Although the thickness of the maximal intensity projections (MIP) was kept to a minimum, this was neither controlled nor recorded between observers or observations. From these reconstructions, the longitudinal separation of the target vessels was measured, again using the bottom of the celiac axis as the point of reference. Renal separation was defined as the difference between the distances measured from the bottom of the celiac axis to the midpoint of each renal artery ostium. Each set of mea-

TABLE 1
Intraobserver Results

	Aquarius (CLL)		Leonardo (MPR)	
	Observer 1	Observer 2	Observer 1	Observer 2
Mean difference, mm	0.6	−0.1	0.1	−0.1
Repeatability coefficient, mm	4.9	4.6	3.9	4.0
Difference >3 mm	2	3	2	1

CLL: central lumen line, MPR: multiplanar reconstruction.

surements consisted of the celiac axis to the upper renal ostium and the celiac axis to the lower renal ostium rounded to the nearest millimeter.

The circumferential position of the target vessel ostia in a plane orthogonal to the visceral aorta was assigned using a "clock-face" protractor with 12-hour gradations over 360° to the nearest 15 minutes (equivalent to 7.5°) according to the planning instructions for fenestrated devices issued by the manufacturers (Cook, Inc., Bloomington, IN, USA). In the case of both workstations, this was achieved by multiplanar reconstruction.

Statistical Analysis

Numerical data representing continuous variables were converted to categorical variables according to set criteria for analysis and descriptive purposes. Proportions of binary variables were expressed as percentages. Repeat measurements differing by >3 mm were considered clinically significant. Since the reference point for assigning clock positions for the target vessel ostia may vary between observers, the relative positions in minutes was calculated and used to determine observer agreement. A clock position discrepancy of 30 minutes or more for the position of target vessel ostia was considered significant.

A paired *t* test was used to compare continuous data between groups, and chi-squared analysis was utilized for dichotomous outcomes. A Student *t* test was used to examine differences in paired observations of raw data. Intra- and interobserver variabilities were measured by calculating the repeatability coefficient given by the mean differences between repeated measures according to the Bland and Altman method. Three-way repeated measures analysis of variance (ANOVA) was utilized to test the individual and combined effects of observer, workstation, and time on measurement variability. Statistical analysis was performed using SPSS software (version 16.0; SPSS Inc, Chicago, IL, USA). $P<0.05$ was considered to indicate a significant difference.

RESULTS

Inter-Renal Separation

In total, 100 paired sets of CTA measurements were generated, falling into 4 groups (Table 1). Intraobserver and workstation-specific repeatability coefficients varied between 3.9 and 4.9 mm. The mean difference between repeat observations was <1 mm in all instances within each group. Analysis of raw data was not significant ($p>0.05$). When data were examined qualitatively, however, 8% of the repeat measurements differed by >3 mm compared to the first measurement of the same observer.

Data relating to interobserver variability is given in Table 2. Interobserver variability was greater, with observer and workstation-specific repeatability coefficients varying between 5.6 and 7.4 mm. There was a tendency toward more consistent measurement between observers using the MPR technique to measure vessel separation The overall mean difference in measurements between observers was also <1 mm, with no significant difference in paired measurements ($p>0.05$). There were, however, more discrepancies between individual measurements, with a >3-mm difference noted in 18% of paired measurements, but this was not statistically

TABLE 2
Interobserver Results

	Aquarius (CLL)		Leonardo (MPR)	
	Observation 1	Observation 2	Observation 1	Observation 2
Mean difference, mm	−0.2	0.5	−0.1	0.1
Repeatability coefficient, mm	7.4	7.4	5.6	6.2
Difference >3 mm	5	2	4	7

CLL: central lumen line, MPR: multiplanar reconstruction.

significant compared with the intraobserver discrepancy (p=0.056).

The results of the 3-way repeated measures ANOVA are given in Table 3. The main individual effect of observer, type of workstation, or time of the observation on the interrenal separation was not significant, but there was a significant interaction among all 3 factors (p=0.022). By subgroup analysis, the interaction between observer and time was significant (p=0.031), but statistical significance was not observed between workstation type and time (p=0.799) or workstation and observer (p=0.585).

Clock-Face Position of Target Vessels

There was no significant intraobserver variation in clock-face measurements. Interobserver variability with ≥30 minutes of discrepancy was noted on 17 occasions, of which 11 (65%) related to the right renal artery position and 6 (35%) of the left renal artery. When analyzed by workstation (Table 4), a discrepancy in interobserver clock-face target vessel position was noted in 12% with the Aquarius workstations and in 6% with the Leonardo workstation, but this difference did not reach statistical significance (p=0.19).

DISCUSSION

Accurate assessment of vascular anatomy is of particular importance with fenestrated stent-grafts since errors may lead to serious consequences. Fenestrated and side-branched devices are tailored based on measurements of both the orientation and separation of target vessels. There are different workstations available to carry out measurements of vascular anatomy and landmarks, with varying but validated software.[6] Measurement of anatomy, even when performed according to a predetermined protocol, may be subject to observer interpretation and potentially be compounded by variations in workstation software. The resulting inter- and intraobserver variations in target vessel measurements for fenestrated stent-graft planning has not been reported previously.

In addition to standard quantitative analyses to examine variance, additional qualitative analysis of the data was also considered important to avoid the possibility of clinically insignificant discrepancies resulting in a statistically significant result or vice versa. For these purposes, a discrepancy of >3 mm in longitudinal vessel separation and of >30 minutes in clock-face measurement were considered significant. These arbitrary limits were chosen by the investigators since lesser degrees of measurement errors were considered unlikely to create serious consequences due to a degree of tolerance within the proximal main stent-graft body that incorporates the fenestrations.

The observers in this study had received training in using both workstations and were

TABLE 3
Three-way ANOVA of Factors Influencing Observer Variability

Factor	dF	F	p
Observer	1	0.784	0.385
Workstation	1	0.584	0.452
Time	1	0.783	0.385
Observer and workstation	1	0.306	0.585
Observer and time	1	5.240	0.031*
Workstation and time	1	0.066	0.799
Observer and workstation and time	1	6.021	0.022*

* Significant interaction between factors.

TABLE 4
Intra- and Interobserver Variability of Target Vessel Clock Position

	Aquarius		Leonardo	
Intraobserver	Observer 1	Observer 2	Observer 1	Observer 2
Right renal artery	0	0	0	0
Left renal artery	0	0	0	0
Interobserver	Observation 1	Observation 2	Observation 1	Observation 2
Right renal artery	3	2	3	3
Left renal artery	3	3	0	0

experienced in their use. Qualitative analysis suggested that intra- and interobserver variation to the extent considered clinically significant occurred with measurement for fenestrated EVAR. When data were examined for variation within workstation and observer-specific sets, the mean difference in repeat measurements was <1 mm in all instances. This, and the fact that the majority of the repeat measurements were within qualitatively tolerable limits of the initial measurement, is reassuring. There were, however, examples of significant measurement discrepancies both on quantitative (repeatability coefficients that exceeded arbitrary limits set for clinical significance) and qualitative analyses, which suggests that some measurements were likely to have been significantly inaccurate. This was true for both longitudinal vessel separation and clock-face assignment. In common with many other studies of image analyses, interobserver variation was greater than intraobserver variation. Furthermore, by 3-way ANOVA, it would appear that this was not a function of the type of workstation/technique used, but rather a result of the interaction between observer and time (repeat measurement), which suggests that interpretation of vascular landmarks remains subjective despite predefined criteria and protocols.

Unique anatomical features, such as angulation within the aorta and the trajectory, tortuosity, and non-planarity of target vessels, likely influence observer interpretation of target vessel position in both longitudinal and cross-sectional orientation. The majority of clock-position discrepancies between the observers related to the right renal artery, a vessel whose course takes a circuitous route behind the inferior vena cava. A higher incidence of target vessel occlusion has been reported with this artery and has been attributed to a higher probability of the renal stent kinking due to the curvature of this vessel.[7] Errors in assigning clock position of the right renal artery could also be a contributory factor.

In addition to the inherently subjective nature of these measurements, there are factors that could have potentially influenced the results. Variations in CTA slice thickness, quality of contrast enhancement, unique anatomical features of the aorta and its branches, distortion from anisotropic voxels in some CTA datasets, and even the hardware used for image acquisition may all have a potential impact on image analysis. Since a number of CTA scans were acquired at different hospitals, it was not possible to reduce heterogeneity of these aspects. Certain workstation functions, in particular semi-automated CLL generation, is influenced by the degree of contrast enhancement[8] and may therefore be responsible for the trend toward consistency with MPR, a technique that relies solely on observer manipulation of the images.

It might not be possible to completely eliminate measurement errors or discrepancies. Furthermore, it should also be recognized that native anatomy may be distorted intraoperatively due to the insertion of rigid stent-graft systems, which could contribute to difficulties in target vessel cannulation in addition to measurement errors. Although encouraging technical success rates are reported,[9] intraoperative difficulties that may ensue from distorted anatomy or device mismatch are seldom reported. It would therefore appear that fenestrated stent-grafts have a degree of tolerance to

mismatch with native anatomy, likely due to flexibility of the proximal main body and incorporation of fenestrations that are larger than the target vessel ostia. Innovations that provide greater tolerance would compensate for measurement errors and also lead to a reduced need for customization.

Conclusion

This study shows that measurements for planning fenestrated EVAR are prone to significant intra- and interobserver discrepancy in a small proportion of patients. Further study is warranted to identify factors that predispose to measurement discrepancies and to develop consensus regarding image interpretation. Stent-graft systems that would allow safe and effective transluminal revascularization of target vessels without relying heavily upon accurate measurement of native anatomy would also be beneficial.

Acknowledgement: The authors would like to acknowledge the late Geoffrey Gilling-Smith for his help and encouragement with this project.

REFERENCES

1. EVAR trial participants. Endovascular aneurysm repair versus open repair in patients with abdominal aortic aneurysm (EVAR trial 1): randomised controlled trial. *Lancet.* 2005;365:2179–2186.
2. Prinssen M, Verhoeven EL, Buth J, et al. A randomized trial comparing conventional and endovascular repair of abdominal aortic aneurysms. *N Engl J Med.* 2004;351:1607–1618.
3. Diehm N, Baum S, Benenati JF. Fenestrated and branched endografts: why we need them now. *J Vasc Interv Radiol.* 2008;19(6 Suppl): S63–7.
4. Sarac TP, Clair DG, Hertzer NR, et al. Contemporary results of juxtarenal aneurysm repair. *J Vasc Surg.* 2002;36:1104–1111.
5. Faggioli G, Stella A, Freyrie A, et al. Early and long-term results in the surgical treatment of juxtarenal and pararenal aortic aneurysms. *Eur J Vasc Endovasc Surg.* 1998;15:205–211.
6. Isokangas JM, Hietala R, Perala J, et al. Accuracy of computer-aided measurements in endovascular stent-graft planning: an experimental study with two phantoms. *Invest Radiol.* 2003;38:164–170.
7. Mohabbat W, Greenberg RK, Mastracci TM, et al. Revised duplex criteria and outcomes for renal stents and stent grafts following endovascular repair of juxtarenal and thoracoabdominal aneurysms. *J Vasc Surg.* 2009;49: 827–837.
8. Wyss TR, Dick F, England A, et al. Three-dimensional imaging core laboratory of the endovascular aneurysm repair trials: validation of methodology. *Eur J Vasc Endovasc Surg.* 2009;38:724–731.
9. Sun Z, Mwipatayi BP, Semmens JB, et al. Short to midterm outcomes of fenestrated endovascular grafts in the treatment of abdominal aortic aneurysms: a systematic review. *J Endovasc Ther.* 2006;13:747–753.

J ENDOVASC THER
2011;18:569–575

◆ISES ENDOVASCULAR RESEARCH COMPETITION, SECOND PLACE

Magnitude of the Forces Acting on Target Vessel Stents as a Result of a Mismatch Between Native Aortic Anatomy and Fenestrated Stent-Grafts

Olufemi A. Oshin, BEng, MBChB, MRCS[1]; Thien V. How, PhD[2]; John A. Brennan, MD, FRCS[1]; Robert K. Fisher, MD, FRCS[1]; Richard G. McWilliams, FRCR[1]; and S. Rao Vallabhaneni, MD, FRCS[1]

[1]Regional Vascular Unit, Royal Liverpool University Hospital, Liverpool, UK. [2]School of Clinical Sciences, Division of Clinical Engineering, University of Liverpool, UK.

Purpose: To quantify the compression force acting on target vessel stents as a consequence of the misalignment between the native aortic anatomy and the fenestrated stent-graft owing to measuring errors during the design of the device.
Methods: The material properties of a fenestrated Zenith stent-graft were determined using a standardized tensile testing protocol. Aortic anatomy was modeled using fresh porcine aortas that were subjected to tensile testing. The net force acting on a target vessel stent due to incremental discrepancy between the target vessel ostia and the stent-graft fenestrations was calculated as the difference in wall tension between the aorta and the stent-graft in diastole and systole. The change in diameter between diastole and systole was set to 8%.
Results: Using the diastole model, underestimation of circumferential target vessel position by 15°, 22.5°, and 30° resulted in net forces on the target vessel stent of 0.6, 0.8, and 1.1 N, respectively. Overestimation of target vessel position by the same increments resulted in net forces of 0.3, 0.6, and 0.9 N, respectively. With the systolic model, underestimating target vessel position by 30° resulted in a 2.1-N maximum force on the stent, which potentially threatened the seal. In the longitudinal direction, underestimating target vessel separation by up to 10 mm resulted in a maximal force on the stent of 6.1 N, while overestimating target vessel separation did not result in any additional force on the stent due to fabric infolding.
Conclusion: The magnitude of the forces generated solely due to mismatch between stent-graft design and native anatomy is modest and is unlikely to cause significant deformation of target vessel stents. Mismatch, however, may cause loss of seal.
J Endovasc Ther. 2011;18:569–575

Key words: Juxtarenal aortic aneurysm, fenestrated stent-graft, target vessel, stent-graft seal, compression force, device planning, balloon-expandable stent

Juxtarenal aortic aneurysms or aneurysms with short infrarenal necks are primary indications for the use of fenestrated-stent grafts during endovascular aneurysm repair (EVAR). These stent-grafts are custom-made and hence require accurate assessment of aortic morphology. Patency of visceral vessels is therefore mainly dependent upon alignment

The annual ISES Endovascular Research Competition held on February 14, 2011, at ICON 2011 (Scottsdale, Arizona, USA) evaluated participants on both their oral and written presentations. ISES congratulates the 2011 winners.

The authors have no commercial, proprietary, or financial interest in any products or companies described in this article.

Address for correspondence and reprints: SR Vallabhaneni, MD, FRCS, Link 8C, Royal Liverpool University Hospital, Prescot Street, Liverpool L7 8XP, UK. E-mail: *fempop@liv.ac.uk*

between the fenestrations and target vessel ostia. Indeed, early clinical experience with fenestrated stent-grafts showed that target vessel patency is best preserved by maintaining alignment between target vessels and fenestrations with balloon-expandable stents.[1]

After deployment, the stent-graft forms a laminar composite structure with the aorta, comprising aortic wall, stent-graft fabric (Dacron), and the metallic sealing stent. Although a degree of mismatch between the location of fenestrations in the stent-graft and the native anatomy may be tolerated without compromising seal, the implanted stent-graft is subject to the pulsatile, expansile hemodynamic movements natural to the aorta. A mismatch between the positions of fenestrations in the stent-graft with their corresponding target vessel ostia will potentially generate compressive forces acting upon the target vessel stents. These forces arise from summation of each of the forces to which individual components of the stent-graft/aorta composite are subjected. Continued target vessel patency is thus reliant on the ability of the target vessel stents to maintain alignment between fenestrations and the target vessel ostia by resisting the rotational and longitudinal forces potentially generated by the stent-graft/native aorta mismatch.

The degree of misalignment that may be tolerated by the target vessel stents without subsequent compromise of target vessel perfusion remains unclear. The aim of this study was to determine the magnitude of the forces brought to bear upon target vessel stents as a consequence of misalignment between stent-graft fenestrations and the target vessel ostia.

METHODS

Study Design and Model

The study device was a 2-fenestration 36-mm Zenith stent-graft (Cook Inc., Bloomington, IN, USA) designed for deployment in a 30-mm-diameter aorta (20% oversizing). The intended target vessels for the fenestrations were the renal arteries located at the same level (inter-renal artery separation of zero) with "clock-face" positions of 2 and 10 o'clock (Fig. 1A). For simplicity, the effect of friction between the stent-graft and lumen of the aorta was ignored, and only the forces acting in the circumferential direction and parallel to the long axis of the stent-graft were considered. The stent-graft was also considered to be uniformly oversized along the circumference, whereas in reality this is not the case (there is a greater degree of oversizing in the posterior aspect because of the need to incorporate diameter-reducing ties into the device to allow implantation).

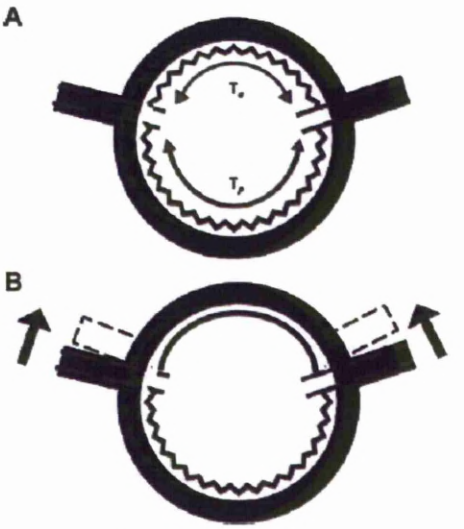

Figure 1 ◆ (A) Net force acting on the target vessel stent is predominantly determined by the tension in the anterior (T_a) and posterior (T_p) sections of the sealing stent during systole. (B) In systole, underestimation of anterior target vessel separation results in anterior displacement of the target vessel ostia.

Compressive forces acting upon target vessel stents when the fenestrations and the target vessels are perfectly aligned were considered negligible since the stent-graft is expected to move harmoniously with the aortic wall during the cardiac cycle. In a situation of mismatch, however, the target vessel stents will be subjected to compressive forces that are exaggerated during the cardiac cycle. These forces arise primarily when the misalignment is severe enough to put the fabric under stretch. This force is opposed by the

hoop strength of the sealing stent. Being elastic, the aorta may deform in response to these forces, accommodating some of the mismatch. Such deformation can be estimated if the elastic properties of aortic tissue are known. Hence, the elastic properties were measured on porcine aortas.

The aortic cross section changes throughout the cardiac cycle as the shock wave created by left ventricular ejection passes through. For the purpose of this study, contraction of the aortic lumen was called the diastolic phase and the enlargement of the aortic cross section was the systolic phase.

As a consequence of oversizing, the sealing stent as a whole is compressed, therefore the majority of the circumferential compressive force acting upon the target vessel stent is the net force generated by the anterior and posterior sections of the sealing stent (Fig. 1A). Since the sealing stent behaves in an elastic manner, the magnitude of these forces is proportional to the arc length of the anterior and posterior sections of the sealing stent and can be determined from experimental measurements.

In systole, the stent-graft fabric is put under stretch if the oversizing is insufficient to permit full expansion of the aorta. This is most likely to occur in the anterior section of the stent-graft if the distance between the target vessel ostia has been underestimated. Since the stiffness and tensile strength of Dacron is higher than that of human aorta,[2–3] this will lead to the target ostia being displaced anteriorly in order to accommodate the diameter change of the aorta during systole (Fig. 1B). This displacement is equivalent to the difference between the anterior circumferential separation of the fenestrations when the stent-graft is at full stretch and the true distance between the target vessel ostia. The resulting compressive force acting upon the target vessel stents is the force required to align the target vessel ostia and fenestrations by stretching the posterior section of the aorta.

In the longitudinal direction, if the inter-vessel separation is underestimated, additional force is required to align the ostia and fenestration. If, however, the inter-vessel separation is overestimated, infolding is likely to occur since Dacron has no columnar strength. Therefore, in this situation, it is unlikely that the target vessel stent will be subjected to any significant additional force.

Measuring the Stiffness of the Sealing Stent

The forces required to extend or compress the sealing stent were measured using a computerized tensile testing machine (Nene Instruments Ltd, Wellingborough, UK). The sealing stent was separated from the fabric of a fenestrated stent-graft and cut open to create a flat zigzag spring. This was divided into 6 V-shaped segments that were tested twice in compression. The gauge length (initial length of the sample) was set at 9 mm, and the rate of compression set at 10 mm/min. Maximum displacement was set at 5 mm. The load displacement was recorded, and the stiffness of the stent segments was calculated.

Measuring the Elastic Properties of the Aorta

Twenty fresh porcine aortas obtained from an abattoir were used as models of human aortas and were subjected to tensile testing according to a standardized protocol. Each aorta was cut into specimens measuring 120×35 mm; a 6-mm-diameter fenestration representing a renal branch ostium was created using a manual hole-punching device. The specimens were mounted onto a specially created jig (Fig. 2) designed to administer varying degrees of strain in both the circumferential and longitudinal directions. For the purposes of this study, 10% and 20% extensions were applied in the longitudinal and circumferential directions, respectively, to simulate the normal wall tension of the aorta as a result of diastolic blood pressure.[4,5] A steel hook terminated by a stainless steel cylinder (7-mm outer diameter) was placed through the "ostium" in the specimen to simulate a target vessel stent. The other end of the hook was connected to the load cell of the tensile tester. The rate of deformation was set to 10 mm/min, and load displacement data were recorded at intervals of 0.01 seconds with maximum displacement set at 10 mm. The tests

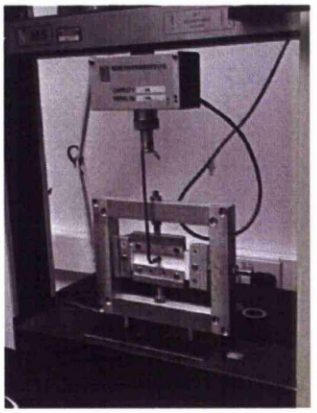

Figure 2 ◆ Tensile testing of aortic specimens.

were performed at room temperature once on 10 individual specimens in both the longitudinal and circumferential directions. Each of the 20 specimens was inspected after testing. The results were discarded when specimen slippage had occurred or where there was evidence that the ostium had been torn during the test. Data are presented as the median and interquartile range (IQR) in Newtons (N).

RESULTS

Tensile Tests

Materials testing of the sealing stent gave a median spring stiffness of 4×10^{-4} N/m for each V-shaped segment. With regard to the porcine aorta, 1 specimen had evidence of a torn ostium after longitudinal testing, while slippage/tearing at the grips occurred in 4 specimens during circumferential testing. These 5 tests were discarded leaving 15 tests eligible for analysis. The median force required to displace the fenestration by 10 mm was 3.97 N (IQR 0.81) in the circumferential direction (at an initial strain of 10%, Fig. 3A) and 6.1 N (IQR 1.6) in the longitudinal direction (at an initial strain of 20%, Fig. 3B).

Forces Acting Upon Target Vessel Stents

Under diastolic conditions, when target vessel separation was underestimated in the circumferential direction by 30 minutes (15°), 45 minutes (22.5°), and 60 minutes (30°), net forces of 0.6, 0.8, and 1.1 N were generated by the sealing stent for each respective grade of discrepancy (Table 1). If target vessel position was overestimated, each gradation of discrepancy resulted in a net force on the stent of 0.3, 0.6, and 0.9 N, respectively.

Stent-graft/aorta mismatch of 15°, 22.5°, and 30° resulted in displacement of the target vessel ostia by 0.4, 2.6, and 4.7 mm, respectively (Table 2). Using the circumferential load displacement data obtained from material testing of the porcine aorta specimens, this was equivalent to median compressive forces of 0.15, 0.77, and 2.1 N, respectively. The magnitude of the longitudinal forces acting on the target vessel stent was derived from the longitudinal load displacement curve of the aortic specimens.

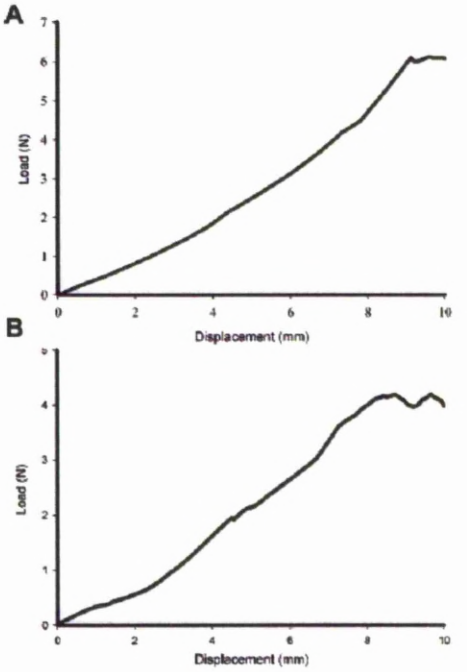

Figure 3 ◆ (A) Longitudinal and (B) transverse (circumferential) load displacement curves for the porcine aorta.

TABLE 1
Summary of the Net Force Generated by Discrepancy Between the Target Vessel Ostia and the Stent-Graft Fenestration

Total Discrepancy Relative to Target Vessel Ostium, ° (minutes)	Lumen Arc Length, mm		Graft Arc Length, mm		Effective Oversizing, %		Net Compressive Force, N
	A	P	A	P	A	P	
0	31.4	62.8	37.7	75.3	20.1	19.9	0.0
−15 (30)	35.3	58.9	37.7	75.3	6.8	27.8	0.6
−22.5 (45)	37.3	56.9	37.7	75.3	1.1	32.3	0.8
−30 (60)	39.3	54.9	37.7	75.3	−4.1	37.2	1.1
+15 (30)	29.4	64.8	37.7	75.3	28.2	16.2	0.3
+22.5 (45)	27.4	66.8	37.7	75.3	37.6	12.7	0.6
+30 (60)	25.4	68.8	37.7	75.3	48.4	9.4	0.9

A: anterior, P: posterior.
Negative values indicate underestimation and positive values overestimation.

DISCUSSION

Accurate assessment of aortic morphology is essential in the design of fenestrated stent-grafts. These measurements, however, are subject to both intra- and interobserver variability.[6,7] By inference, a degree of mismatch between patient anatomy and the design of the fenestrated grafts may be tolerated without target vessel compromise. Since mismatch requires enforced alignment between the stent-graft fenestration and the target vessel ostia, target vessel patency is determined by the structural integrity of the target vessel stent. Despite the potentially disastrous consequences of mechanical failure of these stents, the potential forces to which they are subjected when mismatch occurs have not been investigated.

The reaction of a target vessel stent to deformational forces depends upon its composite materials and its structural design. Although an ability to resist deformation at the level of the fenestration/target vessel ostia is considered a desirable feature in target vessel stents, flexibility is desired away from the ostium due to the movement of the renal arteries with respiration.[8–10] Stiffer target vessel stents, such as the Jostent, though better able to resist deformation and thus cross-sectional area reduction at the ostium, may create a new fulcrum for this movement at the transition between the stent and distal native renal artery, which risks inciting neointimal hyperplasia due to repetitive trauma and subsequent occlusion.

The hoop strength of stents commonly inserted into target vessels during fenestrated

TABLE 2
Compressive Forces Acting Upon Target Vessel Stents as a Result of Displacement of the Target Vessel Ostia

Circumferential Discrepancy, ° (minutes)	Graft/Aorta Mismatch, mm		Total Ostia Displacement, mm	Compressive Force, N
	Anterior	Posterior		
0 (0)	3.8	7.5	0.0	0
15 (30)	−0.4	11.6	0.4	0.15
22.5 (45)	−2.6	13.8	2.6	0.77
30 (60)	−4.7	16.0	4.7	2.10

Negative values denote underestimation of target vessel separation.

EVAR is known.[11] Within the range of our investigation, we have shown that forces capable of compressing the stents and causing a stenosis could be generated solely due to a mismatch. However, in no stent would this reduction create a stenosis >15%. Furthermore, since a flow limiting renal stenosis is defined as a reduction in cross-sectional area of at least 60%,[12–14] greater stent-graft/aorta mismatch may be tolerated without compromising renal perfusion.

Theoretical discrepancies in circumferential target vessel position of up to 60 minutes (30°) were considered in this study. In practice, discrepancies in circumferential target vessel position rarely exceed 30 minutes (15°) between different observers; however, differences in perceived longitudinal target vessel separation are more common.[7] Determining whether this observed difference is significant is often based on an arbitrary figure informed by the size of the target vessel fenestration, which does not take into account the possibility that either the stent-graft or the aorta may deform in order to maintain alignment between the fenestration and target vessel ostia. Since the stent-graft fabric is much stiffer than aortic tissue, underestimation of target vessel separation results in additional tension on the aortic wall in order to maintain alignment. As such, significant displacement in the longitudinal direction is potentially possible without creating a flow-limiting stenosis.

This analysis of longitudinal resistance to crushing does not take into account the hemodynamic forces acting on the graft (in particular those acting at the aortic bifurcation) that are often a major component of caudal migration. It is, however, unlikely that these forces contribute significantly to the forces acting on the target vessel stents due to unique design characteristics of the Zenith fenestrated stent-graft. First, the modular design of the fenestrated stent-graft minimizes transmission of the force acting upon the flow divider of the distal body. This results in modular distraction instead of caudal migration of the proximal main body. Second, after the anti-migration barbs located in the bare metal proximal stents are engaged, a significant additional force (16.8 N)[15] is required to initiate caudal migration of the proximal main body of a fenestrated stent-graft.

Limitations

This model only considered snapshots in the cardiac cycle from which static values for the force acting upon target vessel stents were calculated. In a dynamic environment, the forces acting on the target vessel stents are best described as impulses, though it is not possible to determine if the magnitude of these impulses, which cannot be directly measured, is greater than the static forces calculated in this study. Furthermore, damage to target vessels may occur from additional mechanisms, such as fatigue fractures that potentially could be induced by even the modest forces typified in our results.

Calculation of the force acting on the target vessel stent in the circumferential direction relied upon the assumption that aortic expansion is symmetrical in all directions. However, electrocardiographically-gated magnetic resonance angiography studies have shown that this is not the case due to the close proximity of the aorta to the vertebral column. The mean change in aortic diameter in our study was 8% during systole; however, in some directions, an increase in diameter of up to 22% has been reported.[16,17] The applicability of this observation to everyday clinical practice is unknown since fenestrated stent-grafts are usually designed from computed tomographic angiography images that may be taken from any point within the cardiac cycle.

Friction between the stent-graft and the aortic wall was not considered in order to simplify the boundary conditions of this model. However, friction is more likely to have a significant role where circumferential mismatch is concerned, particularly during the diastolic phase. During the systolic phase, the wall of the aorta stretches and is accommodated by the excess fabric of the oversized stent-graft. In diastole, the aorta remains still while the metal component of the stent-graft attempts to return to its expanded state. It is this potential movement of the fenestrations that is resisted by friction, and rather than adding to the compressive forces on the stent, it probably helps maintain alignment

between the fenestrations and target vessel ostia.

Conclusion

It may not be possible to eliminate errors or discrepancies between observers when planning fenestrated stent-grafts, resulting in a mismatch between native anatomy and stent-graft fenestrations. This study shows that the compression forces developed to act upon target vessel stents due to such mismatch can be tolerated without a significant risk of target vessel stent compression. It is acknowledged that other mechanisms leading to target vessel stent distortion exist.

REFERENCES

1. Muhs BE, Verhoeven EL, Zeebregts CJ, et al. Mid-term results of endovascular aneurysm repair with branched and fenestrated endografts. *J Vasc Surg.* 2006;44:9–15.
2. Salacinski HJ, Goldner S, Giudiceandrea A, et al. The mechanical behavior of vascular grafts: a review. *J Biomater Appl.* 2001;15:241–278.
3. Sarkar S, Salacinski HJ, Hamilton G, et al. The mechanical properties of infrainguinal vascular bypass grafts: their role in influencing patency. *Eur J Vasc Endovasc Surg.* 2006;31:627–636.
4. Kalath S, Tsipouras P, Silver FH. Non-invasive assessment of aortic mechanical properties. *Ann Biomed Eng.* 1986;14:513–524.
5. Silver FH, Snowhill PB, Foran DJ. Mechanical behavior of vessel wall: a comparative study of aorta, vena cava, and carotid artery. *Ann Biomed Eng.* 2003;31:793–803.
6. Malkawi AH, Resch TA, Bown MJ, et al. Sizing fenestrated aortic stent-grafts. *Eur J Vasc Endovasc Surg.* 2011;41:311–316.
7. Oshin OA, England A, McWilliams RG, et al. Intra- and interobserver variability of target vessel measurement for fenestrated endovascular aneurysm repair. *J Endovasc Ther.* 2010;17:402–407.
8. Draney MT, Zarins CK, Taylor CA. Three-dimensional analysis of renal artery bending motion during respiration. *J Endovasc Ther.* 2005;12:380–386.
9. Kaandorp DW, Vasbinder GB, de Haan MW, et al. Motion of the proximal renal artery during the cardiac cycle. *J Magn Reson Imaging.* 2000;12:924–928.
10. Muhs BE, Teutelink A, Prokop M, et al. Endovascular aneurysm repair alters renal artery movement: a preliminary evaluation using dynamic CTA. *J Endovasc Ther.* 2006;13:476–480.
11. Scurr JR, How TV, McWilliams RG, et al. Fenestrated stent-graft repair: which stent should be used to secure target vessel fenestrations? *J Endovasc Ther.* 2008;15:344–348.
12. Hansen KJ, Tribble RW, Reavis SW, et al. Renal duplex sonography: evaluation of clinical utility. *J Vasc Surg.* 1990;12:227–236.
13. Kohler TR, Zierler RE, Martin RL, et al. Noninvasive diagnosis of renal artery stenosis by ultrasonic duplex scanning. *J Vasc Surg.* 1986;4:450–456.
14. Taylor DC, Kettler MD, Moneta GL, et al. Duplex ultrasound scanning in the diagnosis of renal artery stenosis: a prospective evaluation. *J Vasc Surg.* 1988;7:363–369.
15. Zhou SS, How TV, Vallabhaneni SR, et al. Comparison of the fixation strength of standard and fenestrated stent-grafts for endovascular abdominal aortic aneurysm repair. *J Endovasc Ther.* 2007;14:168–175.
16. van Herwaarden JA, Bartels LW, Muhs BE, et al. Dynamic magnetic resonance angiography of the aneurysm neck: conformational changes during the cardiac cycle with possible consequences for endograft sizing and future design. *J Vasc Surg.* 2006;44:22–28.
17. van Prehn J, van Herwaarden JA, Vincken KL, et al. Asymmetric aortic expansion of the aneurysm neck: analysis and visualization of shape changes with electrocardiogram-gated magnetic resonance imaging. *J Vasc Surg.* 2009;49:1395–1402.